uOttawa

L'Université canadienne
Canada's university

FACULTÉ DES ÉTUDES SUPÉRIEURES ET POSTOCTORALES

uOttawa

L'Université canadienne
Canada's university

FACULTY OF GRADUATE AND POSDOCTORAL STUDIES

Ashley Byrnes
AUTEUR DE LA THÈSE / AUTHOR OF THESIS

M.Sc.(Biochemisty:Specialization-Human and Molecular Genetics)
GRADE / DEGREE

Department of Biochemistry, Microbiology and Immunology
FACULTÉ, ÉCOLE, DÉPARTEMENT / FACULTY, SCHOOL, DEPARTMENT

Identification of a Novel Gene for Brachydactyly Type A1

TITRE DE LA THÈSE / TITLE OF THESIS

Dr. Dennis Bulman
DIRECTEUR (DIRECTRICE) DE LA THÈSE / THESIS SUPERVISOR

CO-DIRECTEUR (CO-DIRECTRICE) DE LA THÈSE / THESIS CO-SUPERVISOR

EXAMINATEURS (EXAMINATRICES) DE LA THÈSE / THESIS EXAMINERS

Dr. M-A. Akimenko

Dr. F. Tesson

Gary W. Slater
Le Doyen de la Faculté des études supérieures et postdoctorales / Dean of the Faculty of Graduate and Postdoctoral Studies

Identification of a Novel Gene for Brachydactyly Type A1

By

Ashley M. Byrnes

THESIS
Submitted to the Faculty of Graduate and Postdoctoral Studies
In partial fulfillment of the requirements
For the Master of Science degree in Human and Molecular Genetics

Department of Biochemistry, Microbiology and Immunology
Program in Human and Molecular Genetics
Faculty of Medicine
University of Ottawa

Your file Votre référence
ISBN: 978-0-494-34059-2
Our file Notre référence
ISBN: 978-0-494-34059-2

Abstract

Brachydactyly type A1 (BDA1) is a congenital disorder that affects normal bone development and patterning. Affected individuals have short fingers, broad hands and are generally short in stature. BDA1 was the first human trait described in terms of autosomal dominant Mendelian inheritance. Missense mutations in the Indian hedgehog (*IHH*) gene have been shown to be responsible for the disorder, and a second locus has been mapped to a region on chromosome 5p13.3-p13.2 in a single kindred. We have since obtained DNA from four new BDA1-affected kindreds. We were successful in identifying *IHH* mutations in 3 of these families, thus further supporting a role for *IHH* in the pathogenesis of BDA1.

We have also obtained DNA from a consanguineous BDA1-affected kindred in which mutations in *IHH*, as well as linkage to the chromosome 5p13.3-p13.2 region, have been excluded. Taken together, this data supports existence of a third locus for BDA1. A genome-wide linkage screen was initiated in the family, and linkage was observed at a region on chromosome 20q11.22-q11.23. Subsequent screening of the candidate gene *GDF5*, located in the chromosome 20 disease locus, revealed a homozygous c.1138C>T nucleotide change in all affected members of the sibship. This mutation is hypothesized to disrupt the highly-conserved tertiary structure of the GDF5 monomer which is critical for the dimerization and maturation of GDF5, thus leading to interrupted GDF5 signaling and severe BDA1 pathogenesis in homozygous individuals. This thesis identifies *GDF5* as the second disease gene for BDA1, and describes the first case of BDA1 in a consanguineous family.

Acknowledgements

It is with great pleasure that I may thank the many people who helped make the successful completion of this thesis possible.

It is difficult to express my gratitude to Dr. Dennis Bulman, my thesis supervisor, for his guidance and support throughout graduate school. Without his enthusiasm, good ideas, and sound advice, I would have been lost.

I am deeply indebted to all members of the laboratory, past and present, not only for sharing their extensive knowledge and technical assistance, but also for their camaraderie and support. In particular, I would like to thank Lemuel Racacho, Heather McDonald, Ruobing Zou, Kelly Westaff and Jessica Skof for their considerable contributions to my project.

I am also very grateful to the members of my advisory committee, Drs. Marie-Andrée Akimenko and Robin Parks, for the time they dedicated to help me successfully progress with my project.

To all of my friends and family whose support and guidance have carried me along the way, I cannot thank you enough.

Lastly, and most importantly, I wish to thank my parents and my sister for all of their endless love, teaching, and support. To them I dedicate this thesis.

Table of Contents

List of Figures

List of Tables

List of Abbreviations

2q	Long arm of chromosome 2
5q	Long arm of chromosome 5
7q	Long arm of chromosome 7
9q	Long arm of chromosome 9
12p	Short arm of chromosome 12
12q	Long arm of chromosome 12
17q	Long arm of chromosome 17
20p	Short arm of chromosome 20
20q	Long arm of chromosome 20
∞	Infinity
β	Beta
θ	Theta
ACFD	Acrocapitofemoral Dysplasia
Ala	Alanine
Arg	Arginine
Asn	Asparagine
Asp	Aspartic Acid
ASOH	Allele-Specific Oligo Hybridization
ASPED	Angel-Shaped Phalangoepiphyseal Dysplasia
ATP	Adenosine Triphosphate
BD	Brachydactyly
BDA1	Brachydactyly Type A1
BDA2	Brachydactyly Type A2
BDB	Brachydactyly Type B
BDC	Brachydactyly Type C
BDD	Brachydactyly Type D
BDE	Brachydactyly Type E
BMP	Bone Morphogenetic Protein
BMPR1B	Bone Morphogenetic Protein Receptor 1B
bp	*brachypodism* mouse
c.	Notation for cDNA sequence
C	Cysteine
CDMP-1	Cartilage-Derived Morphogenetic Protein 1)
CGT	Grebe-Type Dysplasia
CHTT	Hunter-Thompson Type Dysplasia
cM	Centimorgan
Cos2	Costal2
cpm	Counts per minute
CVT	Congenital Vertical Talus

Cys	Cysteine
D	Aspartic Acid
D2S2250	Microsatellite marker
ddH_2O	Double distilled water
DHH	Desert Hedgehog
Di	Dinucleotide
Disp	Dispatched
Dlp	Dally-like
DNA	Deoxyribonucleic Acid
dNTP	Deoxy-nucleotide triphosphate
Dsh	*Short digits* mouse
E	Glutamic Acid
EDTA	Ethylene diamine tetracetic acid
FGF	Fibroblast Growth Factor
Fu	Fused
G	Glysine
GDF	Growth and Differentiation Factor
Gli	Glioma associated
Gln	Glutamine
Glu	Glutamic Acid
Gly	Glysine
HCl	Hydrochloric acid
Hh	Hedgehog
HIP	Hedgehog Interacting Protein
His	Histidine
HOXD13	Homeobox Gene D13
HSPGs	Heparan Sulfate Proteoglycans
HTNB	Bilginturin Syndrome
I	Isoleucine
IHH	Indian Hedgehog
K	Lysine
KCl	Potassium chloride
kDa	Kilo Dalton
L	Leucine
LOD	Logarithm of the Odds
Lys	Lysine
M	Molarity, mol/L
Mb	Mega base

MCPP	Metacarpophalangeal Profiles
$MgCl_2$	Magnesium Chloride
mL, µl	Millilitre, microlitre
mM, µM	Millimolar, micromolar
MSX1	Homolog of Drosophila Muscle Segment Homeobox 1
MSX2	Homolog of Drosophila Muscle Segment Homeobox 2
mRNA	Messenger Ribonucleic Acid
N	Asparagine
NCBI	National Center for Biotechnology
NEB	New England Biolabs
Ng	Nanogram
p.	Notation for protein sequence
P	Proline
PCR	Polymerase Chain Reaction
pH	Potential of hydrogen
Ph.D.	Doctor of Philosophy
Ptch1	Patched 1
PTHrP	Parathyroid Hormone Related Protein
Q	Glutamine
R	Arginine
ROR2	Orphan Tyrosine Kinase Receptor
R-Smads	Repressor Smads
S	Serine
SDS	Sodium Dodecyl Sulfate
Ser	Serine
SHH	Sonic Hedgehog
Smo	Smoothened
SNP	Single Nucleotide Polymorphism
SPC	Subtilisin-like Proprotein Convertases
SSPE	Sodium chloride sodium phosphate EDTA
SuFu	Supressor of Fused
SYM1	Proximal Symphalangism 1
SYNS1	Multiple Synostoses Syndrome 1
SYNS2	Multiple Synostoses Syndrome 2
Syn	Synonymous codon
T	Threonine
TD	Touchdown PCR program
Tetra	Tetranucleotide
TM	Temperature PCR program
TGF-β	Transforming Growth Factor beta

Thr	Threonine
Trp	Tryptophan
UTR	Un-Translated Region
V	Valine
X	Any amino acid

Chapter 1. Introduction

1.1 Brachydactyly

The brachydactylies (BDs) are a group of inherited disorders characterized by shortened digits due to malformation or absence of the phalanges and/or metacarpals [1]. Initially classified by Bell into types A1-A3, B, C, D, and E, they have since been reclassified by Temtamy and McKusick and Fitch due to overwhelming phenotype heterogeneity [1-3]. Since this time, additional subtypes A4-A6 have been described, as well as many cases in which affected individuals display features of more than one type of BD [4-6]. This thesis will focus on Brachydactyly type A1 (BDA1).

1.2 Brachydactyly Type A1

Brachydactyly type A1 (BDA1 [MIM 112500]) has the distinction of being the first disorder to be described as an autosomal dominant Mendelian trait in humans [7]. BDA1 was first identified and described by Farabee in his 1903 PhD thesis [7]. BDA1 is characterized by shortness of all middle phalanges of the hands and toes, shortness of the proximal phalanges of the first digit, and short stature [1]. Occasionally, terminal symphalangism may occur, in which the middle and distal phalanges fuse, forming a small chess-pawn shaped bone [3]. BDA1 is thought to occur in approximately 1 in 100,000 live births.

While BDA1 can occur as an isolated malformation, it has also been described as part of complex syndromes. Some of the most commonly reported associated disorders

include nystagmus [8, 9], developmental delay, mental retardation [8-11], scoliosis [8, 12, 13], and club feet [13]. In 1995, Fukushima et al. described a girl with BDA1, flat feet, and Klippel-Feil anomaly [14]. Klippel-Feil anomaly is a defect in cervical vertebrae segmentation, resulting in fused vertebrae. A *de novo* balanced translocation between 5q11.2 and 17q23 was discovered, suggesting that the gene or genes responsible for these traits were located at one of these loci [15].

1.3 Genetics of Brachydactylies

There has been extensive interest in determining the genetic basis for brachydactylies in order to identify novel genes involved in bone development and their purported protein functions. Genes involved in most types of BD have been reported. In many cases, locus heterogeneity has been described, suggesting that mutations in different genes regulating limb development can cause similar phenotypes. Although most cases of BD have been described as autosomal dominant, reports of incomplete penetrance and phenotypic variation stress the impact of genetic and/or environmental modifiers in the development of the disease.

1.3.1 Genetics of Brachydactyly Type A1

Although BDA1 was the first disorder ever reported as having autosomal dominant Mendelian inheritance, investigations disclosing the molecular foundations of BDA1 were not reported until recently. Linkage to chromosome 2q35-36 in two large Chinese kindreds led to the identification of disease-causing mutations in the gene Indian hedgehog (*IHH*) [16, 17]. To date, heterozygous p.E95K, p.E95G, p.D100E, p. D100N,

p.E131K and p.T154I IHH amino acid changes have been associated with BDA1 [16, 18-22]. Following these discoveries, a second locus for BDA1 was reported at chromosome 5p13.3-p13.2 (designated BDA1B [MIM 607004]) in a large Canadian family, implying locus heterogeneity [23]. Furthermore, both the *IHH* gene and the chromosome 5p13.3-p13.2 region were excluded in at least one other family, implicating a third locus in the development of BDA1 [19].

1.3.2 Genetics of Other Brachydactylies

Brachydactyly type A2 (BDA2 [MIM 112600]) is characterized by the shortening of the middle phalange in digit 2 only. Recently, it has been shown that mutations in both growth and differentiation factor 5 (*GDF5*) and its receptor, bone morphogenetic receptor 1B (*BMPR1B*), cause autosomal dominant BDA2 [24, 25].

The brachydactyly type B (BDB [MIM 113000]) phenotype, described as the most severe form of BD, consists of short middle phalanges and absent distal phalanges. Heterozygous mutations in *ROR2*, an orphan tyrosine kinase receptor, cause autosomal dominant BDB [26]. An additional locus on chromosome 9q22 has been reported in at least one family [27].

Brachydactyly type C (BDC [MIM 113100]) is similar to brachydactyly types A1 and A2 in that they each involve malformation of various middle phalanges. However, in BDC, the fourth finger is spared; the phenotype involves shortening of the middle phalanges in digits 2, 3, and 5, and of the first metacarpal. Mutations in *GDF5* have been shown to cause both autosomal dominant and semi-dominant BDC [28, 29]. A

mutation in *BMPR1B* has also been shown to cause a BDC-like phenotype with unusual symphalangism in one individual [30].

Brachydactyly types D (BDD [MIM 113200]) and E (BDE [MIM 113300)] are characterized by a shortened thumb and shortened metacarpals, respectively. Heterozygous mutations in *HOXD13*, a homeodomain transcription factor, were found in one family exhibiting traits of both BDD and BDE [4]. An additional locus for brachydactyly type E has been reported at chromosome 12p12.2-p11.2 [31].

1.4 History of Brachydactyly Type A1

As part of his Ph.D. thesis, Farabee described a large family from Pennsylvania with BDA1 and correctly surmised that the trait was inherited in a dominant manner [7]. A few years later, four additional BDA1 families of English ancestry were described thoroughly by Drinkwater [32-34]. Amongst the families, Drinkwater identified individuals with both mild and severe forms of BDA1, in which the finger length varied from mildly short to less than half the normal expected length (Figure 1.1) [3]. Drinkwater hypothesized that members of his first family (1907) may be related to Farabee's family due to their striking phenotypic similarities [32, 34]. Although ancestors of Drinkwater's first family were known to have immigrated to the United States from England, no last name common to both families was ever confirmed [35]. Members of the Bulman laboratory obtained DNA samples from descendants of both Drinkwater's 1907 and 1915 families, as well as of Farabee's 1903 family. Molecular analysis revealed that all affected individuals in each of the 3 families shared a heterozygous c.298G>A mutation in *IHH* that led to a p.D100N amino acid

Figure 1.1. Pictures of normal hands and hands with Brachydactyly type A1. *(A)* Top hand, unaffected individual; bottom hand, related affected individual with mild BDA1. *(B)* A drawing depicting approximate size differences in the proximal (1), middle (2), and distal (3) skeletal phalanges of A – an unaffected individual, B – an individual with mild BDA1, and C- an individual with severe BDA1. *(C)* Top hand, unaffected individual; bottom hand, related affected individual with severe BDA1.

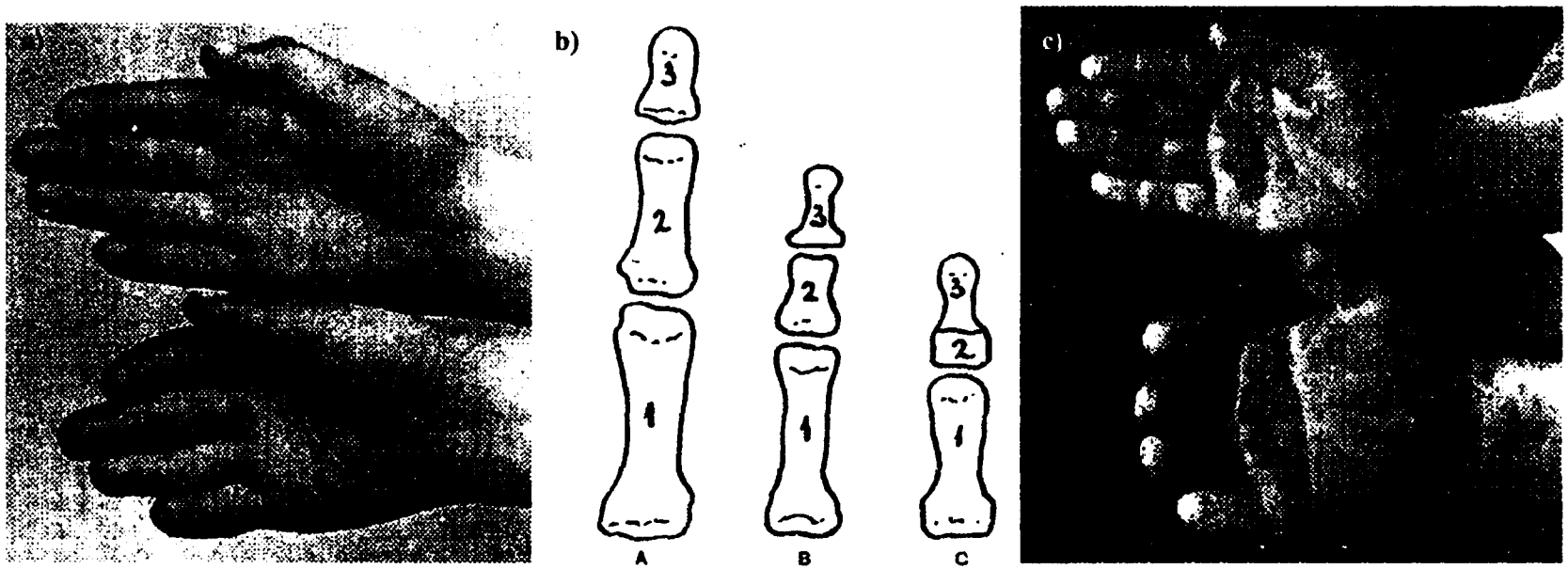

change [21, 22]. This indicated the possibility of a genetic relationship between all 3 families. Microsatellite and Single Nucleotide Polymorphism (SNP) genotyping around the *IHH* gene led to the identification of a haplotype common to all affected individuals in the 3 families. The common haplotype covered a 5cM region between markers D2S2250 and D2S1323 in all individuals except one, in which a recombination occurred [21, 22]. This common haplotype is consistent with the likelihood of a common founder from which all of these families are descendants.

1.5 Endochondral Ossification

In humans, bones can be formed in one of two ways: intramembranous ossification, or endochondral ossification. Intramembranous ossification is the process by which flat bones, such as those of the skull, develop. During intramembranous ossification, mesenchymal progenitor cells differentiate directly into bone cells, called osteoblasts and osteoclasts [36]. Conversely, endochondral ossification, which is particularly important in the formation of the long bones, is a 2-step process. Initially, aggregated mesenchymal cells differentiate into chondrocytes and form cartilaginous precursor elements; these are eventually replaced by bone [37]. The cartilaginous precursor elements serve not only as a scaffold for the bone cells, but also to allow growth of bones [38]. As brachydactyly is a disease with shortened long bones, we will focus on the process of endochondral ossification.

Endochondral bone formation begins with mesenchymal cell recruitment and condensation, followed by differentiation of cells to chondrocytes. Cells at the border of the condensation will differentiate to form the perichondrium, a collar surrounding a

growing long bone (Figure 1.2) [39]. The chondrocytes then pass through phases of resting, proliferation, differentiation and apoptosis (Figure 1.2) [40]. Proliferating chondrocytes arrange into columns, which direct lengthening along one particular axis (proximo-distal in the case of limbs); they then stop proliferating and become pre-hypertrophic chondrocytes (Figure 1.2). The pre-hypertrophic chondrocytes differentiate into terminal hypertrophic cells, which attract blood vessels and bone cells to mineralize the surrounding matrix and induce cells from the perichondrium to differentiate into osteoblasts, forming the bone collar (Figure 1.2) [37, 39]. Continued accumulation of bone cells in the perichondrium leads to radial growth of long bones [41].

Bone length is therefore determined by the rate that proliferating chondrocytes differentiate into terminal hypertrophic chondrocytes [39]. As bones progressively increase in length, secondary ossification centers are established at the ends of long bones where chondrocytes stop proliferating, proceed to hypertrophy, and attract blood vessels and osteoblasts to form new bone [39]. Between the primary and secondary ossification centers of an elongating long bone, the process of chondrocyte proliferation, differentiation and hypertrophy continues at a region called the epiphyseal growth plate (Figure 1.3). As post-natal growth occurs, the growth plates are further separated by the increasing space that is filled with bone following terminal hypertrophy of chondrocytes (Figure 1.3) [40]. In humans, the growth plates normally disappear in adolescence [39].

Many important signaling pathways, such as the fibroblast growth factor (FGF), the bone morphogenetic protein (BMP), and the hedgehog (HH) signaling pathways interact during endochondral ossification to control the rate of proliferation and terminal

Figure 1.2. Schematic of endochondral ossification at the end of a long bone. Adapted from Chung, U.I., et al., J. Clin. Invest., 2001. 107(3): p. 295-304 [57]. Endochondral Ossification of long bones is a 2-step process that begins with the formation of a cartilaginous template, followed by the replacement of cartilage with bone cells called osteoblasts. Initially, mesenchymal cells are recruited to, and condense at, the site of the future bone. Cells will then differentiate into cartilage cells, called chondrocytes. The chondrocytes at the edge of the condensation form the perichondrium, a collar which will surround the growing skeletal element. The remaining chondrocytes pass through numerous phases before being replaced by osteoblasts. Cells proliferate, then become pre-hypertrophic chondrocytes, arranged in columns to direct the growth of the skeletal element lengthwise. The cells then differentiate into hypertrophic chondrocytes, which induces vascularization and mineralization of the surrounding matrix, as well as the differentiation of the perichondrium into the bone collar. Terminal hypertrophic cells apoptose and are replaced by osteoblasts in the vascularized, mineralized matrix. Distal chondrocytes will continue to pass through stages of proliferation, pre-hypertrophy, and terminal hypertrophy, followed by the invasion of blood vessels and osteoblasts. The rate that this process occurs determines the length of a given skeletal element.

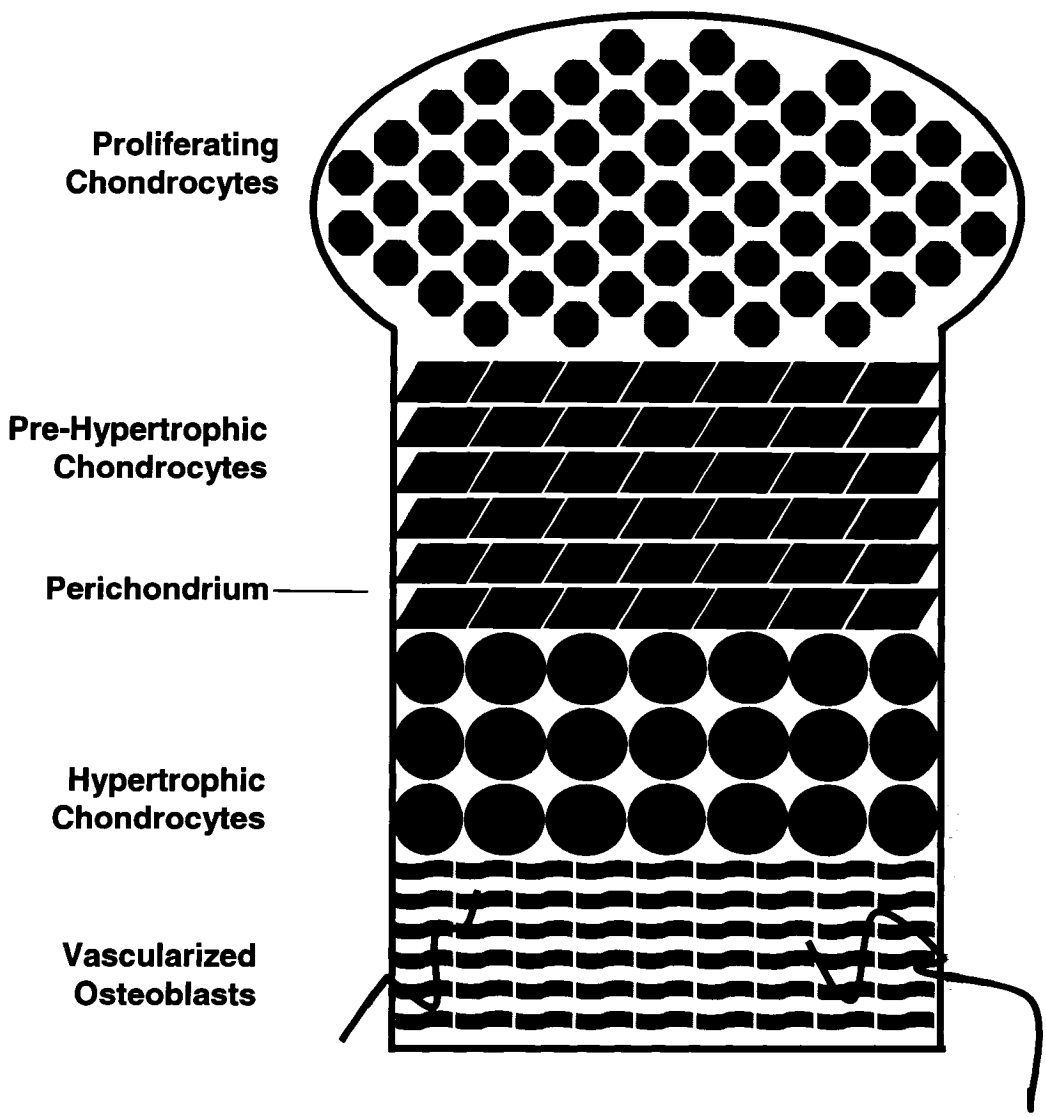
Proliferating Chondrocytes
Pre-Hypertrophic Chondrocytes
Perichondrium
Hypertrophic Chondrocytes
Vascularized Osteoblasts

Figure 1.3. Schematic of the growth plate formed in a long bone during endochondral ossification. Cell types are as defined in Figure 1.1. Chondrocytes pass through stages of proliferation, pre-hypertrophy, and terminal hypertrophy, followed by the invasion of blood vessels and osteoblasts. Initially, terminal chondrocytes induce vascularization and mineralization of the surrounding matrix at the center of the skeletal element (the primary ossification center). As the bone increases in length, hypertrophy of chondrocytes and invasion of blood vessels and osteoblasts occurs at the distal ends of the bone, forming secondary ossification centers. With solid bone forming on both sides, the group of proliferating, pre-hypertrophic and hypertrophic chondrocytes remaining between these ossification centers represents the only area where any subsequent growth can occur. This area is referred to as the growth plate.

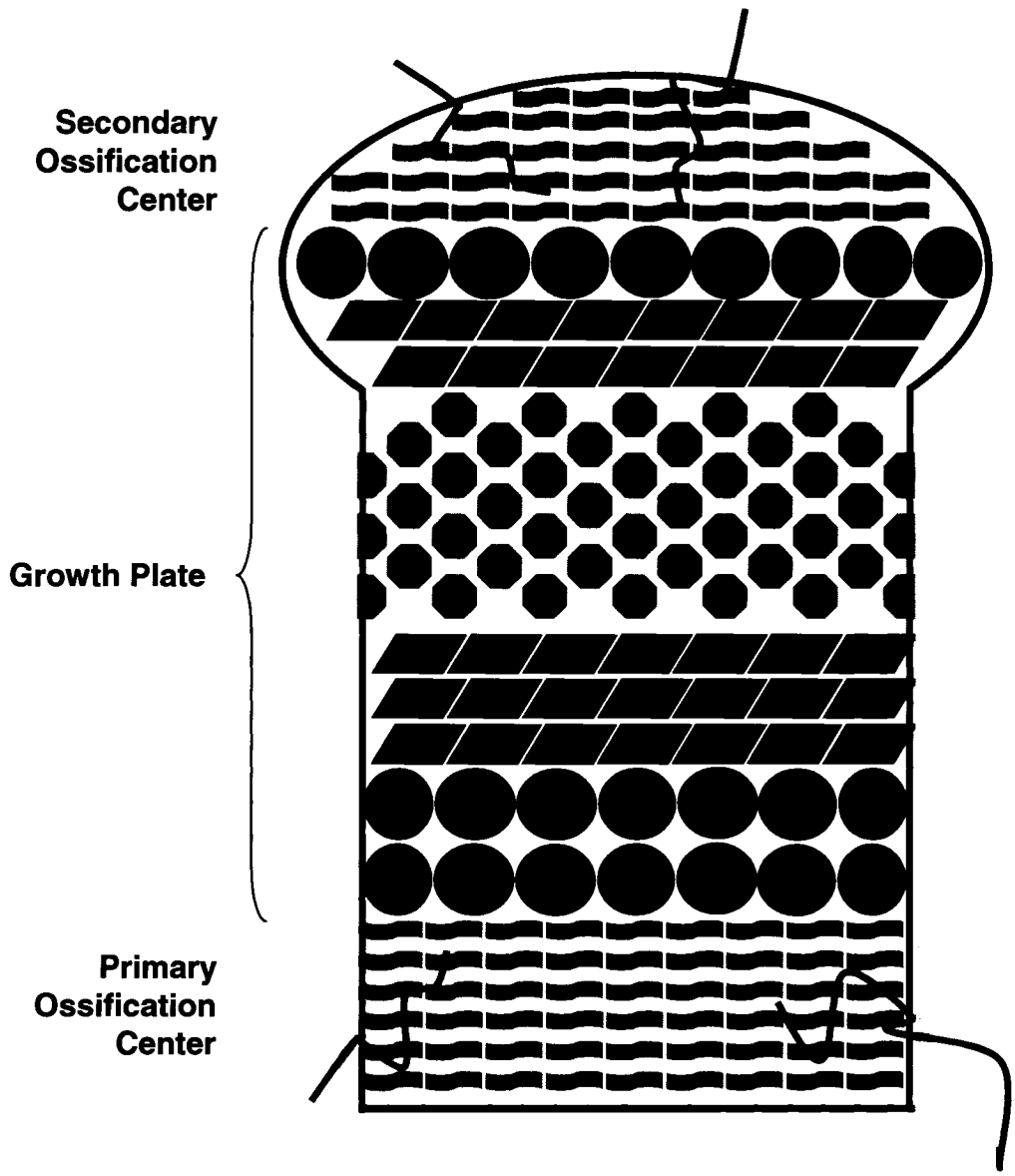
Secondary
Ossification
Center
Growth Plate
Primary
Ossification
Center

differentiation of chondrocytes to prevent the premature ossification of the growth plate [37, 38]. Two members of these pathways, Indian hedgehog (*IHH*) and growth and differentiation factor 5 (*GDF5*), are pertinent to this project and will be discussed in detail.

1.6 Indian Hedgehog

1.6.1 Hedgehog Proteins

Hedgehog signaling proteins are morphogens that contribute to a number of patterning events in vertebrate and invertebrate development. In higher vertebrates, there are 3 members of the hedgehog family: Sonic hedgehog (SHH), Indian hedgehog (IHH), and Desert hedgehog (DHH). Sonic hedgehog, the most extensively studied of the three members, has been implicated in the establishment of left-right asymmetry in both chicks and mice [42, 43], ventral patterning in the central nervous system [44] and antero-posterior patterning in the early limb [45]. Desert hedgehog has been shown to play a critical role in spermatogenesis [46]. Indian hedgehog is most well known for its role in mediating condensation, growth and differentiation of long bone cartilage templates [38]. It is also expressed in the gastrointestinal tract, the pancreas, and the uterus, where dysregulation of IHH can lead to malformations [47-49].

All of the secretory hedgehog proteins are subject to the same post-translational modifications. According to *Drosophila* hedgehog studies, the mature hedgehog mRNA codes for an approximately 45 kDa precursor protein (Figure 1.4A) [50, 51]. Along with the removal of the signal peptide, the precursor protein undergoes autocatalytic cleavage,

Figure 1.4. Cleavage and processing of the Indian hedgehog protein. *(A)* The mature hedgehog mRNA codes for an approximately 45 kDa precursor protein, which is composed of a signal peptide (27 amino acids), an N-terminal fragment (175 amino acids) responsible for all signaling functions, and a C-terminal fragment (209 amino acids) with no apparent function beyond catalysing the cleavage reaction. During hedgehog processing to the mature peptide, *(B)* the signal sequence is cleaved; *(C)* autocleavage of the mature N-terminal portion from the C-terminal portion is catalysed by residues in the C-terminal fragment; and *(D)* palmitate and cholesterol moieties are added to the N-terminus and C-terminus of the N-terminal fragment, respectively.

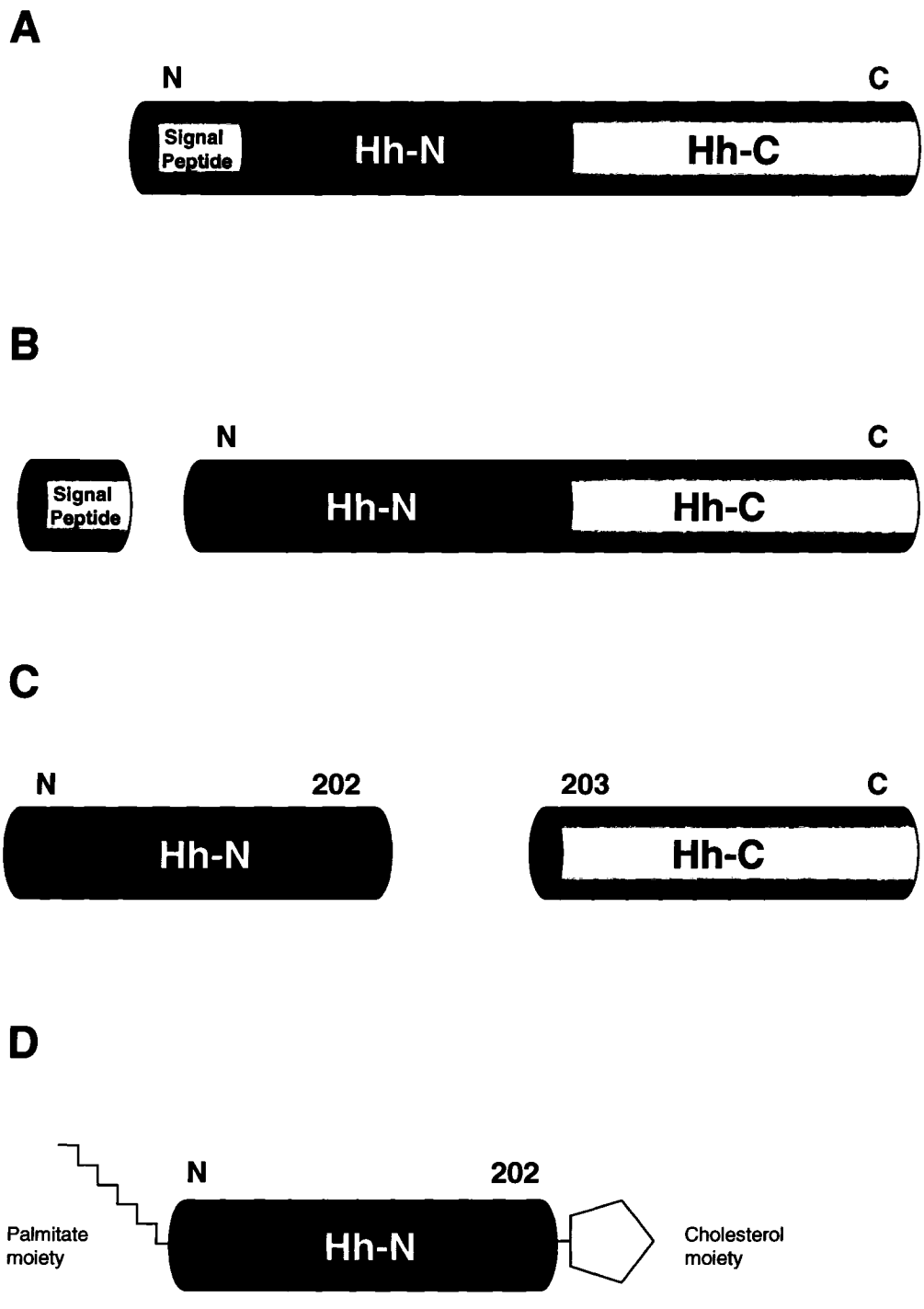
A
N
C
Signal Peptide
Hh-N
Hh-C
B
N
C
Signal Peptide
Hh-N
Hh-C
C
N
202
Hh-N
203
C
Hh-C
D
N
202
Palmitate moiety
Hh-N
Cholesterol moiety

yielding a 16-kDa N-terminal fragment and a 25 kDa C-terminal fragment (Figures 1.4B, 1.4C). While the 16-kDa N-terminal fragment is responsible for all signaling functions, the 25 kDa C-terminal fragment has no apparent function beyond catalyzing the cleavage reaction [50, 51]. Further investigations revealed that the His 275 residue is responsible for initiating cleavage between the Cys 202 and Gly 203 residues of the hedgehog precursor protein (Appendix I: Swiss-Prot UniProt Protein Knowledgebase). During cleavage, the N-terminal fragment is concomitantly modified by the covalent addition of a cholesterol moiety to its C-terminus (Figure 1.4D) [50, 52, 53]. A second reaction, catalyzed by yet-unconfirmed methods, adds a palmitate moiety to the N-terminus of the active N-terminal fragment (Figure 1.4D) [53]. The cholesterol moiety is critical for proper anchoring and transport of hedgehog through biological membranes, thereby regulating distribution of the hedgehog signal and ensuring the correct extracellular gradient [50, 52]. The palmitoylation is hypothesized to increase hydrophobicity of the mature hedgehog molecule, thereby increasing the potency of the hedgehog molecule and increasing its biological activity [50].

1.6.2 Hedgehog Signaling Pathway

Although all hedgehog (Hh) family members have distinct functions, all members employ a common conserved signal transduction pathway. Mature Hh proteins are released from secreting cells with the help of Dispatched (Disp), a transmembrane transporter [54]. Heparan sulfate proteoglycans (HSPGs) Dally and Dally-like (Dlp) are thought to affect the range and distribution of Hh after its release by acting as

transporters or co-receptors, although complete understanding of how this may be achieved is not clear [54].

Hedgehog initiates signaling activity upon binding to its receptor, the 12-transmembrane protein Patched (Ptch1) [55]. When Hh is absent, Ptch1 acts to indirectly inhibit the activity of Smoothened (Smo), a 7-transmembrane protein, possibly by the release of the small inhibitory molecule Vitamin D3 (Figure 1.4A) [55]. With Smo signaling inhibited, a complex comprised of Fused (Fu), Costal2 (Cos2), Suppressor of Fused (SUFU), and microtubules functions to sequester and cleave the transcription factor Glioma associated (Gli) to its repressor form [50, 55]. The repressor Gli then translocates to the nucleus where it suppresses the transcription of Hh target genes (Figure 1.5A) [50].

Conversely, binding of Hh to Ptch1 leads to the receptor's inactivation and internalization, alleviating its inhibition of Smo signaling (Figure 1.5B) [50]. Activated Smo signals through a yet-unknown mechanism to the Fu-Cos2-SUFU complex, preventing it from cleaving Gli to its repressor form (Figure 1.5B). This allows the full-length activated Gli to translocate to the nucleus and initiate transcription of the Hh-target genes (Figure 1.5B) [50].

Interestingly, Hh regulates its own signaling in a negative feedback loop. Ptch1 and Hedgehog Interacting Protein (HIP), a vertebrate membrane glycoprotein Hh inhibitor, are targets of Hh signaling [56]. Therefore, as more Hh is present to activate the cell signaling cascade, more Ptch1 and HIP are available to sequester Hh and diminish the signal [53, 56].

Figure 1.5. Schematic of the hedgehog (Hh) signaling pathway. *(A)* In the absence of Hh, the receptor Patched (Ptch1) acts to indirectly repress the activity of Smoothened (Smo), possibly by the release of Vitamin D3 (D3). With Smo signaling inhibited, a complex made up of Costal 2 (Cos2), Fused, Suppressor of Fused (SuFu), and microtubules is able to sequester the transcription factor Glioma Associated (Gli), cleaving it into a short, repressor form (GliR). GliR then translocates to the nucleus, where it prevents the transcription of Hh target genes. *(B)* Binding of Hh to its receptor Ptch1 causes the internalization of Hh and Ptch1. With the release of the inhibition of Smo signaling, Smo signals to the Cos2-Fused-SuFu-microtubules complex, causing it to loosen and the microtubules to dissociate. This allows the stable full-length Gli to translocate to the nucleus, where it initiates transcription of Hh target genes.

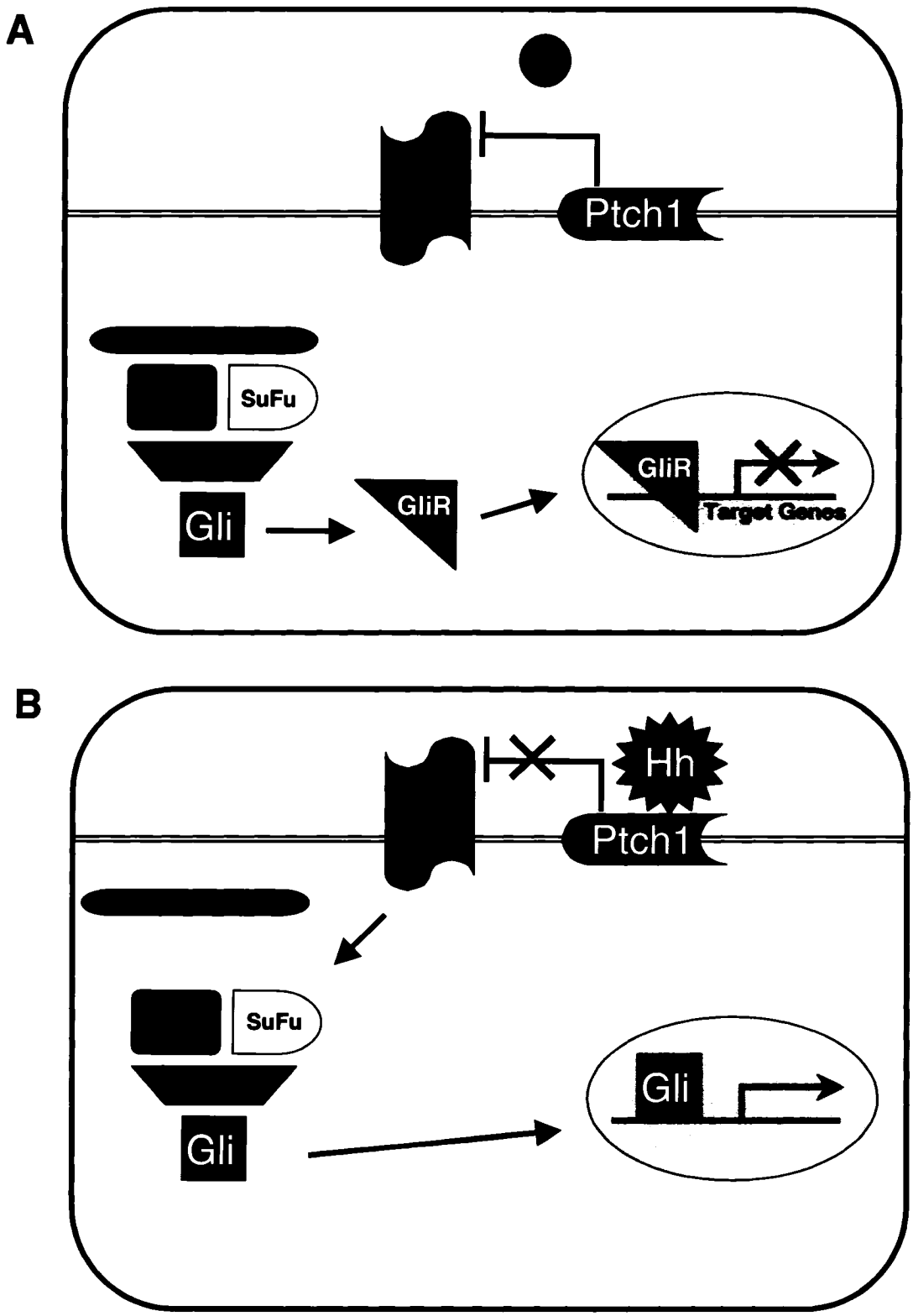
A
Ptch1
SuFu
Gli
GliR
GliR
Target Genes
B
Hh
Ptch1
SuFu
Gli
Gli

1.6.3 Role of Hedgehog Signaling in Bone Development

A chicken homologue of IHH was first isolated and characterized by Vortkamp et al in 1996 [38]. It was found to be expressed in pre-hypertrophic chondrocytes, suggesting an important role for IHH in cartilage differentiation [38]. Ectopic expression of Ihh in chick wings was found to up-regulate expression of Parathyroid Hormone-related Peptide (PTHrP) in the articular perichondrium. Chondrocyte differentiation to the hypertrophic stage was subsequently delayed, and this led to the generation of irregular-shaped bones which underwent an abnormal ossification process and lacked normal growth plates [38]. This phenotype was only observed when PTHrP signaling was intact, implying that PTHrP mediates the effect that Hh signaling has on chondrocyte differentiation [38]. It was hypothesized that Ihh and PTHrP participate in a negative feedback loop to control IHH expression and the site at which chondrocyte differentiation to hypertrophy occurs [38].

However, recent studies have indicated that while IHH is necessary for proper development of skeletal elements, not all of its functions are mediated through PTHrP [57, 58]. St-Jacques et al. (1999) described the multiple bone abnormalities observed in *Ihh*$^{-/-}$ mice, reinforcing a role for Ihh in limb development [41]. The mutant mice had small cartilage elements with reduced chondrocyte proliferation; an increase in delayed, abnormal chondrocyte differentiation to the pre-hypertrophic and hypertrophic stages; and a complete lack of osteoblast development in all bones that develop by endochondral ossification [41]. Karp et al. (2000) proceeded to compare the skeletal elements of *Ihh*$^{-/-}$ mutant mice and those of *Ihh*$^{-/-}$; *PTHrP*$^{-/-}$ double mutants and determined that their phenotypes were indistinguishable [58]. This evidence supports a model whereby Ihh is

necessary for PTHrP function in limb formation [58]. However, a similar comparison of *PTHrP*$^{-/-}$ mice and *Ihh*$^{-/-}$; *PTHrP*$^{-/-}$ double mutants showed drastic differences in the skeletal elements, with the double mutant being much more severely affected. This supports a role for IHH in limb development that is not mediated by PTHrP [58].

Many molecular investigations have elucidated the nature of IHH and PTHrP signaling in growing cartilage elements. PTHrP is secreted from the perichondral cells and proliferating chondrocytes at the distal ends of long bones (Figure 1.6). The receptor for PTHrP, Parathyroid Hormone/Parathyroid Hormone-related Peptide Receptor (PPR), is expressed at low levels in proliferating chondrocytes and at high levels in pre-hypertrophic chondrocytes [39]. PTHrP signals through PPR to keep chondrocytes in the proliferative pool. When the proliferative pool is sufficiently large, the PTHrP signal no longer reaches the distant cells; these chondrocytes then begin to differentiate to pre-hypertrophic chondrocytes and produce Ihh. By means of a yet-unidentified mechanism, Ihh induces the production of more PTHrP from the perichondral cells and chondrocytes at the distal ends of long bones (Figure 1.6). This encourages cells to remain in the proliferative pool and reduces the number of cells proceeding to the pre-hypertrophic stage, thereby decreasing the rate of Ihh production in a negative-feedback mechanism [39]. Ihh also signals through Ptch1 and Smo on neighbouring chondrocytes to increase the rate of proliferation independently of PTHrP (Figure 1.6) [39]. Furthermore, Ihh acts on perichondral cells adjacent to the pre-hypertrophic and hypertrophic zones to stimulate the formation of mature osteoblasts that make up the bone collar (Figure 1.6) [39, 57].

Figure 1.6. Schematic of IHH signaling in endochondral ossification. Adapted from Chung, U.I., et al., J. Clin. Invest., 2001. 107(3): p. 295-304 [57]. Cell types are as defined in Figure 1.1. Pre-hypertrophic chondrocytes express IHH. Through an unknown mechanism, IHH stimulates the production of PTHrP from the perichondral chondrocytes at the end of the skeletal element (A). The PTHrP signals to adjacent proliferating chondrocytes (B), encouraging them to remain in the proliferative pool, thus serving to enlarge the skeletal element. It also reduces the number of cells differentiating to the pre-hypertrophic stage, thus decreasing the amount of IHH expressed in a negative-feedback loop. Once the proliferating chondrocytes become sufficiently distant from the source of PTHrPl, they begin to differentiate into pre-hypertrophic cells, and again IHH is expressed. IHH can also act directly on neighbouring chondrocytes (C) to increase the rate of proliferation independently of PTHrP. IHH also acts to stimulate the formation of the bone collar (D).

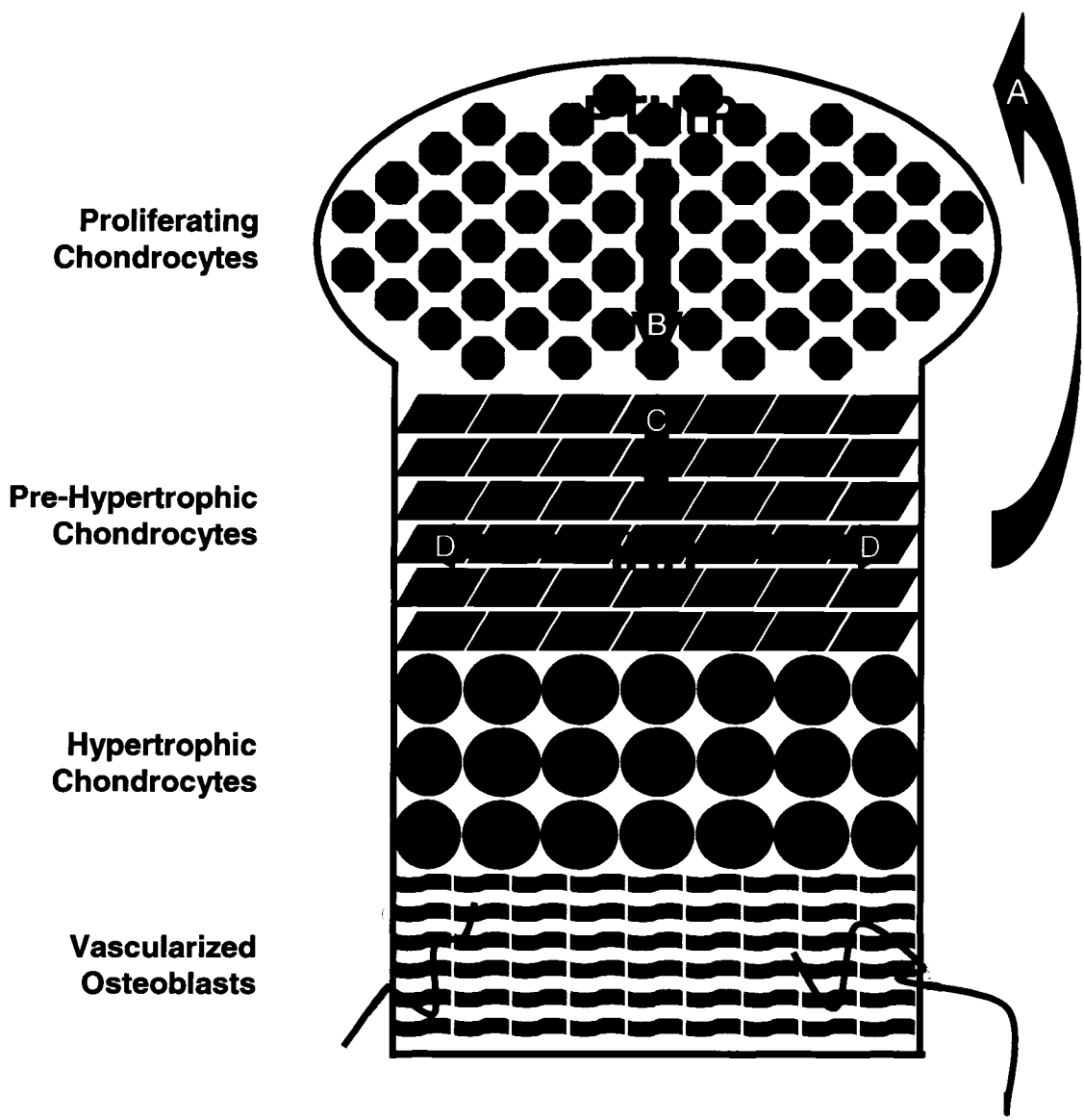
Proliferating Chondrocytes
Pre-Hypertrophic Chondrocytes
Hypertrophic Chondrocytes
Vascularized Osteoblasts
A
B
C
D
D

1.6.4 Human Mutations in Indian Hedgehog

BDA1 is the only disorder known to be caused by heterozygous mutations in *IHH*. However, homozygous mutations in *IHH* have been identified in 2 consanguineous families with Acrocapitofemoral Dysplasia (ACFD [MIM 607778]), so named due to its associated hand and hip abnormalities [59, 60]. ACFD is characterized clinically by brachydactyly, short stature, a narrow thorax and a large head. Radiologically, ACFD is associated with cone-shaped epiphyseal growth plates in the hands, the proximal part of the femur (hips), and sometimes the shoulders, knees and ankles. Premature fusion of the cone-shaped growth plates led to an egg-shaped femoral head and short femoral neck as well as short digits and limbs [59].

The pathogenicity of these *IHH* mutations is not yet known. It has been hypothesized that the mutations causing BDA1 and ACFD have diminished IHH signaling [16, 59]. This may have led to a decrease in cell proliferation, or an increase in the rate at which chondrocytes leave the proliferative pool to become differentiated, pre-hypertrophic chondrocytes. A decrease in these IHH-dependent processes may lead to premature closure of the growth plate and a shortened element. However, it remains to be determined why only certain bones and tissues are affected while others are spared.

Gao et al. (2001) used a model of the crystal structure of the highly-homologous N-terminal fragment of mouse Shh to establish that the BDA1-causing amino acids 95, 100, and 131 are all in very close proximity to one another on a groove in Shh [16]. They hypothesized that the mutations may alter IHH signaling, whereby the mutant IHH may have decreased ability to bind to its normal receptor Ptch1 or increased ability to bind to an alternate receptor [16]. Alternatively, BDA1 could be the result of

haploinsufficiency of IHH. However, *Ihh*$^{+/-}$ mice were not described as having any BDA1-like phenotype [41]. It is possible that mild digit abnormalities were missed, or that mice do not have the same dosage requirements for IHH as humans.

Hellemans *et al.* (2003) used the same mouse Shh model to determine that the ACFD-causing amino acids, 46 and 190, were not in close proximity with each other or the BDA1-causing amino acids 95, 100, and 131 [59]. The homozygous ACFD individuals do not show a phenotype nearly as severe as the *Ihh*$^{-/-}$ knock-out model. This could be attributable to the fact that the ACFD IHH mutants retain some of their function allowing some activity, or perhaps there is a redundant pathway present in humans that does not occur in mice [61].

Interestingly, although the heterozygous parents of two related ACFD patients did display a very mild BDA1-like phenotype, the heterozygous parents of the other ACFD individuals did not show any signs of BDA1 [59]. This indicates that the phenotypic outcome of IHH mutations depends not only on heterozygous or homozygous status, but also on the location and nature of the mutation [59].

1.7 Growth and Differentiation Factor 5

1.7.1 Growth and Differentiation Factors

The growth and differentiation factors (GDFs) belong to the bone morphogenetic protein (BMP) group of the transforming growth factor beta (TGF-β) superfamily of secreted growth, differentiation, and morphogenesis factors [62, 63]. Three members of the family, growth and differentiation factor 5 (GDF5), growth and differentiation factor

6 (GDF6), and growth and differentiation factor 7 (GDF7), were first discovered in mice by degenerate PCR due to their homology to other BMP family members [63]. With the exception of a glycine-rich insert in GDF7, the mature regions of GDF5, GDF6 and GDF7 share 80-86% identity, and are thought to have developed by gene duplication during evolution [63, 64]. These three proteins are highly conserved in vertebrates and are required for the normal formation of bones and joints in the limbs, skull and axial skeleton [63, 65].

All members of the BMP family are expressed as large precursor proteins which are subject to the same post-translational modifications. The mature GDF5 mRNA codes for an approximately 56-kDa precursor protein (Figure 1.7A) [66]. This precursor protein will eventually undergo cleavage by subtilisin-like proteases, yielding the 14-kDa C-terminal fragment responsible for all signaling functions and the N-terminal signal peptide and prodomain (Figures 1.7B, 1.7C) [66]. All highly conserved BMP family members share an Arg-X-X-Arg cleavage site and a 7-cysteine motif in the mature C-terminal region, both of which are critical for proper folding and dimerization of the mature molecule [62, 67, 68]. Following the production of the 56-kDa precursor protein, 6 of the conserved cysteines found in the mature region of the protein are involved in the formation of intra-chain disulfide bonds (Figure 1.7B); the seventh cysteine forms an inter-chain disulfide bond with another monomer, forming a homo- or hetero-dimer (Figure 1.7B) [62]. Subsequent cleavage of the prodomains by subtilisin-like proteases forms the mature, active dimer (Figures 1.7C, 1.7D, 1.8A, 1.8B) [69].

Figure 1.7. Cleavage and processing of the GDF5 protein. *(A)* The mature GDF5 mRNA codes for an approximately 56 kDa precursor protein, which is composed of a signal peptide (27 amino acids), a prodomain (354 amino acids), and the C-terminal signalling fragment (120 amino acids) responsible for all signaling functions. During GDF5 processing to the mature peptide, *(B)* a highly-conserved cysteine found in the mature signaling domain forms an inter-chain disulfide bond with another full-length monomer, forming a homo-dimer, and *(C)* subtilisin-like proteases catalyze the cleavage of the mature signaling domains from their associated prodomains. *(D)* Representation of the mature GDF5 dimer.

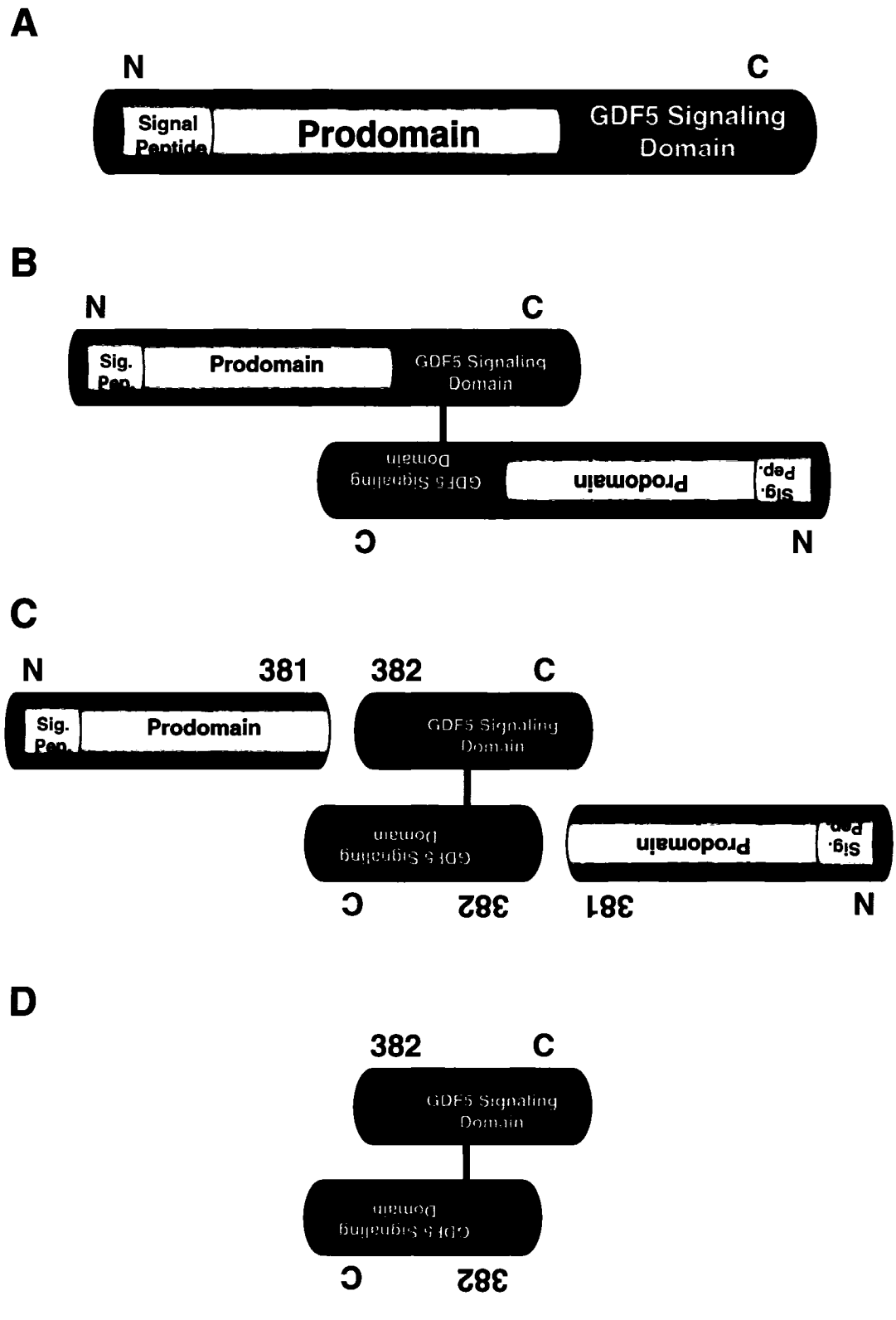
A
N
C
Signal Peptide
Prodomain
GDF5 Signaling Domain
B
N
C
Sig. Pep.
Prodomain
GDF5 Signaling Domain
C
N
C
N
381
382
C
Sig. Pep.
Prodomain
GDF5 Signaling Domain
C
382
381
N
D
382
C
GDF5 Signaling Domain
C
382

Figure 1.8. Schematic of a mature BMP dimer as a representation of a mature GDF5 dimer. *(A)* A mature GDF5 dimer with one monomer shown in green, the other in yellow. Blue-and-orange bars represent the 6 intra-chain disulfide bonds found in each monomer, and the sole inter-chain disulfide bond that maintains the two monomers in a dimer form. *(B)* Two bananas are used as an analogy to depict the shape of the two GDF5 monomers as they join to form a dimer. The A, B and C markers denote the receptor-binding sites for type I and type II receptors.

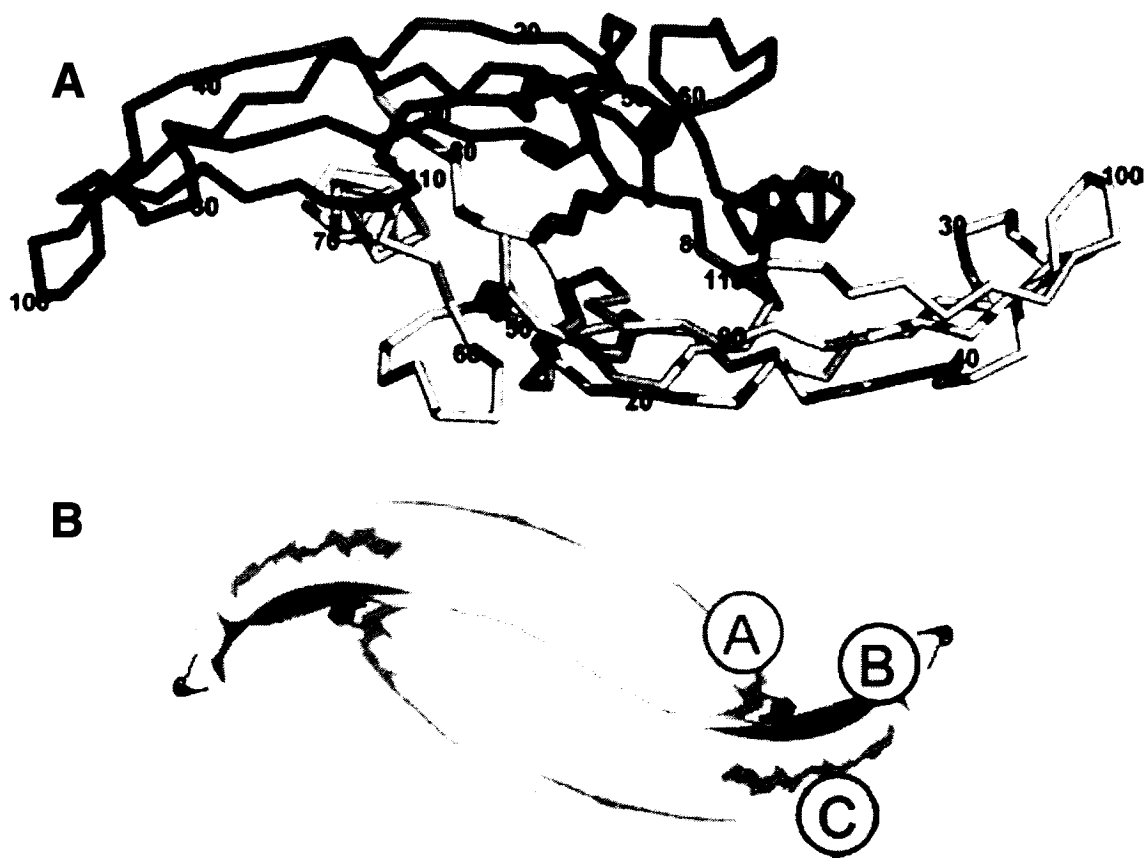

Reprinted from Biochemical and Biophysical Research Communications, 329, Schreuder H., Liesum A., Pohl J., Kruse M., Koyama M., Crystal structure of recombinant human growth and differentiation factor 5: Evidence for interation of the type I and type II receptor-binding sites, Pages 1076-1086, Copyright (2005), with permission from Elsevier.

1.7.2 Growth and Differentiation Factor Signaling Pathway

Although members of the TGF-β superfamily are known to engage in diverse functions, a simple signal transduction pathway is common to all ligands. In summary, the ligand assembles a receptor complex; this activates a family of receptor substrates, which then translocate to the nucleus and act as transcription factors to direct the expression of target genes [70].

BMPs signal through serine/threonine kinase receptors, of which there are type I and type II subtypes [71]. There are many type I and II receptors through which BMPs can bind and propagate a signal; however, GDF5 has been found to bind specifically with high-affinity to the receptor bone morphogenetic protein receptor IB (BMPRIB) [69, 72]. In order to generate a signal, GDF5 binds to BMPRIB, which is catalytically inactive (Figure 1.9A) [70, 72]. However, binding of the ligand to the type I receptor is thought to recruit type II receptors into the heterotetrameric-activated receptor complex, which stimulates the type I receptor to activate the downstream signalling molecules known as Smads (Figure 1.9A) [69-71]. Vertebrates have 8 different Smads, Smad1 to Smad8; some Smads have individual functions, while others are redundant. The activated BMPRIB phosphorylates Smad1, Smad5 and Smad8 at a C-terminal serine (Figure 1.9A) [69, 73]. These receptor-activated Smads (R-Smads) then form a complex with Smad4, and the entire Smad complex translocates to the nucleus where it will interact with transcription factors and the DNA directly to initiate transcription of the GDF5 target genes (Figure 1.9A) [71]. When GDF5 is absent, the receptors cannot activate downstream Smad signalling, and transcription of target genes cannot occur (Figure 1.9B).

Figure 1.9. Schematic of the GDF5 signaling pathway. *(A)* When GDF5 is present, it binds to the type I receptor BMPRIB (shown in blue), which is thought to recruit type II receptors (shown in pink) into the tetrameric complex. This activates BMPR1B, stimulating it to phosphorylate and subsequently activate the downstream signaling molecules Smad1, 5, or 8. The now receptor-activated Smad1, 5, or 8 then complex to Smad4, and the entire complex translocates to the nucleus, where it initiates transcription of GDF5 target genes. *(B)* In the absence of GDF5, the type I and type II receptors do not interact, and therefore are not able to activate the Smad signaling pathway. Transcription of GDF5 target genes cannot occur.

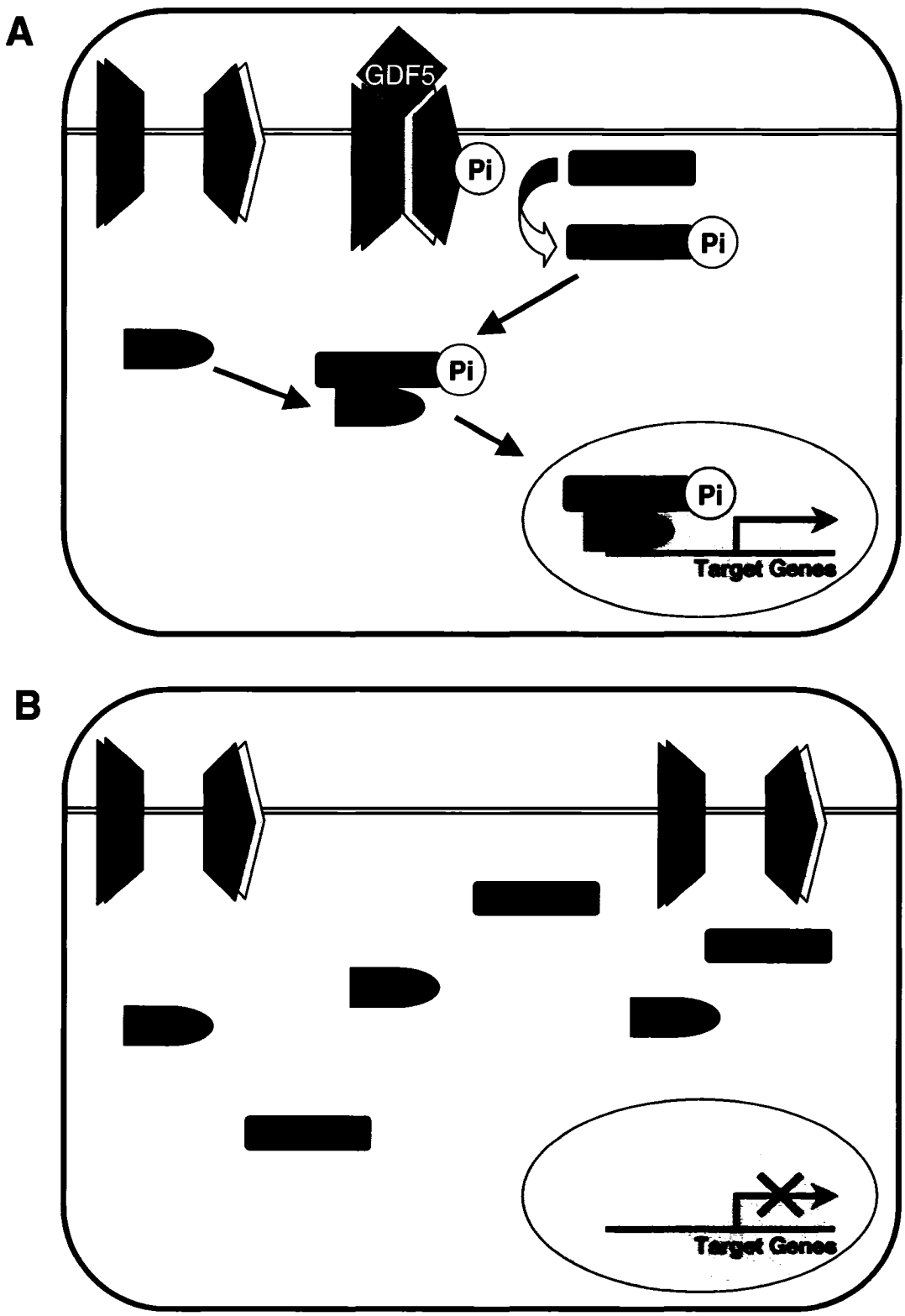
A
GDF5
Pi
Pi
Pi
Pi
Target Genes
B
Target Genes

This signaling pathway can be modulated at both inter- and intra-cellular levels [74]. Firstly, noggin and chordin, two BMP antagonists, could prevent GDF5 receptor binding [75]. Furthermore, expression of the inhibitory Smad6 and Smad7, which is highly regulated by extracellular BMP and TGF-β signals, represents an auto-inhibitory mechanism for signal transduction by down-regulating the R-Smads available to transduce BMP and TGF-β signaling [71, 73]. In addition, the ubiquitin ligases Smurf1 and Smurf2 antagonize BMP and TGF-β signaling by targeting R-Smads for degradation [73].

Recent evidence suggests that receptor tyrosine kinase-like orphan receptor (ROR2) has a role in GDF5 signaling [76]. ROR2 was found to modulate BMPRIB signaling, as the two form a heteromeric complex, with ROR2 capable of repressing Smad signaling. Crossing *Ror2*$^{+/-}$ mice with *BMPRIB*$^{+/-}$ mice and *bp* (*Gdf5*$^{bp\text{-}j}$) mice implied an epistatic effect between the receptors and the ligand, as inactivation of one or two Ror2 alleles in *Gdf5*$^{bp\text{-}j\text{-}}$ mice, and inactivation of one *GDF5* allele or 2 *BMPRIB* alleles in *Ror2*$^{-/-}$ mice led to a considerable reduction in bone length when compared to mutants lacking only one gene [76].

1.7.3 Role of Growth and Differentiation Factor 5 in Bone Development

GDF5 was first reported due to its association with the brachypodism (*bp*) mouse, which has a phenotype of shortened limbs, metacarpals, metatarsals, and absent middle phalanges. Sequencing of the *GDF5* gene in 3 independently-occurring strains of *bp* mice revealed that all 3 carried frameshift mutations representing functional null mutants [63]. The multiple bone abnormalities observed in these GDF5-deficient mice reinforces

a role for GDF5 in limb development. In fact, GDF5 is expressed at sites of cartilage differentiation in the developing limbs [63, 67]. Overexpression of GDF5 in the developing chick wing led to an increase in length and width of skeletal elements, as well as fused joints [77]. Moreover, *in vitro* micromass cultures suggest that GDF5 is important in determining the size of skeletal precursors by increasing mesenchymal cell adhesion and accelerating chondrogenesis in a dose-dependent manner [77]. This gene-dose sensitivity may account for the varying severity of diseases caused by mutations in *GDF5*.

GDF5 expression has also been observed in strong transverse stripes in the future joint space of skeletal precursors, which will eventually subdivide into individual skeletal elements [78, 79]. This expression pattern represents one of the earliest known markers of joint formation (Storm 1996). Interestingly, GDF5 appears to act solely as an inhibitor of BMP signaling in the joint space [75]. Thomas et al (2006) discovered that co-expression of GDF5 with 2 subtilisin-like proprotein convertases (SPCs), Furin and SPC6, is required for processing of GDF5 to mature, active dimmers in *Xenopus*. Co-expression of these 3 proteins does not occur in the joint space; rather, it occurs only at a narrow zone near the distal boundary of the joint space. Noggin and Chordin are expressed in the joint space and antagonize BMP signaling, which allows the joint to form [75, 80, 81]. It has been hypothesized that unprocessed GDF5 present in the joint space also acts as a BMP inhibitor by heterodimerizing with other BMPs and inhibiting their processing and secretion, allowing the joint to form [75].

Recent work has revealed that GDF5-deficient *bp* mice have abnormalities not only in cartilage and joint formation, but also in tendons, intervetebral disks, skin and

bones [74]. Additionally, tendon repair and fracture healing is delayed in these mice [74, 82]. These discoveries have led to increased interest in investigating a role for GDF5 and related molecules in therapeutic applications [74].

1.7.4 Human Mutations in Growth and Differentiation Factor 5

Following the identification of GDF5-null mutations in brachypodism mice, mutations in *GDF5* were found to be the cause of numerous skeletal limb deformities in humans including many chondrodysplasias, brachydactylies and symphalangisms.

Homozygous and compound heterozygous mutations in *GDF5* can cause severe chondrodysplasias such as DuPan syndrome (MIM 228900), Hunter-Thompson type (CHTT/AMDH [MIM 201250]), and Grebe type (CGT/AMDG [MIM 200700]), the most severe of the three disorders [66, 83-87]. DuPan syndrome is characterized by fibular hypoplasia (absent fibula) and complex brachydactyly. Both CHTT and CGT are characterized by a shortening of the bones of the limbs that progresses in a proximal to distal direction with the hands and feet being the most severely affected, much like *bp* mice [66, 84-87]. All three diseases have been described in consanguineous families. In a single case, a mother and daughter with three compound *GDF5* missence mutations on one allele have an autosomal dominant form of DuPan syndrome [88].

A considerable number of brachydactylies have been attributed to mutations in *GDF5*. Heterozygous and homozygous mutations in *GDF5* have been shown to cause both autosomal dominant and partially dominant brachydactyly type C (BDC) [28, 29, 89-93]. The hallmark features of BDC involve shortening of the middle phalanges of digits 2, 3, and 5 as well as shortening of the first metacarpal. Variable expression and

non-penetrance have been observed in many affected families [89, 90, 93]. Heterozygous mutations in *GDF5* were also found to be the cause of brachydactyly type A2 (BDA2), which is characterized by the shortening of the middle phalange in digit 2 only [24, 94]. Furthermore, the heterozygous *GDF5* mutation carriers in the CGT families reportedly exhibit a mild phenotype of brachydactyly types A1, A4, and C [66, 83, 86, 95]. Additionally, heterozygous mutations were identified in two families with angel-shaped phalangoepiphyseal dysplasia (ASPED [MIM 105835]) [92]. Examination of affected family members revealed a phenotype of angel-shaped middle phalanges, hip dysplasia, and teeth abnormalities [92].

Finally, heterozygous mutations in *GDF5* can also cause multiple synostoses syndromes (SYNS1 [MIM 186500] and SYNS2 [MIM 610017]), proximal symphalangism (SYM1 [MIM 185800]), and congenital vertical talus (CVT[MIM 0192950]) [89, 93, 94, 96, 97]. SYM1 and SYNS disorders share a phenotype of a variety of symphalangisms (abnormal union of finger or toe bones) and carpal-tarsal fusions (abnormal union of bones in the wrists or feet). Congenital vertical talus is characterized by the dislocation of the navicular bone with the talus, giving the appearance of a rocker-bottom rigid flatfoot [89].

The pathogenicity of these *GDF5* mutations in humans has been speculated in many instances, but many mechanisms cannot be confirmed. Haploinsufficiency, null mutants, and dominant-negative mutations, in which mutated GDF5 is thought to hinder signaling of other BMP family members, are all hypothesized to lead to this large variety of bone-shortening phenotypes. A decrease in any GDF5-dependent processes may lead to a reduction in the size of the cartilage template on which the bone forms, leading to

the chondrodysplasia and brachydactyly-like phenotypes. Conversely, mutations causing a gain-of-function and aberrant GDF5 signaling are thought to cause the symphalangism phenotypes.

In both cases, non-penetrance and variable expression of the phenotype within and between families implicates a role of genetic and environmental modifiers in the development of the deformities. Furthermore, this shows that the phenotypic outcome of *GDF5* mutations depends on both the heterozygous or homozygous status of the mutation, as well as the specific location and nature of the mutation. It also remains to be determined why only certain bones and tissues are affected in certain individuals, while others are spared.

Chapter 2. Project Goals

2.1 Rationale

We are studying the genetic basis of brachydactyly type A1 in hopes of identifying new genes which, when mutated, can cause BDA1. Although BDA1 is a congenital genetic disease whereby the phenotype develops prior to birth and in itself cannot be cured, investigating the genetic aetiology of BDA1 could lead to the elucidation of novel members of the bone development pathway. There is a need to define these molecular pathways in order to identify novel targets for therapeutic treatments of degenerating bone diseases such as arthritis and osteoporosis.

2.2 Hypothesis

Based on previous reports, we hypothesize that BDA1 is a genetically heterogeneous disorder. Although a subset of our families may have mutations in the Indian hedgehog gene or the chromosome 5 critical region, we hypothesize that there is at least 1, if not more, other genes involved in limb patterning and bone development that, when mutated, can lead to BDA1 pathogenesis.

2.3 Specific Project Objectives

1. To identify novel mutations in the Indian hedgehog gene in individuals with BDA1
2. To identify additional genes that are mutated in individuals with BDA1
    a. To screen a region on chromosome 20 around marker D20S870 which may be linked to BDA1 in some families
    b. To identify and screen any candidate genes in this region for BDA1-causing mutations in some families

Chapter 3. Evaluation of the Indian Hedgehog Gene on Chromosome 2 by Sequence Analysis in Four BDA1 Families

3.1 Introduction

3.1.1 IHH and Skeletal Development

Brachydactyly type A1 has been extensively described over the years, dating back to Farabee's PhD thesis in 1903. While BDA1 can occur as an isolated malformation [17, 18, 20, 23, 32-35, 98-100], it has also been described as part of complex syndromes. Some of the most commonly reported associated disorders include nystagmus [8, 9], developmental delay, mental retardation [8-10], scoliosis [8, 12, 13], and club feet [13]. However, investigations disclosing the molecular foundations of BDA1 were not reported until recently.

Previously, Mastrobattista et al. (1995) used linkage analysis to exclude the candidate genes *HOXD*, *MSX1*, *MSX2*, *FGF1* and *FGF2* in at least one family with BDA1 [99]. In 2000, linkage to chromosome 2q35-36 was described in two Chinese families with BDA1 [17]. Subsequently, heterozygous mutations within the Indian hedgehog (*IHH*) gene were identified in 3 families [16]. The missense mutations co-segregated with affected status in three families and caused p.E95K, p.D100E, or p.E131K amino acid changes. The crystal structure of the highly similar mouse sonic hedgehog (Shh) protein was used to predict that these highly conserved residues were all in close proximity with one another on the receptor-binding site of IHH. It was surmised that the amino acid changes may affect hedgehog receptor binding, and that BDA1

pathogenesis may result from haploinsufficiency of the wild-type protein [16]. To date, additional heterozygous p.E95G, p.D100N, and p.T154I IHH amino acid changes have also been associated with BDA1 [18-22]. Multiple mutations in codons 95 and 100 indicate that these codons may be hot spots for mutations; moreover, they may have a particularly important role in IHH signalling. The protein product of *IHH* is critical for mediating condensation, growth and differentiation of long bone cartilage templates [38]. Furthermore, analysis of an $Ihh^{-/-}$ murine model showed that loss of Ihh lead to uncalcified, severely shortened forelimbs with incomplete joint formation [41]. Homozygous mutations in human *IHH* were found to cause a skeletal dysplasia called ACFD, in which short stature, BDA1, and cone-shaped epiphyses of the hands and hips are the main features.

Following these discoveries, a second locus for BDA1 was described at chromosome 5p13.3-p13.2 in a single family, implying locus heterogeneity [23]. Furthermore, both the *IHH* gene and the chromosome 5p13.3-p13.2 region were excluded in at least one other family, implicating a third locus in the development of BDA1 [19]. It is possible that mutations in other genes involved with the IHH signaling pathway may be responsible for the BDA1 phenotype in some families. To investigate whether heterozygous *IHH* mutations are the cause of BDA1 in four families, *IHH* was evaluated as a candidate gene.

3.1.2 Noggin and Skeletal Development

Noggin is a secreted protein which acts to antagonize members of the bone morphogenetic protein (BMP) family. It is expressed in condensing cartilage, and

Noggin-null mice show a phenotype of excessive cartilage growth and failed joint formation. When not antagonized by noggin, BMP signaling is hypothesized to lead to an increase in cartilage size. Additionally, chondrocytes do not respond to joint-inducing positional cues [80]. Heterozygous mutations in the human *Noggin* gene are known to cause disorders in which the primary features involve joint fusions. Missense and nonsense mutations have been found to cause multiple synostoses syndrome, proximal symphalangism, and carpal-tarsal coalition syndrome, all of which share a phenotype of a variety of symphalangisms (abnormal union of finger or toe bones) and carpal-tarsal fusions (abnormal union of bones in the wrists or feet) [97, 101-104]. They can also cause stapes ankylosis syndrome, which causes conductive hearing loss with or without symphalangism [105]. Here we report one family with a phenotype of BDA1 as well as tarsal fusions, and so both *IHH* and *Noggin* were evaluated as candidate genes in this family.

3.2 Material and Methods

3.2.1 Family and Sample Collection

We studied 4 families affected with BDA1. In all cases, the disease was reportedly passed on in an autosomal dominant fashion from an affected parent. Individuals with BDA1 and their family members were recruited by our collaborators at Stanford University Medical Center in Stanford, California; The University of Hong Kong's Queen Mary Hospital in Hong Kong; and Tel Aviv Sourasky Medical Center in Tel Aviv, Israel. Diagnosis was based on physical examination, radiographic findings

when available, and family history. The study was approved by the Children's Hospital of Eastern Ontario Ethics Review Committee. After receiving informed consent, genomic DNA was extracted from peripheral venous blood or saliva samples with a QIAamp DNA blood mini-kit (Qiagen, Valencia, California) or an Oragene DNA self-collection kit (DNA Genotek, Ottawa, Ontario).

3.2.2 Primer Design

Primers IHHx1, IHHx2, and IHHx3.2 were designed previously (McCready et al, 2002). All other PCR and sequencing primers were designed using the Primer3 online software (Appendix I) or DS Gene software (Accelrys, San Diego, California). All primers were synthesized by Sigma Genosys (Sigma-Aldrich Canada, Oakville, Ontario). Concentrated primer stocks were resuspended in 10 mM Tris-HCl pH 8.0, 0.1mM EDTA, and diluted in ddH_2O to a 17 μM working solution.

3.2.3 Sequence Analysis

IHH

All 3 exons, including flanking splice sites and untranslated regions, were amplified by PCR in one affected individual from each family (arrows, Figure 3.1). Primers pairs were optimized for ideal $MgCl_2$ concentration and annealing temperature prior to amplification (Table 3.1). Each reaction was performed at 25 μl volumes containing 100 ng of genomic DNA, 1.5 mM $MgCl_2$, 10 mM Tris-HCl (pH 8.3), 50mM KCl, 0.2 mM dNTP, 10 μM primers, and 1 Unit *Taq* enzyme. All PCRs were performed on a PTC-225 thermal cycler (MJ Research, Waltham, MA) or an MBS Satellite 0.2G

Figure 3.1. Pedigrees of four families with BDA1 – families 20, 21, 22, and 23. The trait is transmitted in an autosomal dominant fashion in all families. Squares – males. Circles – females. Diamonds – sex unknown. Arrows denote the proband. Numbers represent the sample number assigned to the DNA of individuals who were available to participate in this study.

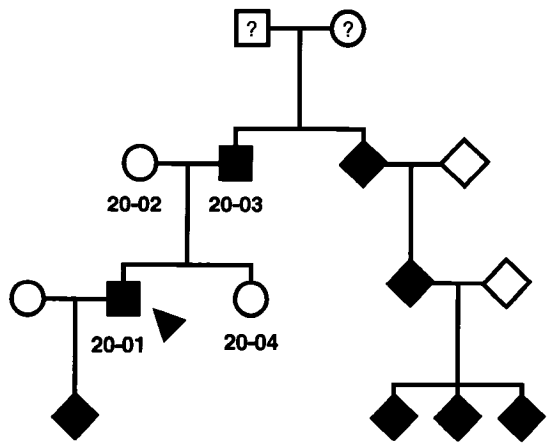

Family 20

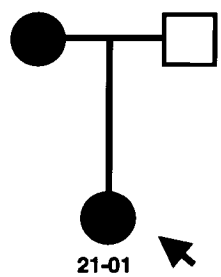

Family 21

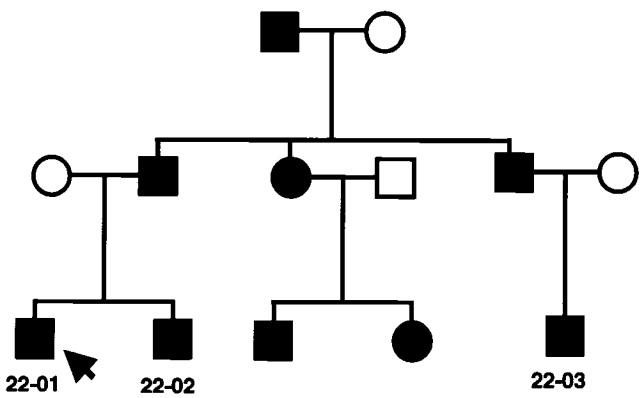

Family 22

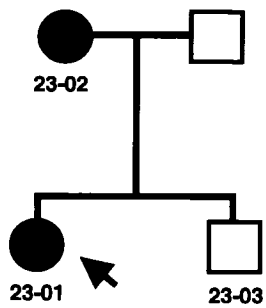

Family 23

Table 3.1. Sequence of primers and conditions used to amplify and sequence the *IHH* gene. Parameters of the amplification programs are described in Appendix II.

IHH Exon	Primer Name	Primer Sequence	Primer Annealing Temperature	Final [$MgCl_2$] (mM)	Additive	PCR Product Size
Upstream of exon 1	IHHsnp12-F	CGCACAGGGAGGAAAGG	60	1.5	---	237 bp
	IHHsnp12-R	GCAGGAGTGTCGGCATC				
1	IHHx1F	TGCCCATCAGCCCACCAG	62	1.5	Betaine	470 bp
	IHHx1R	GAGCGTGCCAGCCAGTCG	(40 cycles)			
2	IHHx2F	CGGCTGATTTCGCTCTG	63	1.5	---	394 bp
	IHHx2R	GGCGGGCTCTTCACCTT				
3	IHHx3.1F	AAGGGAGGGTCGTTGTG	65	1.5	---	494 bp
	IHHx3.1R	TTGTGAGCGGGGCGTAG				
3	IHHx3.2F	TGCTCTTTACGGCTGACAATC	64	1.5	---	531 bp
	IHHx3.2R	CAGAGGAGATGGCAGGAG				
3	IHHx3.3F	TGGGGCGTCTCCTGCTA	58	1.5	---	491 bp
	IHHx3.3R	GCATCGGGTCCAGCCAGA				
3	IHHx3.10F	GTATGGGTTCAAGCCTGCAT	50	1.5	---	569bp
	IHHx3.10R	GCCACGTGTGTAGAGACAGC	(Touchdown)			

thermal cycler (Thermo Electron Corporation, Milford, MA). To degrade unincorporated primers and nucleotides post-amplification, the PCR products were treated with ExoSAP-IT™ (Exonuclease I and shrimp alkaline phosphatase; USB, Cleveland, Ohio) according to manufacturer's suggested protocol. Sequencing was performed in both directions with the BigDye™ v3.1 terminator cycle sequencing kit (Applied Biosystems, Foster City, California) according to the manufacturer's suggested protocol. Sequencing products were evaluated on an Applied Biosystems 3130x1 genetic analyzer.

Noggin

The single-exon gene *Noggin* was amplified and sequenced as described above in the proband of family 20 only. Primers and optimized conditions are described in Table 3.2.

3.2.4 Restriction Digest

IHH exon 2 with *Pst*I

To detect the presence of a c.383G>A nucleotide change in the *IHH* gene of members of family 20, exon 2 was first amplified by PCR in DNA samples 20-01, 20-02, 20-03 and 20-04. Restriction digest was performed in 20 μl volumes, containing 5 μl PCR product, 2.0 μl of 10X Amersham Buffer H, 0.2 μl of the *Pst*I enzyme, and 12.8 μl ddH_2O. Reactions were incubated on a PTC-225 thermal cycler (MJ Research, Waltham, MA) at 37°C for 2 hours. Products were loaded on to a 1.5% agarose gel containing ethidium bromide, electrophoresed for 40 minutes at 100V, and photographed

Table 3.2. Sequence of primers and conditions used to amplify and sequence the *Noggin* gene. Parameters of the amplification programs are described in Appendix II. Primers denoted with an asterix were used for sequencing purposes only.

Noggin Exon	Primer Name	Primer Sequence	Primer Annealing Temperature	Final [$MgCl_2$] (mM)	Additive	PCR Product Size
5'UTR, Exon 1	Nog F2	ACCTCATCGAACACCCAGAC	60	1.5	---	572bp
	Nog R1.2e	CCGAGTTCTAGCACGAGCA				
Exon 1, 3'UTR	Nog CDS F	GCCAACTTGTGTGCCTTTCT	55	1.5	6% DMSO	999 bp
	Nog CDS R	GAGCGTGCCAGCCAGTCG				
	Nog R1*	AGCCCTCGGAGAACTCTAGC				
	Nog F2*	ACCTCATCGAACACCCAGAC				

under UV light. This procedure was repeated with 200 control DNA samples.

IHH exon 2 with *BstE*II

To detect the presence of a c.389C>A nucleotide change in the *IHH* gene of family 22, exon 2 was amplified by PCR in DNA samples 22-01, 22-02, 22-03 and 200 control DNA samples. Restriction digest was performed in 20 μl volumes, containing 5.0 μl PCR product, 2.0 μl of 10X NEB buffer #3, 2.0 μl of BSA, 0.2 μl of the *BstE*II enzyme and 10.8 μl ddH_2O. Reactions were incubated at 60°C for 2 hours. Products were loaded on to a 1.5% agarose gel containing ethidium bromide, electrophoresed for 40 minutes at 100V, and photographed under UV light.

3.3 Results

3.3.1 Phenotype of BDA1 Families

Individuals from 4 families of diverse ethnic and regional backgrounds were examined at this locus. While sporadic cases of BDA1 have been reported, all of the families presented here show an autosomal dominant pattern of inheritance. In family 21, variable expression of the phenotype is observed as the proband's mother only has affected foot bones. Syndromic forms of BDA1 have also been described in conjunction with other features, but this is not the case in these families. Consequently, all of the families described here share the general diagnosis of autosomal dominant familial BDA1. Clinical features of each patient have been summarized in Table 3.3.

Table 3.3. Clinical features of affected individuals 20-01, 21-01, 21-02, 22-01 and 23-01. A "-" indicates the information was not made available for this study.

Patient	20-01	21-01	21-02	22-01	23-01
Phalanges, metacarpals, metatarsals	Hands/feet: Short middle phalanges and proximal phalange of digit 1	Hands/feet: Short middle phalanges and proximal phalange of digit 1	Toes only: short 4,5 metatarsals; absent middle phalanges	Hands/feet: Short middle phalanges and proximal phalange of digit 1	Hands/feet: Short middle phalanges and proximal phalange of digit 1
Terminal Symphalangism	Digit 2, right hand only	-	-	Possibly in digits 2 and 5	All digits 2-5
Carpal/Tarsal bones	Tarsal coalition Limited dorsiflexion	-	-	-	-
Stature	Short arms Normal stature – 5'10"	Short	-	Short	Short
Other features reported in affected family members	Palate problems in a 2nd cousin	Treated for unrelated conditions	-	None	None

Family 20

We studied 4 members of an American family with BDA1 segregating in at least 4 generations. This family's ancestors are of German, Scottish and Irish descent, with most of the United States migrants settling in the southern states. The family was ascertained when an ultrasound revealed that a third-trimester fetus had short limbs. The family was referred to Stanford University Medical Center where our proband (individual 20-01 in Figure 3.1), the 43-year-old father of the fetus, was diagnosed with BDA1 on the basis of clinical and radiographic evaluations (Figure 3.2). The middle phalanges were very short, especially those in digits 2 and 5. The proximal phalange of digit 1 was also quite short. The proband had short arms, but normal stature at 5'10" (175 cm) tall. Other phenotypic findings included limitation of dorsiflexion of his feet (limitations in turning the feet upward) and tarsal coalition (abnormal fusion of tarsal bones in the feet). The proband's father (individual 20-02 in Figure 3.1) and the father's sibling were reported to have BDA1. The father's sibling had an affected child, who in turn had 3 affected children. The sex of any of these family members is not known. One of the children was reported to have a "problem with the palate" that did not require repair. No further abnormalities were described in the family.

Family 21

We studied 3 members of an American family in which the proband was affected with BDA1, and the mother displayed a milder phenotype. The family was referred to Stanford University Medical Center, where the 6-year-old female proband (individual 21-01 in Figure 3.1) was diagnosed with BDA1 based on clinical and radiographic

Figure 3.2. Hand radiographs of the proband of family 20. Radiographs are of the a) right and b) left hands of individual 20-01. The middle phalanges are very short, especially in digits 2 and 5. Fusion between the middle and distal is noted in digit 2 of the right hand. The proximal phalanges of both thumbs are also quite short.

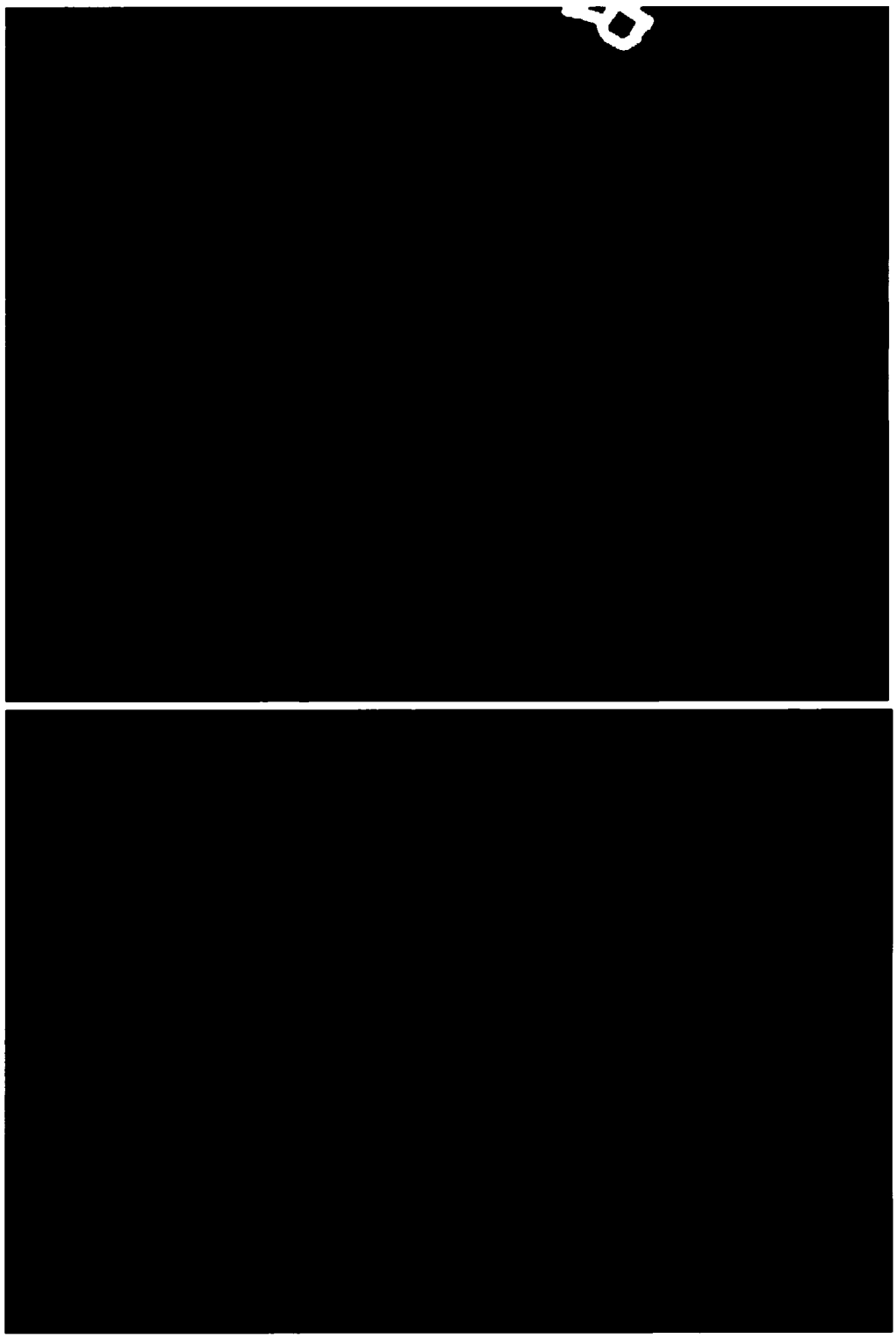

evaluations. The proband also had short stature, and had reportedly been treated for unrelated conditions. The proband's mother (individual 21-02 in Figure 3.1) had short fourth and fifth metatarsals with absent phalanges involving only the toes. Although the mother lacks involvement of the hand bones in her diagnosis, a phenotype similar to BDA1 in her feet implies that a mutation causing BDA1 in the little girl may have been inherited in a dominant fashion from the mother. Variable expression of the phenotype between family members could be accounted for by genetic or environmental modifiers [106].

Family 22

We studied 3 members of a family of Indian descent with BDA1 segregating in at least 3 generations. The proband (individual 22-01 in figure 3.1) was referred to The University of Hong Kong's Queen Mary Hospital, where he was diagnosed with type A1 brachydactyly based on clinical evaluations. Radiographs were not available. The middle phalanges were very short, and likely missing or fused to the terminal phalange in digits 2 and 5. Photographs of the proband's flexed hands indicated that there was only one interdigital joint in digits 2 and 5. Interestingly, all of the proband's blood relatives on his father's side are reported to have BDA1. We have obtained DNA from the brother and a cousin (individuals 22-02 and 22-03 in Figure 3.1) of the proband. To our knowledge, there were no other developmental problems in the family.

Family 23

We studied 3 members of an Ashkenazi Jewish family from Israel with BDA1 reportedly segregating in at least 4 generations. The family was ascertained when the 34-year-old female proband (individual 23-01 in Figure 3.1) was referred to the Tel Aviv Sourasky Medical Center in Tel Aviv, Israel for preimplantation genetic diagnosis of BDA1 prior to undergoing *in vitro* fertilization. The proband was diagnosed with BDA1 based on clinical and radiological findings (Figure 3.3). The middle and distal phalanges were replaced with a single small chess-pawn shaped bone in digits 2-5, and she had very short proximal and distal phalanges in digit 1. Her mother was also affected with the disorder. No further abnormalities were described in this family.

3.3.2 Evaluation of the *Noggin* Gene by DNA Sequencing in Family 20

In family 20, the *Noggin* gene was evaluated by DNA sequencing of the single exon and flanking splice sites in the proband (individual 20-01, Figure 3.1). No polymorphisms or sequence variants were present in the proband's DNA sequence.

3.3.3 Evaluation of the *IHH* Gene by DNA Sequencing in Four Families

Four families (20, 21, 22, 23) were evaluated for *IHH* mutations by DNA sequencing of the three exons, flanking splice sites, and associated untranslated regions in the proband of each family (Figure 3.1, arrows). Three exonic polymorphisms were detected in the sequence, all of which were present in the NCBI single nucleotide polymorphism (SNP) database (Appendix I) or the Ensembl Genome Browser Transcript Report (Appendix I). All of these polymorphisms were silent, coding for synonymous

Figure 3.3. Hand radiographs of the proband of family 23. Radiographs are of the hands of individual 23-01. The middle and distal phalanges of digits 2 through 5 were replaced by a small chess-pawn shaped bone in every case. The proximal phalanges of both thumbs are also very short.

amino acids and not creating any splice sites (Table 3.4). Frequencies of SNP alleles observed in our diverse probands will not be discussed, as historical isolation of different ethnic groups has led to wide-ranging allele frequencies [106].

A heterozygous c.383G>A nucleotide change, which creates a *Pst*I restriction site, was present in the DNA of individual 20-01 (Figure 3.4A). To determine if this change co-segregated with affected status in this family, we screened the DNA of all four available family members by restriction digest with *Pst*I. Analysis showed that both affected individuals carried the c.383G>A change. Neither of the unaffected family members carried the nucleotide change. In order to determine if this change was simply a rare polymorphism, the DNA of 200 control individuals was amplified and digested with *Pst*I. The c.383G>A nucleotide change was not seen in any of the 400 control chromosomes evaluated.

A heterozygous c.389C>A nucleotide change was present in the DNA of individual 22-01 (Figure 3.4B). To determine if this change co-segregated with affected status in this family, we screened the DNA of all 3 available family members by restriction digest with *BstE*II. Analysis showed that all affected individuals carried the c.389C>A change. To exclude the possibility that the change is a rare polymorphism, DNA of 200 control individuals was amplified and digested with *BstE*II. The c.389C>A nucleotide change was not seen in any of the 400 control chromosomes evaluated.

A heterozygous c.391G>A nucleotide change was present in the DNA of 23-01 (Figure 3.4C). To determine if this change co-segregated with affected status in this family, we screened all three available family members by sequence analysis. The results demonstrated that both affected individuals carried the nucleotide change, while

Table 3.4. List of nucleotide and amino acid changes seen in the *IHH* gene of individuals 20-01, 20-02, 20-02, 21-01, 22-01, and 23-01.

IHH exon	Nucleotide change	Position of nucleotide change	SNP status	Codon change	Amino acid or splice site change	Genotypes observed
Exon 2	G>A	c. 383	--	CGG>CAG	Arg128Gln	G/A, G/G
Exon 2	C>A	c. 389	--	ACC>AAC	Thr130Asn	C/A, C/C
Exon 2	G>A	c. 391	Reported as disease-causing in another BDA1 family	GAG>AAG	Glu131Lys	G/A, G/G
Exon 3	G>A	c. 600	rs3731878	ACG>ACA	Syn	G/A, G/G
Exon 3	T>C	c. 753	rs3731881	CCT>CCC	Syn	T/C, T/T
Exon 3	T>C	c. 1128	rs394452	ACT>ACC	Syn	T/T, T/C, C/C

Figure 3.4. Chromatograms showing the heterozygous *IHH* mutations found in affected members of families 20, 22, and 23. (*A*) Heterozygous c.383G>A nucleotide change (arrow) predicted to lead to the amino acid substitution R128Q in members of family 20. (*B*) Heterozygous c.389C>A nucleotide change (arrow) predicted to lead to the amino acid substitution T130N in members of family 22. (*C*) Heterozygous c.391G>A nucleotide change (arrow) predicted to lead to the amino acid substitution E131K in members of family 23.

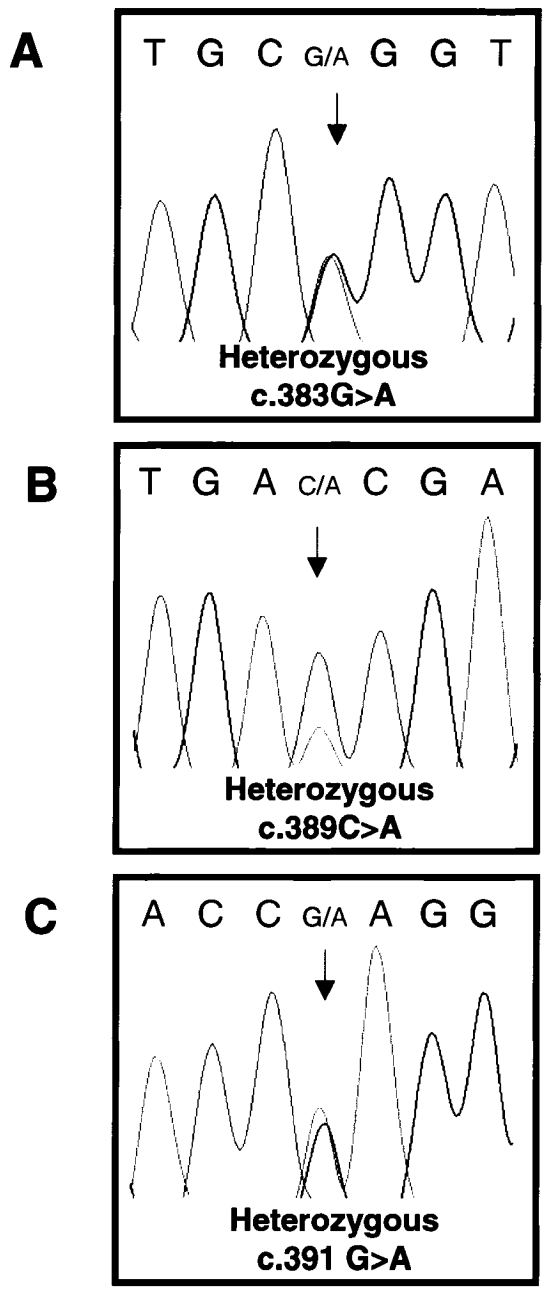
A
T G C G/A G G T
Heterozygous
c.383G>A
B
T G A C/A C G A
Heterozygous
c.389C>A
C
A C C G/A A G G
Heterozygous
c.391 G>A

the unaffected family member did not. As this nucleotide change has already been reported to cause BDA1 in another family, we did not screen control individuals for the change.

In summary, we have identified heterozygous nucleotide changes in affected individuals in three families. In the remaining family, we have excluded mutations in the transcribed region and flanking sequences of *IHH* as the cause of BDA1.

3.4 Discussion

To date, the occurrence of Brachydactyly type A1 in the population has not been reported, though it is thought to be fairly rare. Reports of BDA1 in families of many different ethnic backgrounds have been published since the first report by Farabee in 1903. Recently, Gao et al. (2001) discovered that heterozygous mutations in the Indian hedgehog gene cause autosomal dominant Brachydactyly type A1[16]. We have investigated the possibility that heterozygous mutations in *IHH* are causing BDA1 in four of our families. These families all share a diagnosis of BDA1 with features including short or absent middle phalanges in digits 2-5 and a short proximal phalange in digit 1. BDA1 is thought to be transmitted as an autosomal dominant disorder in each family, as every proband has one affected parent. Although most cases of BDA1 are autosomal dominant conditions, Tsukahara et al. (1989) reported a case where autosomal recessive inheritance was suspected [9]. They described a young girl affected with a combination of BDA1, dwarfism, ptosis, ocular anomalies, mixed partial hearing loss, microcephaly and mental retardation who was born to unaffected, consanguineous parents. Furthermore, homozygous mutations in *IHH* have been found to cause the

recessive disorder Acrocapitofemoral Dysplasia (ACFD), in which BDA1 and short stature are main features of the disorder [59].

3.4.1 Phenotypic Heterogeneity

In spite of the common diagnosis of BDA1, families described worldwide show considerable inter- and intra-familial heterogeneity. In the families examined here, detailed clinical descriptions of affected family members were not made available. However, clinical descriptions of our 4 probands do support a great deal of inter-familial heterogeneity. In BDA1, reports of distal symphalangism have occurred in some families. In this study, we found varying severity of phenotypes: individual 20-01 had distal symphalangism in one digit only, individual 22-01 had distal symphalangism in digits 2 and 5 of both hands, and individual 23-01 had distal symphalangism in all digits 2-5 of both hands. Furthermore, individual 20-01 had a complex BDA1 phenotype that included short arms, tall stature, tarsal coalition and limitations to dorsiflexion, none of which were described in the other 3 families. Tall stature in a BDA1 family has been described by Sillence et al. (1978) [13]. However, this family had a more severe form of BDA1 with distal symphalangism, scoliosis, and club foot. Short arms has never been described as a marked feature in most BDA1 families, but arm measurements given in Drinkwater's 1915 paper indicate that the forearms of many affected individuals in those families were slightly shorter than their unaffected family members. Mesomelic shortening of the limbs has also been described in a family with Osebold-Remondini Syndrome, also referred to as Brachydactyly type A6 (MIM 112910) [6]. Affected

individuals in this family also had small or absent middle phalanges, radial deviation of index fingers, and abnormal carpal and tarsal bones.

3.4.2 Molecular Findings

The recent identification of heterozygous mutations in the *IHH* gene of 3 Chinese families with BDA1 [16] drew attention to investigating the genetic cause of BDA1 in many other families. To date, 6 different heterozygous mutations in just 4 codons have been found in the *IHH* gene of BDA1-affected families [16, 18-22]. In this study, we report 2 novel and one previously described *IHH* mutations in 3 of the 4 families examined here.

We have identified a heterozygous c.383G>A mutation in family 20, an American family. The mutation co-segregated with affected status in the family, and was not seen in 400 control chromosomes evaluated. This nucleotide change caused an arginine to glutamine amino acid substitution at position 128. We also identified a heterozygous c.389C>A mutation in family 22, a family of Indian descent. The mutation co-segregated with affected status in the family, and was not seen in 400 control chromosomes evaluated. This nucleotide change caused a threonine to asparagine amino acid substitution at position 130. No mutations have ever been reported in either of these two codons before. The importance of a particular codon in the overall function of a protein can be estimated by observing cross-species conservation, as disease-causing mutations are more likely to occur in amino acids conserved throughout evolution [106]. Conservation of these particular amino acids in many hedgehog proteins supports the hypothesis that these are disease-causing mutations in families 20 and 22 (Figure 3.5).

Figure 3.5. Alignment of the partial amino acid sequence of IHH with those of other species, as well as with human SHH and DHH. The human IHH (amino acids 28 to 202) was aligned with IHH proteins from a number of species, namely the mouse IHH, chicken IHH, African clawed frog (banded hedgehog) and zebrafish (echidna hedgehog). They were also aligned with the human SHH and DHH proteins. Residues associated with disease are indicated by an arrow. Heterozygous mutations D100N, R128Q, T130N and E131K are associated with BDA1 in this study (denoted by an asterisk). BDA1-causing heterozygous mutations E95K, D100E, and E131K were described by Gao et al (2001); D100N was described by McCready et al (2002), Giordano et al (2003), and McCready et al (2005); E95G was described by Kirkpatrick et al (2003); and T154I was described by Liu et al (2006). Homozygous mutations P46L and V190A were described by Hellemans et al (2003) and are associated with ACFD.

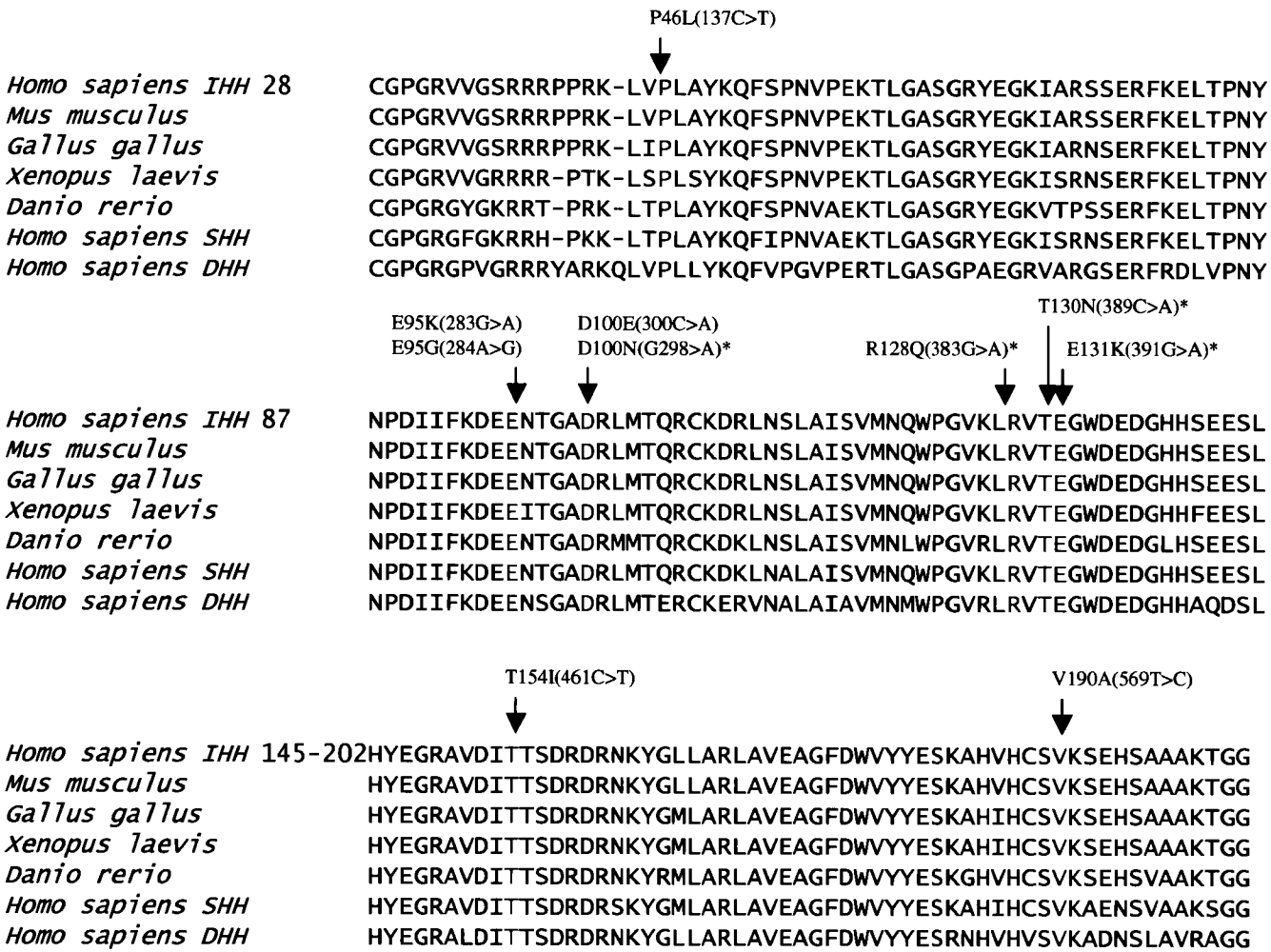
P46L(137C>T)
Homo sapiens IHH 28 CGPGRVVGSRRRPPRK-LVPLAYKQFSPNVPEKTLGASGRYEGKIARSSERFKELTPNY
Mus musculus CGPGRVVGSRRRPPRK-LVPLAYKQFSPNVPEKTLGASGRYEGKIARSSERFKELTPNY
Gallus gallus CGPGRVVGSRRRPPRK-LIPLAYKQFSPNVPEKTLGASGRYEGKIARNSERFKELTPNY
Xenopus laevis CGPGRVVGRRRR-PTK-LSPLSYKQFSPNVPEKTLGASGRYEGKISRNSERFKELTPNY
Danio rerio CGPGRGYGKRRT-PRK-LTPLAYKQFSPNVAEKTLGASGRYEGKVTPSSERFKELTPNY
Homo sapiens SHH CGPGRGFGKRRH-PKK-LTPLAYKQFIPNVAEKTLGASGRYEGKISRNSERFKELTPNY
Homo sapiens DHH CGPGRGPVGRRRYARKQLVPLLYKQFVPGVPERTLGASGPAEGRVARGSERFRDLVPNY
T130N(389C>A)*
E95K(283G>A)
E95G(284A>G)
D100E(300C>A)
D100N(G298>A)*
R128Q(383G>A)*
E131K(391G>A)*
Homo sapiens IHH 87 NPDIIFKDEENTGADRLMTQRCKDRLNSLAISVMNQWPGVKLRVTEGWDEDGHHSEESL
Mus musculus NPDIIFKDEENTGADRLMTQRCKDRLNSLAISVMNQWPGVKLRVTEGWDEDGHHSEESL
Gallus gallus NPDIIFKDEENTGADRLMTQRCKDRLNSLAISVMNQWPGVKLRVTEGWDEDGHHSEESL
Xenopus laevis NPDIIFKDEEITGADRLMTQRCKDRLNSLAISVMNQWPGVKLRVTEGWDEDGHHFEESL
Danio rerio NPDIIFKDEENTGADRMMTQRCKDKLNSLAISVMNLWPGVRLRVTEGWDEDGLHSEESL
Homo sapiens SHH NPDIIFKDEENTGADRLMTQRCKDKLNALAISVMNQWPGVKLRVTEGWDEDGHHSEESL
Homo sapiens DHH NPDIIFKDEENSGADRLMTERCKERVNALAIAVMNMWPGVRLRVTEGWDEDGHHAQDSL
T154I(461C>T)
V190A(569T>C)
Homo sapiens IHH 145-202 HYEGRAVDITTSDRDRNKYGLLARLAVEAGFDWVYYESKAHVHCSVKSEHSAAAKTGG
Mus musculus HYEGRAVDITTSDRDRNKYGLLARLAVEAGFDWVYYESKAHVHCSVKSEHSAAAKTGG
Gallus gallus HYEGRAVDITTSDRDRNKYGMLARLAVEAGFDWVYYESKAHIHCSVKSEHSAAAKTGG
Xenopus laevis HYEGRAVDITTSDRDRNKYGMLARLAVEAGFDWVYYESKAHIHCSVKSEHSAAAKTGG
Danio rerio HYEGRAVDITTSDRDRNKYRMLARLAVEAGFDWVYYESKGHVHCSVKSEHSVAAKTGG
Homo sapiens SHH HYEGRAVDITTSDRDRSKYGMLARLAVEAGFDWVYYESKAHIHCSVKAENSVAAKSGG
Homo sapiens DHH HYEGRALDITTSDRDRNKYGLLARLAVEAGFDWVYYESRNHVHVSVKADNSLAVRAGG

A heterozygous c.391G>A mutation was identified in family 23, a family of Ashkenazi Jewish descent residing in Israel. The mutation co-segregated with the affected status in the family. The exact same nucleotide change was reported by Gao et al (2001) in a Miao Chinese kindred affected with BDA1 [16]. This group screened 100 Miao Chinese control chromosomes and did not observe the change in any of them. The nucleotide change caused a glutamic acid to lysine substitution at position 131. This residue is highly conserved in many hedgehog proteins (Figure 3.5). Because these two families hail from different regional and ethnic backgrounds, it seems unlikely that this mutation is the result of a common ancestor. Rather, this mutation likely arose independently in both families, indicating that Glu131 may represent a hot spot for mutations in BDA1. Interestingly, affected individuals in the Chinese family are reported to be missing the middle phalanges in digits 2-5, and radiographs show the presence of the same chess pawn-shaped distal bone observed in affected individuals in our Israeli family. This phenotype common to both families suggests a particularly important role for Glu131 in IHH function during skeletal development as both families are affected with a more severe BDA1 phenotype.

Indian hedgehog is critical for mediating condensation, growth and differentiation of long bone cartilage templates [38]. St-Jacques et al. (1999) reported that loss of Ihh in a murine model (*Ihh*$^{-/-}$) led to uncalcified, severely shortened forelimbs with incomplete joint formation [41]. In humans, the BDA1 phenotype may be caused by haploinsufficiency of IHH during development, leading to shortened cartilage elements with occasional incomplete joint formation. It has also been suggested that the mutations may alter IHH signaling, whereby the mutant IHH may have decreased ability

to bind to its receptor Ptch1 or increased ability to bind to an alternate receptor [16]. However, heterozygous *Ihh*$^{+/-}$ mice were not described as having any BDA1-like phenotype [41]. It is possible that mild digit abnormalities were missed, or that mice do not have the same dosage requirements for Ihh as humans. To study the effects these amino acid replacements have on BDA1 pathogenesis, *in vitro* or *in vivo* studies could be conducted; however, these tasks are beyond the scope of this thesis.

Although we did not find any disease-causing mutations in the coding region of one family (21), the possibility remains that a mutation in a non-coding regulatory element or a mutation creating a cryptic splice site may exist. Mutations in a regulatory element can affect transcriptional regulation of a given gene, with tissue-specific loss or gain of a product leading to a novel phenotype [107]. Splice site mutations can lead to deleterious effects due to the loss of an entire exon, the inclusion of an intron, or the introduction of a splice site in the middle of an exon or intron [108]. Unfortunately, a lack of additional family members prevented us from formally excluding non-coding mutations at the *IHH* locus by linkage analysis. However, only 10% and 1% of disease-causing mutations originate in splice sites and regulatory elements, respectively [106]. This adds to the likelihood that mutations at another locus are the cause of BDA1 in this family. Following the identification of mutations in the *IHH* gene of BDA1 families, a second locus for BDA1 was described at chromosome 5p13.3-p13.2 in a single family [23]. Furthermore, both the *IHH* gene and the chromosome 5p13.3-p13.2 region were excluded in at least one other family, implicating a third locus in the development of BDA1 [19]. The proband of family 21 will be included in further studies to identify other genes responsible for BDA1 pathogenesis.

3.4.3 Conclusions

In summary, the identification of *IHH* mutations in 3 new kindreds with BDA1 from American, Indian and Israeli regional ethnic groups supports ongoing findings implicating IHH in the pathogenesis of a proportion of BDA1 cases. These mutations are predicted to cause amino acid substitutions at highly conserved codons Arg128, Thr130, and Glu131. Finally, *IHH* coding mutations were not seen in one of our families, but the low occurrence of non-coding mutations in disease points towards additional loci as the cause of BDA1 pathogenesis in this family.

Chapter 4. Assessment of an Ancestral Indian Hedgehog Mutation in a New Zealand Kindred with Brachydactyly Type A1

4.1 Introduction

Brachydactyly Type A1 has the distinction of being the first disorder to be described as an autosomal dominant Mendelian trait in humans. As part of his Ph.D. thesis in 1903, Farabee described a large family from Pennsylvania with BDA1 and correctly surmised that it was inherited in a dominant manner [7]. A few years later, four additional BDA1 families of English ancestry were described by Drinkwater [32-34]. He hypothesized that members of his first family may be related to Farabee's family; however, no common last name was ever confirmed [32, 35].

In 1933, Nissen reported a BDA1 family that emigrated from England to Australia around 1840 [100]. One branch of the family migrated to New Zealand around 1850. Members of this branch were examined and found to have characteristic deformities similar to Drinkwater and Farabee's families [100]. Descendants of this family have since been obtained for a genetic study to determine the molecular basis of BDA1 in their family.

In 2001, mutations in the Indian hedgehog gene (*IHH*) were identified in several BDA1 families [17]. Subsequently, two of the Drinkwater families and Farabee's family were found to share a common c.298G>A mutation resulting in a p.D100N amino acid substitution in IHH [21, 22]. In addition, they were found to share a common haplotype surrounding the *IHH* gene, indicating that these families shared a common founder [21, 22]. Prior to the initiation of this master's research project, descendants of Nissen's

original family were screened for mutations in the *IHH* gene. The same c.298G>A nucleotide change was found in the proband, implying probable common ancestry [21, 109].

To investigate whether this founder mutation is responsible for BDA1 in Nissen's New Zealand kindred, seven family members have been genotyped at 12 markers surrounding the *IHH* gene to determine if the family shares a haplotype with the Farabee and Drinkwater families.

4.2 Material and Methods

4.2.1 Family and Sample Collection

We studied a New Zealand kindred with ancestral origins in England and Australia. The family was previously reported in 1933 by Nissen. The disease can be traced back in an autosomal dominant fashion for at least 7 generations. Individuals with BDA1 and their family members were recruited by our collaborators at Central and Southern Regional Genetics Services, Wellington Hospital, Wellington, New Zealand. Diagnosis was based on physical examination, radiographic findings, and family history. The study was approved by the Children's Hospital of Eastern Ontario Ethics Review Committee. After receiving informed consent, genomic DNA was extracted from peripheral venous blood by standard methods.

4.2.2 Sequence Analysis of *IHH*

Mutational analysis in individuals 16-01 and 16-02 (Figure 4.1) was performed prior to the initiation of this research project [109]. In the remaining family members, the *IHH* gene was amplified and sequenced as described in section 3.2.3.

4.2.3 Establishment of the "Farabee Haplotype" on Chromosome 2

4.2.3.1 Microsatellite Markers

Seven markers from Marshfield's sex-averaged genetic map were examined (D2S2250, D2S433, D2S163, D2S1242, D2S424, D2S1323, and D2S126). See appendix III for primer details. The DNA of individuals 16-01 to 16-07 was genotyped along with the proband of Farabee's family (see [21]) to ensure that alleles co-segregating in the New Zealand kindred were exactly the same as those found in Farabee's family. Each locus was amplified in 10 μl volumes with 100 ng of genomic DNA, 1.5 mM $MgCl_2$, 10 mM Tris-HCl (pH 8.3), 0.2 mM dNTP, 0.12 μM M13-tailed forward primer, 0.12 μM reverse primer, 0.12 μM IRD-700 labelled M13 primer (LI-COR, Lincoln, NE), and 1 Unit *Taq* enzyme. Products were separated on 8% acrylamide gels using the LI-COR DNA sequencer model 4000 and analyzed with RFLPscan software (version 3.0).

Figure 4.1. Extended pedigree of the brachydactylous family described by Nissen (1933). Individuals above the dashed line were originally published. Squares-males, circles-females. Numbers represent sample number assigned to DNA of individuals who were available for this study.

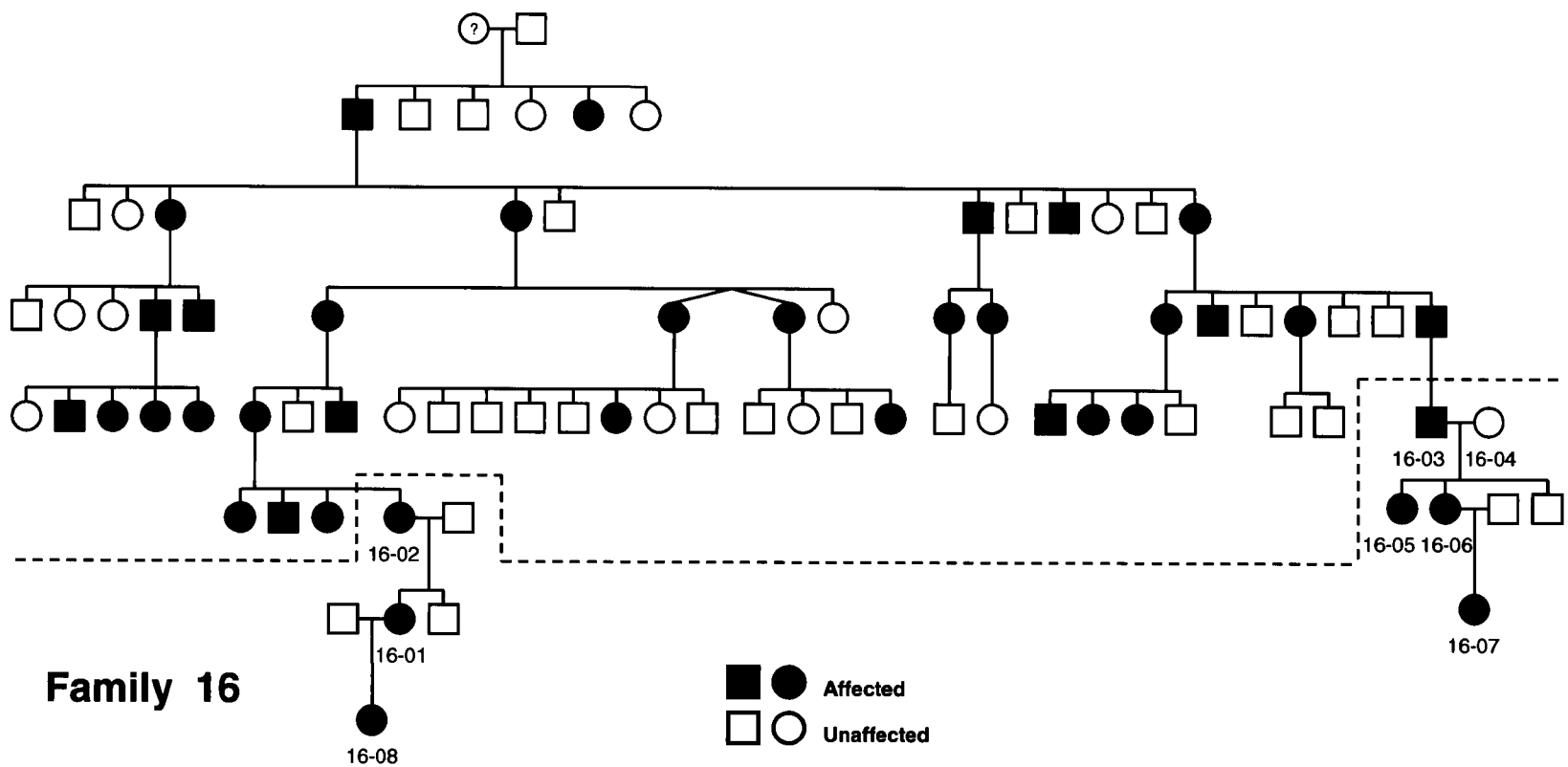
?
16-03
16-04
16-05
16-06
16-07
16-02
16-01
16-08
Affected
Unaffected

Family 16

4.2.3.2 Single Nucleotide Polymorphisms

Analysis of 2 single nucleotide polymorphisms (SNPs) located upstream of exon 1 of *IHH* and 3 SNPs in exon 3 of *IHH* was performed. These SNPs have been previously described by McCready *et al.* in 2002 (Figure 4.2) [22]. Primer details can be found in appendix III. SNPs A and B were amplified with primers IHHsnp12, which bind to a region upstream of exon 1. SNP E was amplified with primers IHHx3.1. Genotypes for these SNPs were established by PCR amplification and sequencing as described in section 3.2.3.

Genotypes at SNP C were ascertained by amplifying IHHx3.2 by PCR in all available family members. Restriction digest was performed in 20 μl volumes, containing 2 μl PCR product, 2.0 μl of 10X NEB Buffer #4, 0.2 μl of the *Sma*I enzyme, and 15.8 μl ddH_2O. Reactions were incubated on a PTC-225 thermal cycler (MJ Research, Waltham, MA) at 25°C for 2 hours. Products were loaded on to a 1.5% agarose gel containing ethidium bromide, electrophoresed for 40 minutes at 100V, and photographed under UV light.

Genotypes at SNP D were ascertained by amplifying IHHx3.3 by PCR in all available family members. Restriction digest was performed in 20 μl volumes, containing 8 μl PCR product, 2.0 μl of 10X NEB Buffer #2, 0.2 μl of the *Bst*UI enzyme, and 9.8 μl ddH_2O. Reactions were incubated at 60°C for 2 hours. Products were loaded on to a 1.5% agarose gel containing ethidium bromide, electrophoresed for 40 minutes at 100V, and photographed under UV light.

Figure 4.2. Schematic representation of 7 microsatellite markers (above band), 5 SNPs and the c.G298A mutation (below band) located on chromosome 2q35-36.1. Genotypes obtained at these markers in family 16 suggest relation to Farabee and Drinkwater's families. The region bounded by markers D2S2250 and D2S126 is 4.82 cM, which corresponds to approximately 2.5 Mb and contains approximately 37 genes. The enlargement shows the structure of the 3-exon *IHH* gene: short boxes, UTR; large boxes, coding region; line, introns. Adapted from information taken from the UCSC genome browser, May 2004 assembly.

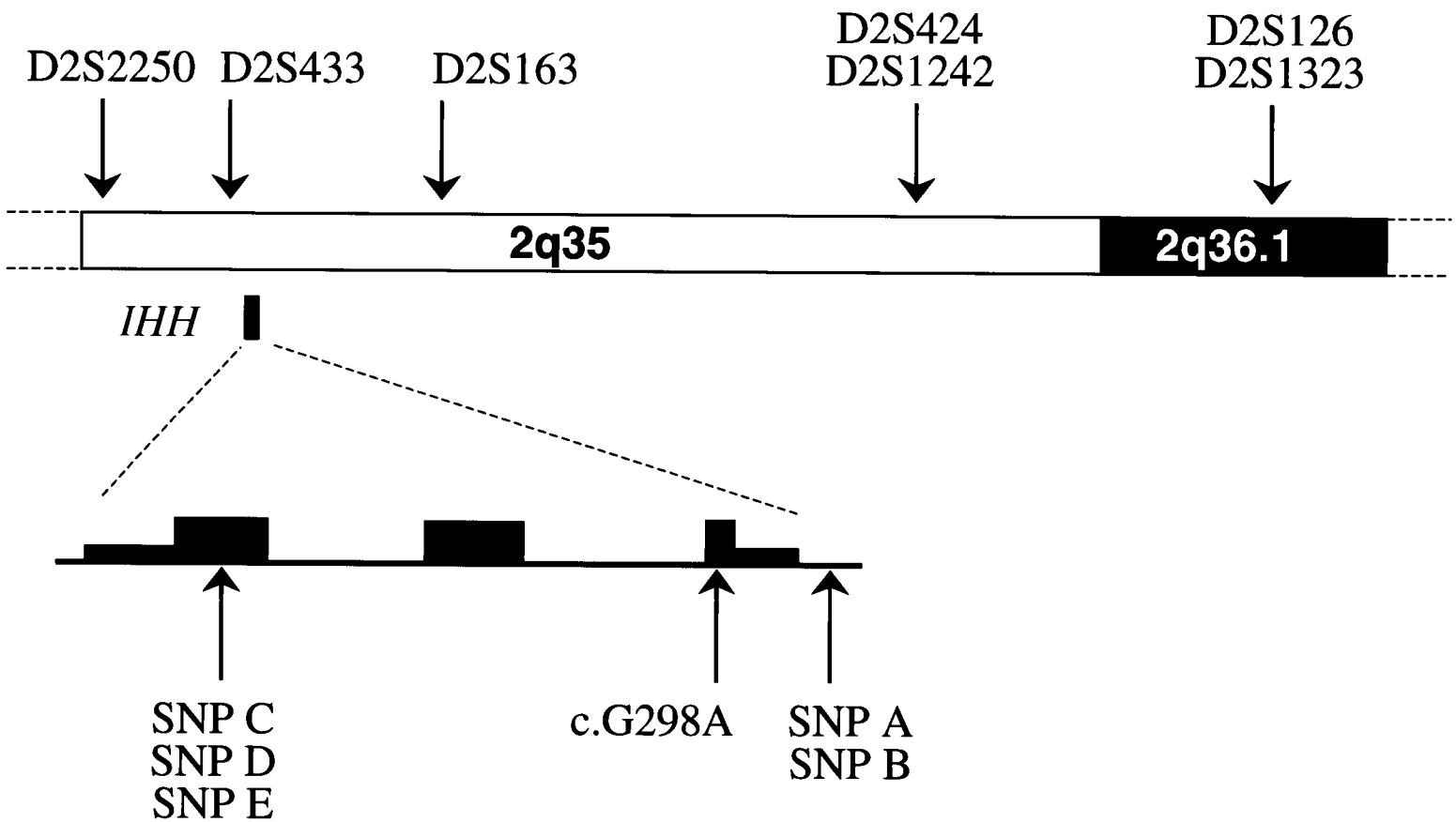
D2S2250
D2S433
D2S163
D2S424
D2S1242
D2S126
D2S1323
2q35
2q36.1
IHH
SNP C
SNP D
SNP E
c.G298A
SNP A
SNP B

4.3 Results

4.3.1 Phenotype of Family 16

We studied 7 members of a New Zealand family with BDA1 segregating as an autosomal dominant, fully penetrant disorder in at least 7 generations. The family's ancestors originated from England, with branches of the family settling in both Australia and New Zealand. The 35-year-old female proband (individual 16-01 in Figure 4.1) initially came to attention after being referred to the genetics clinic for a diagnosis assessment of short fingers. Radiographic analysis showed absent middle phalanges in digits 2-5 of hands and feet, as well as shortened proximal phalanges in digit 1 (Figure 4.3). There was a single interphalangeal joint in each digit, and the proband could not bend her thumbs. Brachydactyly type A1 was diagnosed. Other findings included syndactyly (digit fusion) of the second and third toes, aching back and knees, hallux vulga (lateral deviation of big toe), and absent lateral incisors. She had a normal blood pressure and lipid profile. Her height was 163cm, 25^{th}-50^{th} percentile.

At 33 years of age, the proband became pregnant and desired prenatal screening for BDA1 to prepare for having an affected child. Ultrasonography at 18 weeks' gestation revealed shortening of the fingers, and BDA1 was diagnosed (Figure 4.4A). Pregnancy progressed uneventfully. At term, a female infant with short fingers was born, confirming the BDA1 diagnosis (Figure 4.4B).

On examination at 59 years of age, the proband's affected mother (individual 16-02 in Figure 4.1) had painful lower back, knees, toes and arches of feet. From the age of 44, she had raised blood pressure which was difficult to control. Other features observed

Figure 4.3. Radiographs of the proband of family 16. (A) Radiographs of the hands of individual 16-01 showing a shortened proximal phalange in digit 1 and fusion of the middle and terminal phalanges in digits 2-5. (B) Radiographs of the feet of individual 16-01 showing absent middle phalanges in digits 2-5.

A

B

Figure 4.4. Photographs and ultrasound of the hands of individual 16-08. (A) Ultrasound picture of the fetal hand of individual 16-08 at 18 weeks, showing evidence of short digits. (B) Pictures of the hands of individual 16-02 at approximately 6 months, showing short fingers and confirming the pre-natal diagnosis of BDA1.

A

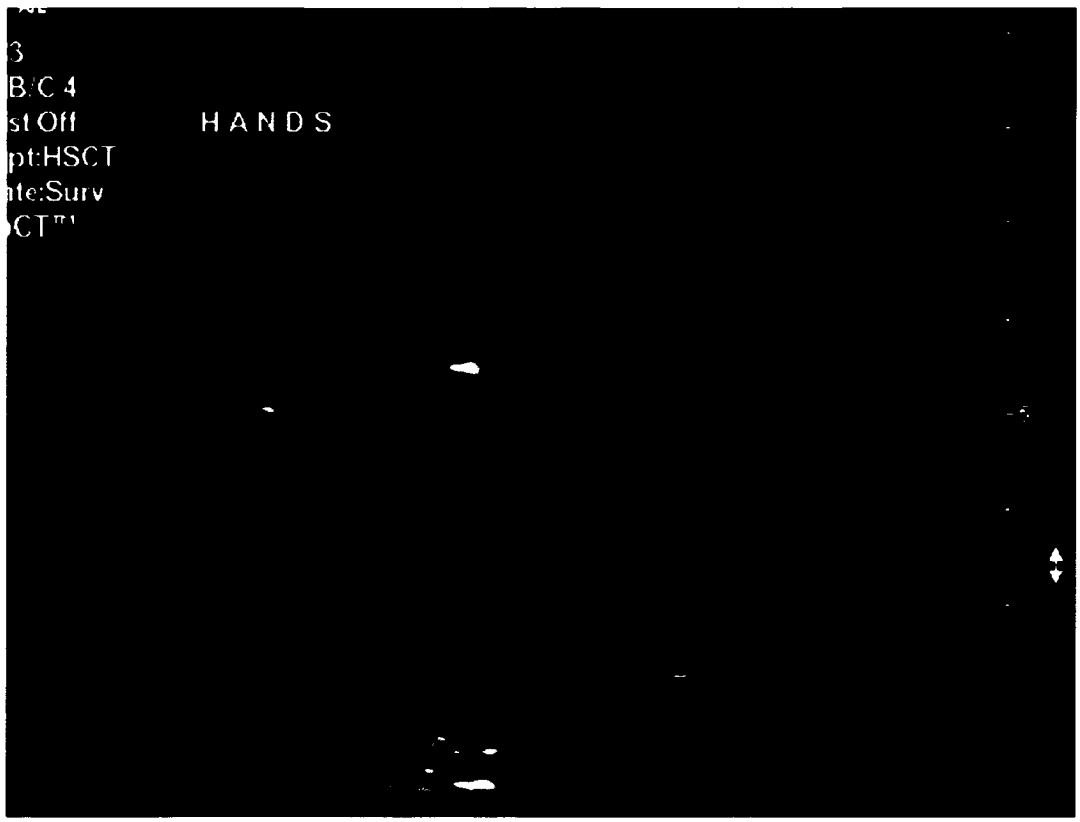

B

in the extended family included lumbar lordosis, extra teeth, and a shortened fifth metacarpal (Table 4.1). The family distinguished affected members as having either "short-short" or "long-short" fingers, indicating heterogeneity in the severity of the phenotype. The family also noted that affected individuals tended to be shorter than their unaffected siblings. All of the family are of normal or high intellect. Further familial assessment showed a strong family history of BDA1, hypertension and vascular disease.

4.3.2 Mutation Detection

A heterozygous c.298G>A nucleotide change was present in the DNA of individual 16-01 and 16-02. To determine if this change co-segregated with the affected status in this family, we screened the DNA of all five additional family members by sequence analysis. The results showed that all six affected individuals carried the c.298G>A change (Figure 4.5). As this nucleotide change has already been reported to cause BDA1 in another family, we did not screen control individuals for the change.

4.3.3 Haplotype Analysis

Based on reports that this family's ancestors are from England, we addressed a possible association of the New Zealand kindred to the Drinkwater and Farabee families by evaluating whether affected members of the family carried the same ancestral haplotype. We studied seven polymorphic markers and 5 SNPs spanning a 4.82 cM region around the *IHH* gene (Figure 4.2). Alleles were compared to the Drinkwater and Farabee ancestral alleles [21, 22]. Results revealed a common shared haplotype between markers D2S2250 and D2S1323 for all 4 families (Table 4.2).

Table 4.1. Clinical features of affected descendants of Nissen's 1933 family. A "+" indicates affected, a "–" indicates unaffected. A "?" indicates the information was not made available for this study.

Patient	16-01	16-02	16-03	16-05	16-06	16-07
Terminal Symphalangism	+	?	?	?	?	?
Thumbs reduced flexion at IP joint	+	+	+	+	+	+
Short 5th metacarpal	-	-	-	-	-	+
2-3 toe syndactyly	+	+	-	-	+	+
Hallux Vulga	(+)	(+)	+	+	+	+
Painful hips	Early 20's	-	50's	Late 20's	Late 20's	-
Absent incisors	+	+	-	-	-	-
Extra teeth	-	-	+	-	-	-
Lumbar lordosis	-	-	-	+	+	-
Height	25th - 50th %	2nd %	9th %	25th - 50th %	0.4th - 2nd %	9th %
Blood Pressure	Normal	Increased	Slight Inc	Normal	Normal	-
Nystagmus	-	-	-	-	-	-

Figure 4.5. Chromatogram showing the DNA sequence of individual 16-01. A heterozygous c.298G>A nucleotide change (arrow), predicted to lead to the amino acid substitution p.D100N, was found in all affected descendants of Nissen's 1933 family.

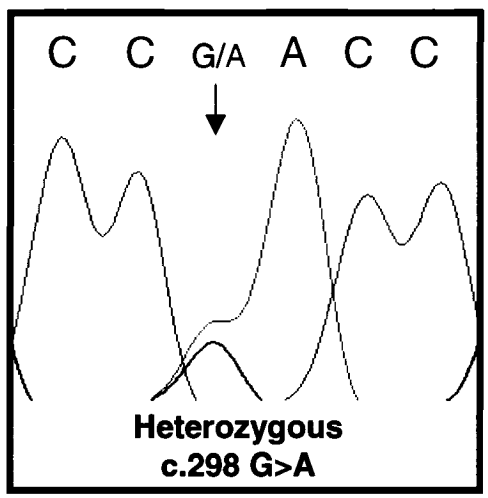
C C G/A A C C
Heterozygous
c.298 G>A

Table 4.2. Analysis of polymorphic markers and SNPs flanking the *IHH* gene on chromosome 2q in individual 16-01 and a descendant of the Farabee family (see McCready et al, 2005). Genotyping data shows a common shared haplotype between markers D2S2250 and D2S126 in BDA1-affected descendants of both Nissen's 1933 family and Farabee's 1903 family. The disease-causing mutation is shown in red.

Marker	Position	Individual	
		16-01	Farabee
D2S2250	216.31	5	5
D2S433	216.31	1	1
SNPd	N/A	G	G
SNPc	N/A	C	C
SNPe	N/A	C	C
c.G298A	N/A	A	A
SNPb	N/A	A	A
SNPA	N/A	A	A
D2S163	218.45	5	5
D2S1242	218.45	4	4
D2S424	218.45	3	3
D2S1323	221.13	2	2
D2S126	221.13	1	1

4.4 Discussion

Here we present molecular, clinical, and ultrasound data on a New Zealand family with BDA1. The condition presents as an autosomal dominant, fully penetrant disorder through at least seven generations and is caused by c.298G>A change in the *IHH* gene. We have also shown images of a fetus in which prenatal diagnosis of BDA1 was made by ultrasound at 18 weeks' gestation. The diagnosis was confirmed at birth.

4.4.1 Molecular Findings

This kindred consented to participate in a genetic study to determine the molecular basis of BDA1 in their family. To investigate whether heterozygous *IHH* mutations are the cause of BDA1 in the family, we determined the sequence of the three exons encoding *IHH* in our proband. We have identified a heterozygous c.298G>A mutation in all affected members of family 16. The mutation caused an aspartic acid to asparagine substitution at position 100. The exact same nucleotide change was reported in the descendants of three BDA1-affected families originally described by Farabee (1903) and Drinkwater (1908, 1915) [7, 21, 22, 32, 34]. One-hundred ninety-four unrelated non-BDA1 control chromosomes were previously screened for the mutation, and the change was not observed in any of them [22].

A common haplotype surrounding the c.298G>A mutation has been previously identified in descendants of the three kindreds with BDA1 first reported by Drinkwater and Farabee, indicating that these families are likely related [21, 22]. This founder mutation is speculated to have originated at least 12 generations ago. Based on reports that the New Zealand family's ancestors hail from England, we addressed a possible

association of the New Zealand family to the Drinkwater and Farabee families by evaluating whether affected members of the family carried this ancestral haplotype. Twelve markers spanning the *IHH* locus were genotyped, and alleles were compared to the Drinkwater and Farabee ancestral alleles. Results revealed a common shared haplotype between markers D2S2250 and D2S1323 for all 4 families (Table 4.2). These results are consistent with the existence of a common founder from whom all four families originated and inherited the mutation. Recombination events previously reported in Drinkwater's 1907 family [22] that were not seen in the other three kindreds may represent a more distant relation to Farabee's family, Drinkwater's 1915 family, and the New Zealand family.

In this study, we have identified a historic mutation and haplotype flanking the *IHH* gene in members of a 7-generation New Zealand family. To date, 3 other families have been shown to share this common c.298G>A mutation and ancestral haplotype. Additionally, two other BDA1-affected families of Italian and American descent have been found to share this same *IHH* mutation [18, 21]. While these mutations may have occurred independently, it remains possible that either of these families may be descendants of this same common founder. Another mutation, c.300C>A, is associated with BDA1 in a Chinese family [16]. This nucleotide change causes an aspartic acid to glutamic acid substitution at position 100. The existence of at least 2 independent mutations in this codon suggests that Asp100 may represent a highly mutational region for BDA1 mutations and that it may play an important role in IHH function during skeletal development. Conservation of this particular amino acid in many hedgehog

proteins supports the hypothesis that these amino acid changes are responsible for BDA1 pathogenesis in these families (Chapter 3, Figure 3.5).

4.4.2 Phenotypic and Genetic Heterogeneity

These four families all share a general diagnosis of Brachydactyly type A1 with symmetrically affected hands and feet and short stature. The middle phalanges of the feet were usually missing, while the middle phalanges in the hands were short or fused to the terminal phalanges. Drinkwater hypothesized that digit shortening was due to a shortened bone shaft, the absence of an epiphysis, or the premature ossification of the epiphysis and bone [33]. Radiographs of affected children as young as 2 years old have shown premature ossification of the epiphyses in the middle phalanges [33, 34].

Other features observed in descendants of Drinkwater's 1908 family were abnormalities of the patella; back, hip and foot pain; inability to squat; and normal stature [22]. A descendant of Drinkwater's 1915 family was reported to have bilateral valgus deformities of his hindfeet, a double scoliosis, and hand and knee deformities. Nystagmus, a squint, and developmental delay were also described [8]. It is not clear whether these traits are the results of the *IHH* mutation found in this family or not.

In the family described by Nissen, all affected individuals had bilateral shortening of the middle phalanges of digits 2-5 and the proximal phalange of digit 1. Distal symphalangism (fusion of the middle and distal phalanges) was frequently present, as were deformities in the carpal and tarsal bones [100]. The proband's aunt was described at age 5 by Nissen, establishing that the remaining individuals examined here are descendants of that family [100]. A diagram of the original x-ray showed absent middle

phalanges, and a virtually absent proximal phalange in digit 1. The most striking feature was the appearance of both normal and basal epiphyses in the metacarpals [100].

Descendants of the family examined in this study showed remarkable phenotypic heterogeneity. Although all six reported having shorter stature than their unaffected siblings, the affected family members distinguished themselves as having "short-short" or "long-short" fingers. Radiographs were not available for all members, but the degree of shortening of the middle phalanges and the presence or absence of distal symphalangism presumably account for these differences. Only one individual, 16-07, had shortened fifth metacarpals. All affected individuals examined could not bend their thumbs at the interphalangeal joints, and had bilateral hallux valgus. Hallux valgus, in which the big toe bends in towards the other toes, has previously been associated with brachydactyly in a family where phalangeal shortness was observed primarily in the feet [110].

Four of the six affected individuals examined here reported 2-3 syndactyly of the toes. Syndactyly has been previously associated with brachydactyly in 2 individuals of a family with a complicated phenotype of brachydactyly, bone fragility, fibromuscular dysplasia, hypertension, congenital cardiac defects, and learning disabilities [10]. One patient had syndactyly of bilateral fingers 4:5, while the other family member had more extensive syndactyly of left fingers 2:3:4, right fingers 3:4, and bilateral toes 2:3 as observed in our kindred [10]. Syndactyly is also frequently a feature of brachydactyly type B [27].

Two sisters, individuals 16-05 and 16-06, were noted to have lumbar lordosis. Lumbar lordosis is a condition which is characterized by an increased curve in the

lumbar region of the lower back and a forward-tilted pelvis, leading to a visibly protruding abdomen and posteriorly protruding buttocks [111]. This posture is thought to be caused by an imbalance in pelvic femoral muscles [111]. Lumbar lordosis has only been described in conjunction with brachydactyly in some individuals with much more severe diagnoses of achondroplasia and/or hypochondroplasia [112-114]. Other vertebral anomalies, such as scoliosis and kyphosis, have also been associated with brachydactyly [8, 12, 13, 115-117]. As no other individuals in the family are reported to be affected with lumbar lordosis, it is possible that this trait was inherited independently of the BDA1 phenotype.

Interestingly, individuals 16-01 and 16-02 were missing lateral incisors, while another affected family member, 16-03, reported having extra teeth. As individual 16-03 is the fourth and third cousin of 16-01 and 16-02 respectively, it is possible that these teeth phenotypes may have been inherited independently from the BDA1 phenotype. However, various supernumerary teeth and dental anomalies have been described in conjunction with brachydactyly in types B and E, angel-shaped phalangoepiphyseal dysplasia (ASPED), and autosomal recessive and dominant Robinow syndromes [92, 118-122].

A large degree of phenotypic heterogeneity, in which mutations in the same gene yield a range of phenotypes [123], has also been observed in BDA1 kindreds with mutations in *IHH*. Wide variation in clinical expression of BDA1 amongst Nissen's, Drinkwater's, and Farabee's families, who share the same heterozygous c.298G>A *IHH* mutation, may reflect the interaction of other genetic alterations or environmental factors with the mutant allele. Evidence exists that modifier genes can control penetrance,

dominance, expressivity and pleitropy of characteristics thought to segregate strictly as Mendelian traits [124]. A mutation or polymorphism at a locus, as well as epigenetics, can influence a phenotype caused by a mutation in a different gene [123, 125]. These modifiers can cause novel, more extreme, less extreme, or wild-type phenotypes in carriers of a particular mutant genotype [124]. Genetic and environmental modifiers are likely responsible for the appearance of additional muscoskeletal and neurological traits described in these BDA1 families.

4.4.3 Brachydactyly and Hypertension in the Family

The New Zealand family has a strong family history of BDA1, vascular disease and hypertension. This association mandated concern of Bilginturan syndrome, also known as brachydactyly with hypertension (HTNB [MIM 112410]). The association of brachydactyly with hypertension was first described in a large Turkish family [126]. Affected individuals had short stature, shortening of various metacarpals and phalanges, and hypertension. The brachydactyly co-segregated completely with hypertension in this family, leading investigators to conclude that both disorders were transmitted in a dominant fashion and were caused either by pleiotropic action of one gene or by two closely positioned genes [126]. The disorder was eventually mapped to 12p12.2-p11.2 [31]. The existence of this HTNB locus was further supported by the discovery of a *de novo* chromosomal deletion, 12p11.21p12.2, in a sporadic case of HTNB [127] (Nagai 1995). Of the individuals examined in the New Zealand kindred, only the proband's affected mother and third cousin were noted to have hypertension. Hypertension was not described in members of Farabee's family or either of Drinkwaters' family. There was

no evidence to suggest that BDA1 is co-segregating with hypertension in the family, as the remaining affected individuals examined had normal blood pressure.

4.4.4 Prenatal Diagnosis

Ultrasonography at 18 weeks' gestation revealed that the proband was carrying a fetus with short digits, and BDA1 was diagnosed. Pregnancy progressed uneventfully and at term, an affected female infant was born, confirming the BDA1 diagnosis. To our knowledge, we have presented only the second report on prenatal diagnosis of BDA1 in an affected family. The diagnosis at 18 weeks' gestation is the earliest currently reported. Ultrasonography had been used previously to diagnose BDA1 in an affected fetus from a 3-generation Dutch family [128]. Following the identification of the structural anomaly at 19 weeks gestation, amniocentesis revealed a normal karyotype and alpha-fetoprotein level. A diagnosis of BDA1 was confirmed at birth, and no other skeletal anomalies were observed [128]. As the Dutch family was published prior to the identification of *IHH* as a BDA1 candidate gene, no findings were ever published revealing the molecular basis for the disorder in this family.

Although the BDA1 phenotype is relatively benign, the ability to diagnose this type of malformation at 18 weeks gestation is important because of the potential to detect syndromes associated with the Brachydactylies. Bronshtein et al. (1995) pioneered reports on prenatal ultrasound diagnosis of digit abnormalities in fetuses between 13 and 17 weeks of gestation [129]. They report that examination of all fingers and phalanges is possible as early as 12-13 weeks gestation. Results suggested that examination of the fingers is preferably done in the first half of gestation, when the fetus tends to keep the

hands open and fingers extended. In the second half of gestation, examination of the fingers can be more difficult as the fetus usually keeps one or both hands closed [129, 130]. Abnormally prolonged fisting is often a feature of aneuploidy in a fetus [129]. Through ultrasound examination, a variety of digit abnormalities were observed in 25 of 20000 fetuses studied, 60% of which were later attributed to syndromes or chromosomal abnormalities [129]. These studies recommended including fetal hand evaluation as part of routine sonography because of its potential for detecting aneuploidy, even in cases at low risk for fetal anomalies [129, 130].

4.4.5 Conclusions

In summary, we have presented evidence that Nissen's 1933 kindred is related to Farabee and Drinkwater's original families through a common ancestor. Genetic and environmental modifiers may be responsible for variable expression of the BDA1 phenotype and involvement of additional muscoskeletal, neurological, and hypertension problems in some individuals [106]. In Nissen's family, hypertension does not co-segregate with the BDA1 phenotype, eliminating concern of Bilginturan syndrome. Furthermore, we have presented the earliest reported diagnosis of BDA1 in an unborn fetus.

Chapter 5. Mapping of a Third BDA1 Locus to Chromosome 20q11.22-q11.23 in Two Families

5.1 Introduction

5.1.1 Positional Candidate Approach to Disease Gene Discovery

Many human diseases have an obvious genetic basis. Understanding the mechanisms by which genetic mutations influence a phenotype can advance research towards improved detection and treatment of these diseases. The positional candidate approach has been successful in identifying many genes responsible for diseases with a hereditary basis. This technique has superseded both the candidate gene approach, in which functional information about the disease is used to guess the mutated gene, and the positional cloning approach, in which the mutated gene is located solely on the basis of map position [131]. The positional candidate approach combines both methods, relying on a combination of mapping the disease gene to a specific chromosomal region, and subsequently scanning that region for potential candidate genes based on functional information [131].

In 1980, Botstein et al. described the use of naturally occurring polymorphic DNA sequence variants to trace genetic inheritance. Since this time, rapid progress in disease gene identification has been aided by the initiation of the Human Genome Project (HGP) and the discovery of thousands more polymorphic variants [131-133]. The first step in the positional candidate strategy involves scanning polymorphic microsatellite markers on each chromosome to determine which genetic variants (alleles) are present

[132, 134]. Markers are amplified by PCR and subject to separation by gel or capillary electrophoresis, revealing the alleles present in each individual [133]. Genotypes are analyzed at each marker by haplotype or linkage analysis to assess if any allele is co-inherited strictly with the disease phenotype. Evidence for co-inheritance implies that the chromosomal region that is linked to the trait may harbor variants influencing the phenotype [132]. Subsequently, genotyping additional nearby markers allows one to define a critical region linked to the trait. This region is defined by the closest flanking recombinant markers, in which alleles are no longer co-inherited with the disease [132]. Finally, this critical region can be screened for candidate genes based on functional information.

5.1.2 Exclusion of Existing BDA1 Candidate Genes

The brachydactylies (BDs) are a group of inherited disorders characterized by shortened digits due to malformation or absence of the phalanges and/or metacarpals. Although most cases of BD have been described as autosomal dominant, reports of incomplete penetrance and phenotypic variation stress the impact of genetic and/or environmental modifiers in the development of the disease. Genes involved in most types of BD have been reported. In many cases, locus heterogeneity has been described, suggesting that mutations in different genes regulating limb development can cause similar phenotypes. To date, Brachydactyly type A1 (BDA1) has been described as a fully penetrant, autosomal dominant condition. Missense mutations in the *Indian hedgehog* (*IHH*) gene have been shown to be responsible for the disorder [16] and a second locus has been mapped to 5p in a single kindred [23]. Furthermore, an inversion

of the Sonic hedgehog (*Shh*) locus has been demonstrated to yield a murine BDA1 phenotype in heterozygous *Short digits* (*Dsh/+*) mice [135]. We will use linkage and haplotype analysis to evaluate these loci as candidate genes in 2 families with BDA1.

We sought out polymorphic markers spanning our loci of interest in order to conduct haplotype and linkage analysis on 2 families. Two markers flanking the 5p critical region, D5S2854 and D5S663, as well as one marker within the region, D5S583, were selected to determine if the region was linked to the disease in family 18. The 5p critical region had already been excluded by haplotype analysis as disease-causing in family 4 [136]. Although sequence analysis had been used to exclude mutations in the *IHH* coding region in both of these families [19, 109], three markers positioned around the *IHH* gene on chromosome 2q (D2S164, D2S433, and D2S1242) were selected to exclude non-coding mutations in *IHH* as the cause for BDA1 in the family. Finally, three markers positioned around the *SHH* gene on chromosome 7q (D7S3070, D7S1823, and D7S2465) were selected to examine *SHH* as a candidate gene in both of these families. With all three loci excluded in both families, a 25-cM genome-wide linkage screen was initiated.

5.2 Materials and Methods

5.2.1 Family and Sample Collection

We studied 2 families affected with BDA1 (Figure 5.1). In family 4, the disease was transmitted in an autosomal dominant fashion from an affected parent. In family 18, the proband was born to reportedly unaffected, consanguineous parents, suggesting an

Figure 5.1. Pedigrees of two families with Brachydactyly Type A1, families 4 and 18. The trait is transmitted in an autosomal dominant fashion in pedigree 4, while it is transmitted in an autosomal recessive or co-dominant fashion in pedigree 18. Squares – males. Circles – females. Numbers represent the sample number assigned to the DNA of individuals who were available to participate in this study.

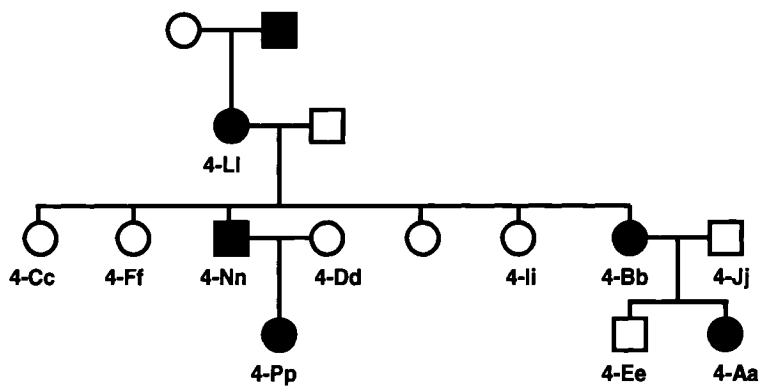

Family 4

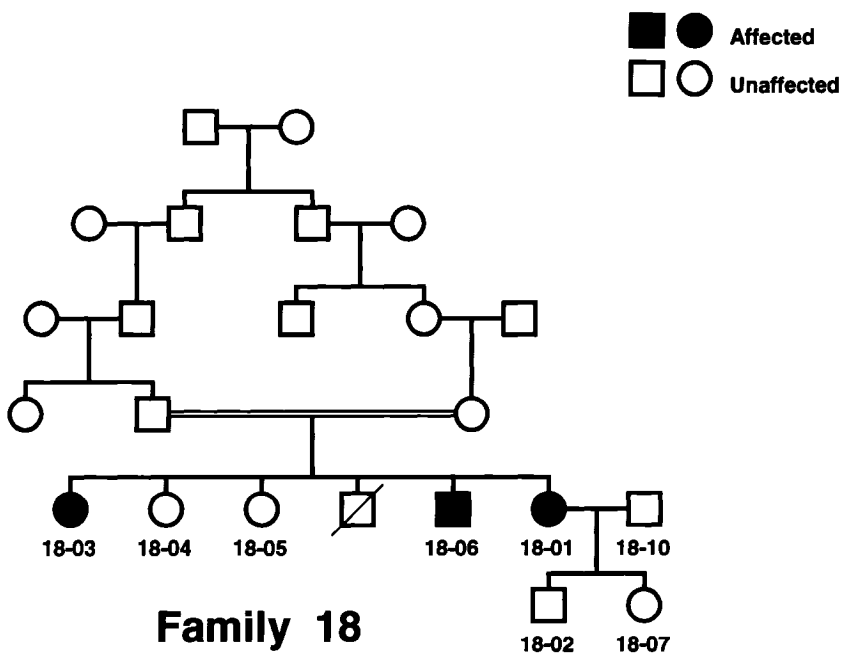

Family 18

autosomal recessive or a partially dominant mode of inheritance. Individuals with BDA1 and their family members were recruited by our collaborators at the Shriners Hospital for Children in Houston, Texas, and the Children's Hospital of Eastern Ontario in Ottawa, Ontario. Diagnosis was based on physical examination, radiographic findings when available, and family history. The study was approved by the Children's Hospital of Eastern Ontario Ethics Review Committee. After receiving informed consent, genomic DNA was extracted from peripheral venous blood or saliva samples with a QIAamp DNA blood mini-kit (Qiagen, Valencia, California) or an Oragene DNA self-collection kit (DNA Genotek, Ottawa, Ontario).

5.2.2 Exclusion of Linkage to the Chromosome 5 Critical Region, the *IHH* Gene, and the *SHH* Gene

Nine microsatellite markers from Marshfield's sex-averaged genetic map were examined (D2S164, D2S433, D2S1242, D7S3070, D7S1823, D7S2465, D5S2854, D5S583, and D5S663) (Table 5.1). Primer sequences are available in Appendix III. An M13 primer tail sequence was added to the forward primer (CACGACGTTGTAAAACGAC). Each locus was amplified in 10 μl volumes with 100 ng of genomic DNA, 1.5 mM $MgCl_2$, 10 mM Tris-HCl (pH 8.3), 0.2 mM dNTP, 0.12 μM M13-tailed forward primer, 0.12 μM reverse primer, 0.12 μM IRD-700 labelled M13 primer (LI-COR, Lincoln, NE), and 1 Unit *Taq* enzyme. Products were separated on 8% acrylamide gels using the LI-COR DNA sequencer model 4000 and analyzed with RFLPscan software (version 3.0). Linkage analysis was performed using the MLINK program of the LINKAGE package (version 4.0). LOD scores for family 4 were

Table 5.1. Polymorphic microsatellite markers used to genotype families 4 and 18 at chromosomes 2, 5, and 7.

Chromosome	Marker	Chrom. Band	Position (cM)	Variation Type	Heterozygosity	Distance from previous marker (cM)
2	D2S164	2q35	214.71	di	0.8408	---
	D2S433	2q35	216.31	tetra	N/A	1.6
	D2S1242	2q35	218.45	tetra	0.9380	2.14
5	D5S2854	5p13.3	41.06	tetra	N/A	---
	D5S583	5p13.3	47.09	tetra	0.8571	6.03
	D5S663	5p13.2	51.99	di	0.8329	4.9
7	D7S3070	7q36.1	163.03	tetra	N/A	---
	D7S1823	7q36.2	173.71	tetra	N/A	10.68
	D7S2465	7q36.3	180.24	di	0.8321	6.53

calculated using an autosomal dominant model. Due to the consanguineous nature of family 18, LOD scores were calculated using an autosomal recessive model. A penetrance of 100%, disease allele frequency of 0.000001, equal marker allele frequencies, and equal recombination frequencies between males and females was assumed.

5.2.3 Genome-Wide Linkage Screen

A 25-centimorgan genome-wide scan was initiated using 208 primer sets from the MapPairs™ polymorphic microsatellite marker set (Research Genetics, Huntsville, Alabama) including markers on chromosomes 1-22. Nine additional markers from Marshfield's sex-averaged genetic map were subsequently examined (D20S471, D20S912, D20S486, D20S601, D20S106, D20S914, D20S870, D20S865, and D20S834) (Table 5.2). See appendix IV for primer information. Each locus was amplified as described above. Products were separated on 8% acrylamide gels using the LI-COR DNA sequencer model 4000 (LI-COR, Lincoln, Nebraska) and analyzed with LI-COR's Saga Generation 2 software. Linkage analysis was performed as described above.

5.3 Results

5.3.1 Mode of Inheritance in Two Families

Individuals from 2 families of different ethnic and regional backgrounds were genotyped at many loci on chromosomes 1-22. One family shows a clear autosomal dominant pattern of inheritance, and we have obtained DNA from 5 affected individuals

Table 5.2. Polymorphic microsatellite markers used to genotype families 4 and 18 at chromosome 20.

Marker	Chromosomal Band	Position (cM)	Variation Type	Heterozygosity	Distance from previous marker (cM)
D20S482	20p13	13.21	tetra	N/A	---
D20S851	20p12.3	24.70	di	0.74	11.49
D20S604	20p12.1	32.94	tetra	N/A	8.24
D20S470	20p12.1	39.25	tetra	N/A	6.31
D20S471	20p11.23	42.28	tetra	N/A	3.03
D20S912	20p11.23	46.71	di	0.81	4.43
D20S486	20p11.21	49.22	tetra	N/A	2.51
D20S601	20q11.22	50.81	tetra	N/A	1.59
D20S106	20q11.22	50.81	di	0.71	0
D20S914	20q11.23	50.81	di	0.56	0
D20S870	20q11.23	50.81	di	0.67	0
D20S865	20q11.23	50.81	di	0.74	0
D20S834	20q11.23	51.36	di	0.72	0.55
D20S478	20q11.23	54.09	tetra	N/A	2.73
D20S481	20q13.12	62.32	tetra	N/A	8.23
D20S480	20q13.2	79.91	tetra	N/A	17.59
D20S171	20q13.32	95.70	di	0.78	15.79

and 6 unaffected individuals (Figure 5.1). The other family shows an unclear potentially recessive or partially dominant pattern of inheritance, and we have obtained DNA from 3 affected individuals, and 5 unaffected individuals (Figure 5.1). Both families shared an initial diagnosis of BDA1.

5.3.2 Determining the Theoretical Maximum LOD Scores in Two Families

Because of the small number of individuals in each pedigree, we knew that neither family would be able to yield a LOD score of 3.0 that is generally required to be considered significant evidence in favour of linkage (Ott 1999). Using an autosomal dominant model, the maximum possible LOD scores we could obtain was 2.11 ($\theta = 0$) for family 4. Using an autosomal recessive model, the maximum possible LOD score we could obtain for family 18 was 2.15 ($\theta = 0$).

5.3.3 Exclusion of the 5p13.3-p13.2 Region, the *IHH* Gene, and the *SHH* Gene by Haplotype and Linkage Analysis in Two Families

Sequencing of the *IHH* gene and haplotype analysis of the 5p13.3-p13.2 critical region in family 4 prior to the initiation of this Master's project excluded these regions as disease-causing candidates [19, 136]. Haplotype analysis showed that none of the markers surrounding *IHH* or *SHH* co-segregated with the disease in this family. Linkage analysis was performed with an autosomal dominant model, and LOD scores of $-\infty$ ($\theta = 0$) at all markers formally excluded these loci in this family (Table 5.3).

Sequencing of the *IHH* gene in family 18 was performed prior to the initiation of this Master's project and excluded this region as disease-causing in the family [109].

Table 5.3. Chromosome 2q (*IHH*) and 7q (*SHH*) LOD scores for pedigree 4, calculated with an autosomal dominant model at 100% penetrance.

			LodScore at θ=						
Chromosome	**Marker**	**Map position**	**0.00**	**0.01**	**0.05**	**0.10**	**0.20**	**0.30**	**0.40**
2	D2S164	214.71 cM	-∞	-1.11	-0.44	-0.19	-0.01	-0.07	-0.06
	D2S433	216.31 cM	-∞	-1.61	-0.77	-0.40	-0.09	0.03	0.04
	D2S1242	218.45 cM	-∞	-5.91	-3.16	-2.03	-0.98	-0.45	-0.15
7	D7S3070	163.03 cM	-∞	-1.92	-0.63	-0.17	0.13	0.16	0.09
	D7S1823	173.71 cM	-∞	-1.11	-0.44	-0.19	0.01	0.07	0.06
	D7S2465	180.24 cM	-∞	-1.92	-0.63	-0.17	0.13	0.16	0.09
Theoretical Maximum	-	-	2.11	2.07	1.93	1.74	1.33	0.87	0.39

Haplotype analysis showed that none of the markers surrounding the 5p13.3-p13.2 critical region, *IHH* or *SHH* co-segregated with the disease in this family. Linkage analysis was performed with an autosomal recessive model, and LOD scores of $-\infty$ (θ = 0) at all markers formally excluded these loci in this family (Table 5.4).

5.3.4 Linkage of BDA1 to a Region on Chromosome 20q11.22-q11.23 in Two Families

A genome-wide linkage screen yielded weakly positive LOD scores in both families at nearby regions on chromosome 20q. Initially, the consanguineous nature of family 18 was not known, and LOD scores from both families were calculated using an autosomal dominant model and were considered to be additive. Positive LOD scores of 1.51 and 1.81 at markers D20S478 and D20S481 were seen in family 4, and a positive LOD score of 1.20 at the adjacent marker D20S470 was seen in family 18.

Nine additional polymorphic markers spanning the 14.84 cM region between markers D20S470 and D20S478 were genotyped (Figure 5.2, blue arrows). A region of homozygous alleles in affected members of family 18 at all markers between D20S601 and D20S865 drew attention to the consanguineous nature of the family (Figure 5.3). LOD scores for family 18 were re-calculated under an autosomal recessive model (Table 5.5).

By analyzing the families separately, we were able to define separate critical regions in both families. A novel recombination event between markers D20S601 and D20S106 in patient 4-Cc allowed us to define a large 45-cM critical interval in family 4 from marker D20S601 to at least marker D20S171 that co-segregated with the disease in

Table 5.4. Chromosome 5p13.3-p13.2, 2q (*IHH*), and 7q (*SHH*) LOD scores for pedigree 18, calculated with an autosomal recessive model at 100% penetrance.

Chromosome	Marker	Map position	LOD Score at θ=						
			0.00	0.01	0.05	0.10	0.20	0.30	0.40
5	D5S2854	41.06 cM	-∞	-2.26	-0.97	-0.49	-0.15	-0.04	-0.01
	D5S583	47.09 cM	-∞	-3.77	-1.83	-1.10	-0.49	-0.20	-0.06
	D5S663	51.99 cM	-∞	-3.80	-1.83	-1.08	-0.45	-0.18	-0.04
2	D2S164	214.71 cM	-∞	-2.10	-0.88	-0.48	-0.22	-0.11	-0.03
	D2S433	216.31 cM	-∞	-1.21	-0.56	-0.32	-0.13	-0.05	-0.01
	D2S1242	218.45 cM	-∞	-1.62	-0.38	0.03	0.23	0.18	0.07
7	D7S3070	163.03 cM	-∞	-2.10	-0.88	-0.48	-0.22	-0.11	-0.03
	D7S1823	173.71 cM	-∞	-3.77	-1.83	-1.10	-0.49	-0.20	-0.06
	D7S2465	180.24 cM	-∞	-1.77	-0.51	-0.09	0.15	0.14	0.05
Theoretical Maximum	-	-	2.15	2.10	1.91	1.66	1.17	0.68	0.28

Figure 5.2. Schematic representation of chromosome 20 showing the approximate locations of 17 microsatellite markers used to genotype families 4 and 18. Markers denoted by a red arrow were used in the initial screen; markers denoted with a blue arrow were used to narrow down the region of overlapping linkage in both families. The expanded region is showing many microsatellite markers used to refine the critical region.

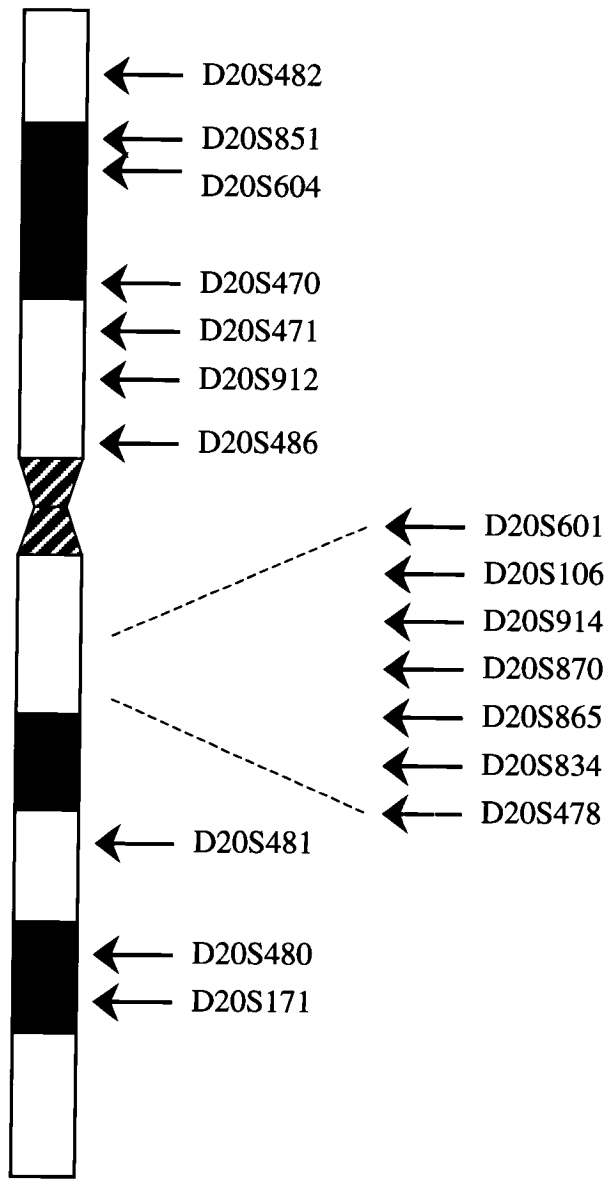
D20S482
D20S851
D20S604
D20S470
D20S471
D20S912
D20S486
D20S601
D20S106
D20S914
D20S870
D20S865
D20S834
D20S478
D20S481
D20S480
D20S171

Figure 5.3. Haplotype of members of family 18 at microsatellite markers spanning a 49 cM region of chromosome 20q. The red bar represents the disease haplotype bounded by non-recombinant markers D20S601 and D20S865. Alleles in brackets are inferred data. Squares – males. Circles – females. Numbers represent the sample number assigned to the DNA of individuals who were available to participate in this study.

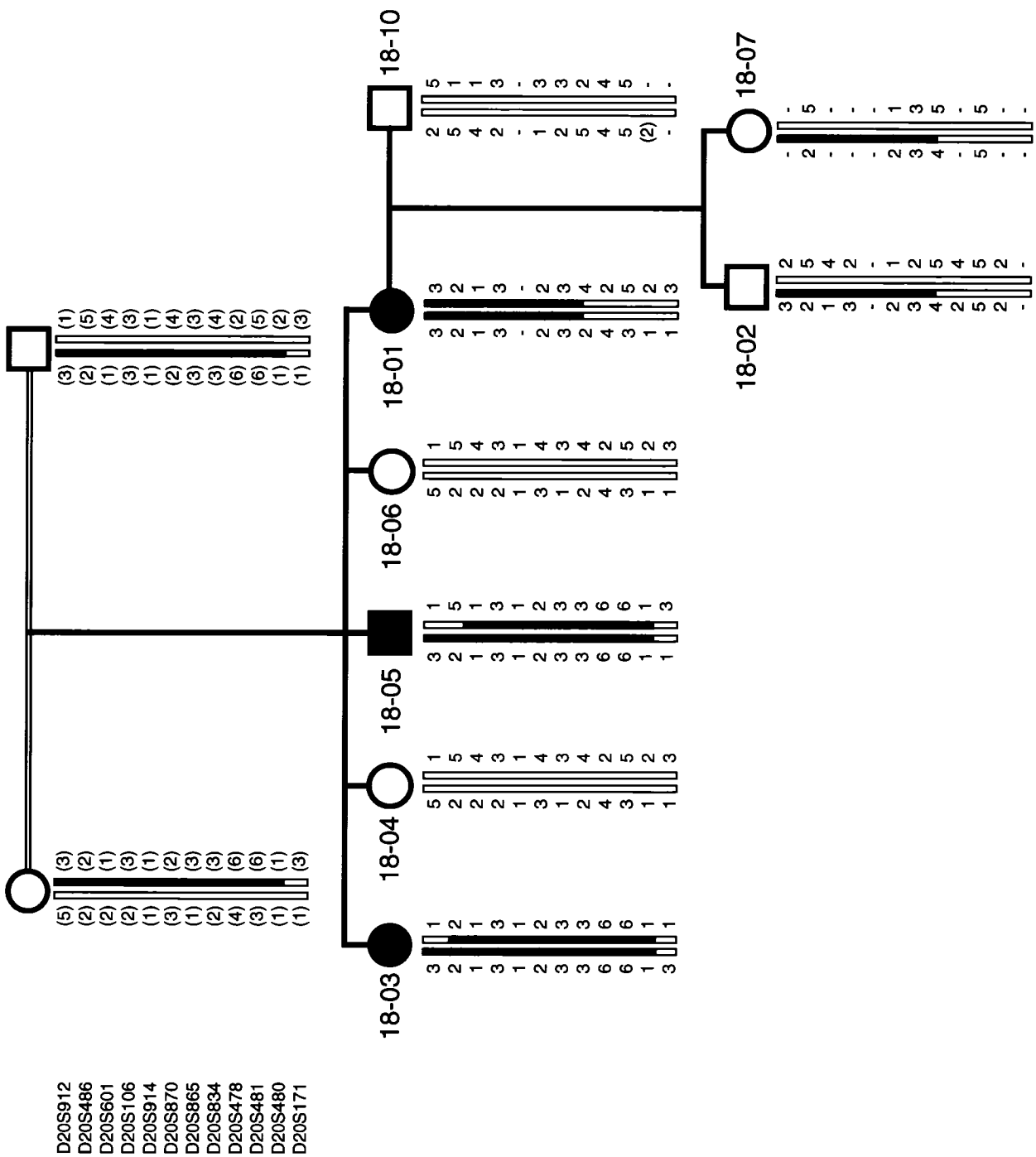
18-10
18-07
18-01
18-02
18-06
18-05
18-04
18-03
D20S912
D20S486
D20S601
D20S106
D20S914
D20S870
D20S865
D20S834
D20S478
D20S481
D20S480
D20S171

Table 5.5. LOD scores of microsatellite markers for pedigree 18, calculated with an autosomal recessive model at 100% penetrance.

Marker	Map position	LOD Score at θ=						
		0.00	0.01	0.05	0.10	0.20	0.30	0.40
D20S482	13.21	-∞	-3.59	-1.66	-0.95	-0.39	-0.15	-0.03
D20S851	24.70	-∞	-2.36	-1.05	-0.56	-0.19	-0.06	-0.02
D20S604	32.94	-∞	-0.48	0.10	0.25	0.26	0.16	0.06
D20S470	39.25	-∞	-2.07	-0.79	-0.34	-0.03	0.02	0.01
D20S471	42.28	-∞	-1.72	-0.48	-0.08	0.13	0.11	0.04
D20S912	46.71	-∞	-1.55	-0.32	0.08	0.26	0.21	0.08
D20S486	49.22	-∞	-0.25	0.27	0.36	0.28	0.15	0.05
D20S601	50.81	2.06	2.01	1.82	1.59	1.11	0.64	0.22
D20S106	50.81	1.48	1.44	1.28	1.08	0.71	0.38	0.13
D20S914	50.81	0.26	0.25	0.20	0.15	0.08	0.03	0.01
D20S870	50.81	2.15	2.10	1.91	1.66	1.17	0.68	0.24
D20S865	50.81	1.63	1.59	1.41	1.19	0.78	0.43	0.14
D20S834	51.36	-∞	-1.89	-0.65	-0.23	0.01	0.05	0.03
D20S478	54.09	-∞	-1.82	-0.58	-0.17	0.06	0.07	0.04
D20S481	62.32	-∞	-1.76	-0.52	-0.12	0.09	0.09	0.05
D20S480	79.91	-∞	-0.68	-0.11	0.03	0.07	0.04	0.01
D20S171	95.70	-3.12	-1.13	-0.49	-0.25	-0.08	-0.03	-0.01
Theoretical Maximum	-	2.15	2.10	1.91	1.66	1.17	0.68	0.28

the family (Figure 5.4). Unfortunately, no markers beyond D20S171 were available to determine if there were any recombination events closer to the telomeric end of 20q. A maximum LOD score of 2.05 ($\theta = 0$) was observed at marker D20S834 (Table 5.6). In family 18, recombination events were identified between markers D20S486 and D20S601 in patient 18-05, as well as between markers D20S865 and D20S843 in patient 18-01. This defined a 2.1 cM critical interval that was inherited on both chromosomes of affected individuals for that family. A maximum LOD score of 2.15 ($\theta = 0$) was observed at marker D20S870 (Table 5.5).

Because linkage analysis was performed with different models for the 2 families, LOD scores were no longer additive. However, positive LOD scores in both families at markers D20S106 to D20S865 supported the existence of one gene causing BDA1 in both of these families. Recombination events in both families narrow the critical region of potential overlap down to a 0.55 cM, 2.5 Mb region on chromosome 20q11.22-q11.23 containing approximately 50 genes.

5.4 Discussion

This project was initiated in order to identify loci which are responsible for BDA1 in two families. BDA1 is a genetically heterogeneous disorder, as at least 2 candidate loci have been identified in humans and an additional candidate was identified in a mouse. Since 2001, many teams have described mutations of the Indian hedgehog (*IHH*) gene in many BDA1 families of various ethnic and regional backgrounds [16, 18-22]. Subsequently, a second locus for BDA1 was mapped to 5p13.3-p13.2 in a single Canadian kindred [23]. More recently, a German group described a radiation-induced

Figure 5.4. Haplotype of members of family 4 at microsatellite markers spanning a 49cM region of chromosome 20q. The black bar represents the disease haplotype bounded by non-recombinant markers D20S106 and D20S171. Alleles in brackets are inferred data. Squares – males. Circles – females. Numbers represent the sample number assigned to the DNA of individuals who were available to participate in this study.

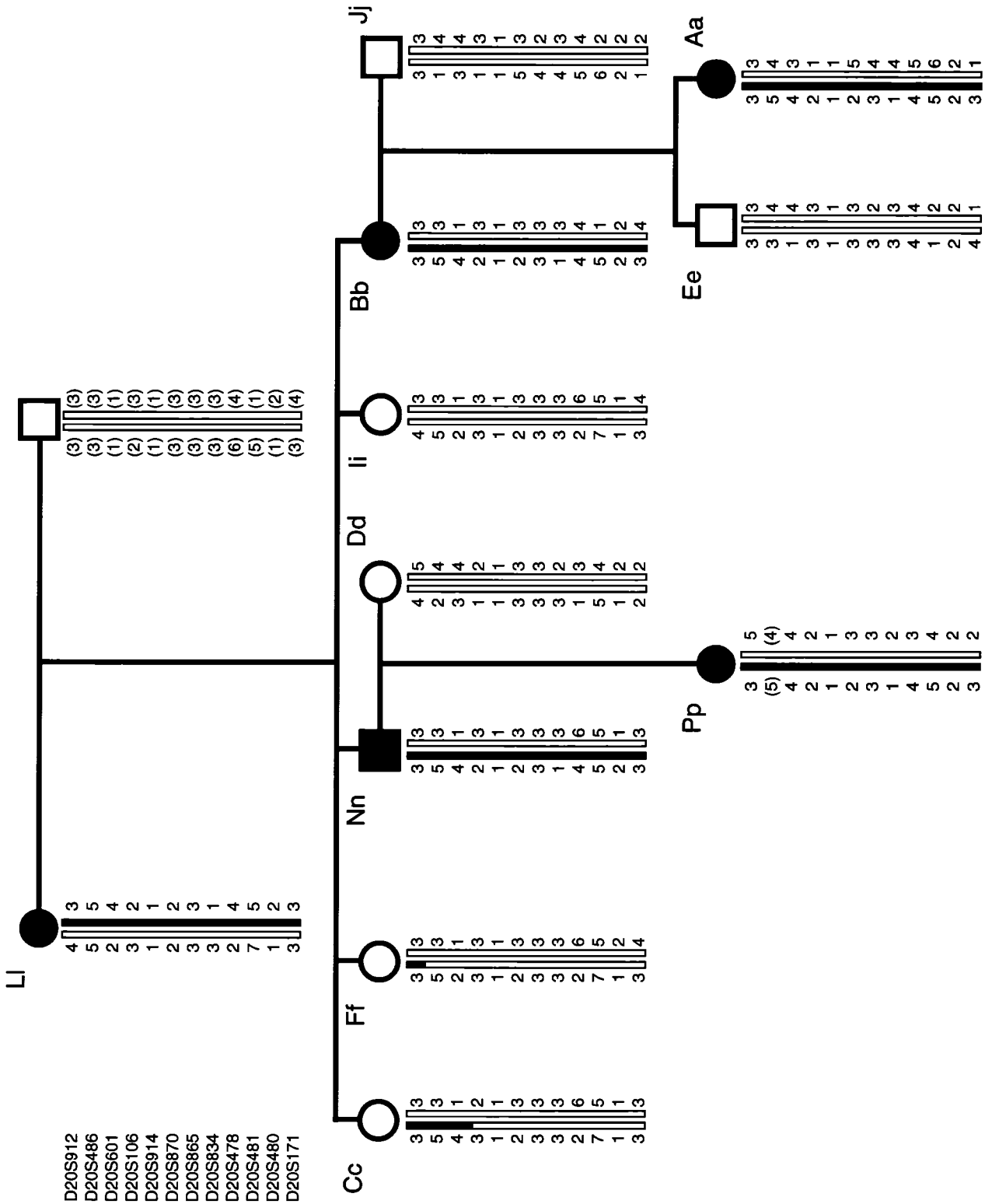
Jj
Aa
Bb
Ee
Ii
Dd
Ll
Nn
Pp
Ff
Cc
D20S912
D20S486
D20S601
D20S106
D20S914
D20S870
D20S865
D20S834
D20S478
D20S481
D20S480
D20S171

Table 5.6. LOD scores of microsatellite markers for pedigree 4, calculated with an autosomal dominant model at 100% penetrance.

Marker	Map position	LOD Score at θ=						
		0.00	0.01	0.05	0.10	0.20	0.30	0.40
D20S482	13.21	-∞	-4.21	-2.19	-1.38	-0.67	-0.35	-0.16
D20S851	24.70	-∞	-7.90	-4.44	-2.98	-1.58	-0.82	-0.33
D20S604	32.94	-∞	-1.80	-0.94	-0.54	-0.17	-0.01	0.03
D20S470	39.25	-∞	-2.51	-1.18	-0.67	-0.25	-0.09	-0.02
D20S471	42.28	-∞	-1.45	-0.79	-0.53	-0.27	-0.12	-0.03
D20S912	46.71	-∞	-2.80	-1.44	-0.89	-0.39	-0.15	-0.04
D20S486	49.22	0.60	0.59	0.56	0.51	0.41	0.29	0.16
D20S601	50.81	-∞	0.08	0.65	0.79	0.74	0.53	0.27
D20S106	50.81	0.71	0.75	0.82	0.82	0.69	0.46	0.21
D20S914	50.81	0.00	0.00	0.00	0.00	0.00	0.00	0.00
D20S870	50.81	0.90	0.89	0.84	0.77	0.61	0.44	0.24
D20S865	50.81	0.00	0.00	0.00	0.00	0.00	0.00	0.00
D20S834	51.36	2.05	2.01	1.87	1.68	1.27	0.82	0.35
D20S478	54.09	1.51	1.48	1.37	1.23	0.92	0.58	0.23
D20S481	62.32	1.81	1.78	1.65	1.49	1.13	0.73	0.31
D20S480	79.91	0.90	0.88	0.79	0.68	0.45	0.23	0.06
D20S171	95.70	0.60	0.59	0.56	0.51	0.41	0.29	0.16
Theoretical Maximum	-	2.11	2.07	1.93	1.74	1.33	0.87	0.39

mouse mutant in which a chromosomal inversion involving the *Shh* gene lead to ectopic expression of Shh during endochondral ossification [135]. The heterozygote mice display a phenotype very similar to human BDA1 [135]. It is feasible that similar changes in the human *SHH* gene expression could cause a BDA1 phenotype in humans, making *SHH* an additional candidate for BDA1.

In order to examine each of these loci as candidates in our two families, multiple markers that flanked each locus were genotyped in members of both families. Alleles were assessed by haplotype and linkage analysis, and results indicate that none of these 3 loci are responsible for the disease in either family. It can therefore be concluded that we are looking for additional disease candidates in these 2 families.

A genome-wide linkage screen of chromosomes 1-22 with markers spaced approximately 25 cM apart was initiated. Positive LOD scores were observed on chromosome 20 for both families, prompting the addition of several more markers in the region to the linkage screen. Although it remains possible that 2 separate loci on chromosome 20 can cause BDA1, we did identify a 0.55 cM region of overlapping linkage at chromosome 20q11.22-q11.23 in both families. Haplotype and linkage analysis identified recombination events in families 4 and 18 that defined the centromeric and telomeric ends of the overlapping critical region, respectively.

Despite the fact that BDA1 has been described in sporadic forms, usually in conjunction with other features, all of the families described to date have shown autosomal dominant, fully penetrant transmission of the disease [7, 16-23, 32-34, 137]. Although BDA1 does segregate as an autosomal dominant, fully penetrant disease in family 4, the inheritance pattern in family 18 was not as clear. The 3 affected siblings

were born to reportedly unaffected parents. It was conceivable that the trait showed incomplete penetrance in this family, and that one of the unaffected parents carried the mutation but had a normal phenotype. However, the occurrence of a stretch of 5 adjacent markers on chromosome 20 at which only the affected individuals were homozygous for identical alleles drew attention to the familial relation of the parents. The clinician was able to confirm that the parents of the sibship were second cousins, identifying the possibility of recessive inheritance in this consanguineous pedigree.

In summary, linkage analysis has excluded the *IHH* gene, the *SHH* gene, and the chromosome 5p13.3-p13.2 critical region as disease-causing candidates in at least 2 families with BDA1. By way of a genome-wide linkage screen, linkage was observed at regions of chromosome 20 in both families. There is a 0.55 cM region of overlapping linkage in both families that may contain a BDA1 candidate gene common to both families.

Chapter 6. Establishment of Growth and Differentiation Factor 5 as a Second Gene for Brachydactyly Type A1

6.1 Introduction

6.1.1 A Third Locus for BDA1 Resides at Chromosome 20q11.22-q11.23

The results of the genome-wide linkage screen discussed in chapter 5 drew attention to chromosome 20 as the prospective location for a third BDA1 locus. Both families 4 and 18 showed linkage to numerous markers on chromosome 20, with a 0.55 cM region of overlap in the two families. This region spans chromosome 20q11.22-q11.23, and is flanked by recombinant markers D20S601 and D20S834 (Figure 6.1). Assuming these 2 families share a common disease gene, we scanned this region on the NCBI and UCSC databases (Appendix I) for candidate genes whose protein products were known or thought to contribute to bone development. One gene, growth and differentiation factor 5 (*GDF5*), drew our immediate attention due to its known role in cartilage differentiation and joint formation in the limbs [63]. To investigate whether mutations in *GDF5* can cause BDA1, *GDF5* was evaluated as a candidate gene in one control individual, the probands of families 4 and 18, and in 8 other cases of BDA1 in which a disease-causing mutation had not yet been identified.

6.1.2 *GDF5* as a Candidate Gene for Brachydactyly Type A1

The gene *GDF5* encodes growth and differentiation factor 5, which is closely related to the bone morphogenetic proteins (BMPs), members of the transforming growth

Figure 6.1. Schematic representation of 6 microsatellite markers located on chromosome 20q11. Genotypes obtained at these markers in families 4 and 18 suggested potential linkage of this region to the BDA1 phenotype in both families. The region bounded by markers D20S601 and D20S834 is 0.55 cM, which corresponds to approximately 2.5 Mb and contains approximately 50 genes. The candidate gene *GDF5* is located in the 20q11.22 chromosome band and encodes a cartilage growth & differentiation factor critical for the development of the appendicular skeleton. The enlargement shows the structure of the 2-exon *GDF5* gene: short boxes, UTR; large boxes, coding region; line, introns. Adapted from information taken from the USCS genome browser, March 2006 assembly.

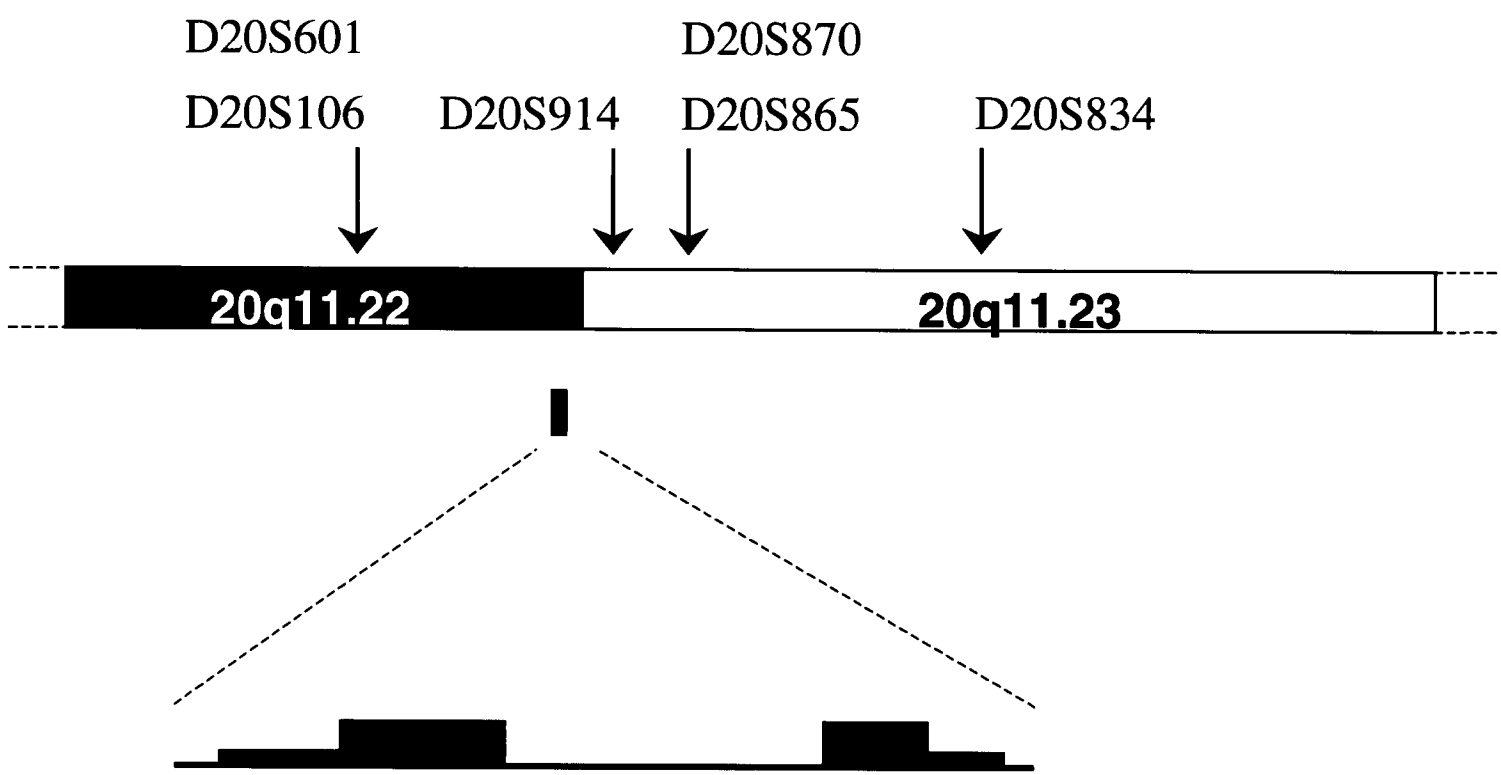

GDF5: 2 exons
span 4,878 bases
of genomic DNA

factor beta (TGF- β) family of secreted growth, differentiation, and morphogenesis factors [63, 70]. The gene has 2 exons and was mapped to chromosome 20q11.2 [138]. *GDF5*, also known as *CDMP1* (cartilage-derived morphogenetic protein 1) encodes a 501 amino acid precursor peptide with a 27 amino acid N-terminal signal peptide, a 354 amino acid prodomain, and a 120 amino acid C-terminal active domain [63] (Swiss Prot UniProt protein knowledgebase, Appendix I). All highly conserved TGF-β members share an Arg-X-X-Arg cleavage site and a 7-cysteine motif critical for proper folding and dimerization of the mature molecule [62, 63, 67]. They are initially produced as large precursor molecules, and 6 of the conserved cysteines are involved in the formation of intra-chain disulfide bonds; the seventh cysteine forms a disulfide bond with another monomer, forming a homo- or hetero-dimer [62]. Subsequent cleavage of the prodomains by subtilisin-like proteases forms the mature, active dimer (Figures 1.6D, 1.7A, 1.7B) [69].

GDF5 and 2 other related molecules, GDF6 and GDF7, were first discovered in mice by degenerate PCR because of their homology to other BMP family members [63]. GDF5 is expressed at sites of cartilage differentiation in the developing limbs [63, 67]. Overexpression and *in vitro* studies suggest that GDF5 is important in determining the size of skeletal precursors by increasing cell adhesion and accelerating chondrogenesis in a dose-dependent manner, which may account for the varying severity of diseases caused by mutations in *GDF5* [77]. GDF5 expression has also been observed in strong transverse stripes in the future joint space of skeletal precursors, representing one of the earliest known markers of joint formation [63, 79]. Recent work has proposed that

unprocessed GDF5 in the joint region acts to antagonize BMP signalling, preventing ossification and thus allowing the joint to form [75].

GDF5 was first reported because of its association with the *brachypodism* (*bp*) mouse, as 3 strains with functionally null *GDF5* mutants display a phenotype of shortened limbs, metacarpals, metatarsals, and absent middle phalanges [78]. Mutations in *GDF5* have also been found to be responsible for many chondrodysplasias and other appendicular skeleton deformities in humans.

Homozygous and compound heterozygous mutations in *GDF5* can cause severe chondrodysplasias such as DuPan syndrome, Hunter-Thompson type (CHTT), and Grebe type (CGT), as well as brachydactyly type C (BDC) [29, 83-87, 139]. Heterozygous mutations in *GDF5* have been shown to cause DuPan syndrome, BDC, brachydactyly type A2 (BDA2), angel-shaped phalangoepiphyseal dysplasia (ASPED), and congenital vertical talus (CVT) [24, 28, 88-94]. Furthermore, the heterozygous *GDF5* mutation carriers in the CGT families reportedly exhibit a mild phenotype of brachydactyly types A1, A4, and C [66, 83, 86, 95]. Finally, in addition to causing chondrodysplasias and brachydactylies in humans, heterozygous mutations in *GDF5* can cause multiple synostoses syndromes (SYNS1 and SYNS2) and proximal symphalangism (SYM1) [94, 96, 97].

In summary, *GDF5* is a good candidate for BDA1 pathogenesis because of its known role in determining the size of cartilage skeletal precursor elements. Furthermore, missense and null mutations in *GDF5* have already been associated with many other types of skeletal malformations in both humans and mice, including chondrodysplasias, brachydactylies and limb symphalangisms.

6.2 Materials and Methods

6.2.1 Primer Design

All *GDF5* PCR and sequencing primers were designed using DS Gene software (Accelrys, San Diego, California) or the Primer3 online software (Appendix I). All primers were synthesized by Sigma Genosys (Sigma-Aldrich Canada, Oakville, Ontario). Concentrated primer stocks were resuspended in 10 mM Tris-HCl, pH 8.0, 0.1mM EDTA, and diluted in ddH_2O to a 17 μM working solution.

6.2.2 Sequence Analysis

GDF5

The two-exon gene *GDF5* was amplified and sequenced as described in section 3.2.3 in the probands of families 4 and 18. It was also amplified in the proband of family 21 (see chapter 3), and six sporadic cases of BDA1: 6-03, 8-01, 9-01, 11-01, 17-01, and 19-01 (see Appendix V). Primers and optimized conditions are described in Table 6.1.

6.2.3 Investigation of Nucleotide Changes in *GDF5*

6.2.3.1 Sequencing

GDF5 exon 1 variant in family 17

Sequencing of the region flanked by markers GDF5x1F2.2/x1R2.2 in individuals 17-02 and 17-03 (Appendix V) was performed as described in section 3.2.3 to detect the presence of a c.349G>T nucleotide change seen in the proband 17-01.

Table 6.1. Sequence of primers and conditions used to amplify and sequence the *GDF5* gene. Parameters of the amplification programs are described in Appendix II. Primers denoted with an asterix were used for amplification and sequencing of families 4 and 18 only.

GDF5 Exon	Primer Name	Primer Sequence	Primer Annealing Temperature	Final $[MgCl_2]$ (mM)	PCR Product Size
5' UTR	GDF5x1F1	CGCCATTCTTCCTTCTTGG	60	1.5	391 bp
	GDF5x1R1	AGAAAGTGAGGAGTTTGGGG			
Exon 1	GDF5x1F2*	TGCTGCCGCTGTTCTCTTTG	65	1.5	425 bp
	GDF5x1R2*	TGTCCTTTTGGGGTCACAGTCC			
Exon 1	GDF5x1F2.2	TCCTTCTGCTGCTACTGCTG	65	1.5	555 bp
	GDF5x1R2.2	CTGGGGACAGATCCTGCTT			
Exon 1	GDF5x1F3	CCAAACAAGGCAGGCTACAG	65	1.5	403 bp
	GDF5x1R3	ATGCACACAGTGTCTCCCAC			
Exon 2	GDF5x2F1b	TGGTGAGGTTGCAGGGAATG	68	2.0	382 bp
	GDF5x2R1b	TCCAGATGTCGAACACCTCC			
Exon 2	GDF5x2F2	TGGGAGGTGTTCGACATCTG	68	1.5	414 bp
	GDF5x2R2	GTGGAAAGCCTCGTACTCAAG			
Exon 2	GDF5x2F3	GGAAGGCACTGCATGTCAAC	62	1.5	406 bp
	GDF5x2R3	TGTGTAGATGCTCCTGCCAC			
Exon 2	GDF5x2F4	TCCTGCACTCCTGGAATCAC	60	1.5	421 bp
	GDF5x2R4	CTCTTCTCTCCCACTCTTGC			
3' UTR	GDF5x2F5	CTCCTCAAATCACATTTGTGC	58	1.5	388 bp
	GDF5x2R5	TTTGGAAGGAACAGGAATGC			
Exon 2	GDF5x2F6*	AAGAAGCCCTCGGACACG	58	1.5	700 bp
	GDF5x2R6*	GGATGCTGATGGGACTCAG			

6.2.3.2 Restriction Digest

GDF5 exon 2 variant in family 17

To detect the presence of a g.2345T>C nucleotide change in the *GDF5* gene of members of family 17, the region flanked by markers GDF5x2F5/x2R5 was first amplified by PCR in DNA samples 17-01, 17-02 and 17-03. Restriction digest was performed in 20 μl volumes, containing 8 μl PCR product, 2.0 μl of 10X Amersham Buffer H, 0.2 μl of the *Hinf*I enzyme, and 9.8 μl ddH_2O. Reactions were incubated on a PTC-225 thermal cycler (MJ Research, Waltham, MA) at 37°C for 2 hours. Products were loaded on to a 1.5% agarose gel containing ethidium bromide, electrophoresed for 40 minutes at 100V, and photographed under UV light.

6.2.3.3 Allele-Specific Oligonucleotide Hybridization

GDF5 exon 2 variant in family 4

To detect the presence of a c.1138C>T nucleotide change in the *GDF5* gene of family 4, all members were examined by sequence analysis. Allele-specific oligonucleotide hybridization (ASOH) was performed on the proband and 100 control individuals to confirm genotypes and eliminate the possibility that the change was a rare polymorphism. Oligonucleotides specific to both the wild-type (GGCGAAAACGGCGGGCC) and mutant (GGCGAAAATGGCGGGCC) alleles were end-labelled with γ-^{32}P ATP using T4 polynucleotide kinase (USB, Cleveland, Ohio) according to manufacturer's suggested protocol. Unincorporated phosphates were removed with a G-25 Sephadex spin column (GE Healthcare, Fairfield, CT) according to the manufacturer's suggested protocol. Probe activity was measured with a scintillation

counter. A region of *GDF5* exon 2 was amplified in all family members and 100 control individuals by PCR as described in section 3.2.3. PCR products were electrophoresed through 1.5% agarose gels and transferred onto Hybond-N membranes (GE Healthcare, Fairfield, CT) for three hours under denaturing conditions (0.5 N NaOH, 1.5 M NaCl). The blots were then neutralised (1M Tris-Cl, pH 7.5, 1.5 M NaCl) for 15 minutes. The DNA was UV crosslinked to the membranes. Membranes were then prehybridized with 10 mL of prehybridization solution (5X SSPE, 5X Denhardt's, 1% SDS) for 1 hour at hybridization temperature. The labelled probe was denatured at 95°C for 5 minutes, and 0.8 x 10^6 cpm of labelled probe was added per ml of hybridization solution. Blots were probed for 1 hour with hybridization solution containing either the wild-type probe at 62°C or the mutant labelled probe at 60°C. Membranes were washed twice for 15 minutes with 100 ml of wash solution (2X SSPE, 0.1% SDS) at hybridization temperature and then exposed to x-ray film at -80°C for 2-3 hours. This procedure was repeated for both primers.

GDF5 exon 2 variant in family 18

To detect the presence of a c.1195C>T nucleotide change in the *GDF5* gene of family 18, all members were examined by sequence analysis. ASOH was performed on the proband and 100 control individuals to confirm genotypes and eliminate the possibility that the change was a rare polymorphism. The procedure was performed as described above. Blots were probed with wild type probe (5'-CTTAAGGCTCGCTGCAGT- 3') at 56°C or mutant probe (5'-CTTAAGGCTTGCTGCAGT- 3') at 54°C.

6.3 Results

6.3.1 Phenotype of BDA1 Families

Individuals from 3 familial BDA1 cases and 6 sporadic cases of diverse ethnic and regional backgrounds were examined (Appendix V). Families 4 and 18 will be described here. Family 21 was described in section 3.3.1, and the 6 sporadic cases have been previously described (Appendix V) [109, 136]. Of the 6 sporadic cases of BDA1 examined, many are syndromic forms, having been described in conjunction with other features. Consequently, the families here share a general diagnosis of BDA1, but vary in the severity, associated features, and familial or sporadic transmission of the trait.

Family 4

We studied 11 members of an American family of Scandinavian descent with BDA1 reportedly segregating as an autosomal dominant, fully penetrant disorder in at least 6 generations. The family was referred to the Shriners Hospital for Children in Houston, Texas, where the 2-year-old female proband (individual 4-Pp in Figure 5.1) was diagnosed with brachydactyly and bilateral deformities of the feet. She had short fingers and short first and third to fifth metacarpals. A single bilateral simian crease replaced the usual 3 creases. She also had congenital bony malformations of the lower extremities, especially the feet. She was placed in multiple casts in attempt to correct her foot deformities. The proband had pes planus (flat feet), but this was likely inherited independently of the BDA1 phenotype as her unaffected mother also had pes planus. There was a remarkable family history for brachydactyly; the proband's father,

grandmother and great-grandfather were all known to be affected, as well as an aunt and cousin. No further abnormalities were described in the family.

Family 18

We studied 8 members of a French Canadian family with BDA1 segregating potentially as an autosomal recessive syndrome, or a semi-dominant syndrome. The proband (individual 18-01 in Figure 5.1) came to attention after her daughter was referred to the Genetics Clinic for an unrelated condition. BDA1 was suspected and confirmed on radiological imaging. The family history revealed that a brother and sister had similar findings and there were also two unaffected sisters. Another brother, who may have had brachydactyly, passed away at an early age. The parents were second cousins (Figure 5.1) and were reportedly unaffected. Among her siblings, the proband was the only affected individual to have children. Radiographs of the hands and feet of the proband and her son were obtained for detailed examination (Figures 6.2B, 6.3B). Metacarpophalangeal profiles (MCPP) of the proband and her heterozygous son were completed by the physician using the ANTRO program. The radiographs and MCPP of the proband demonstrated significantly shortened middle phalanges of digits 2-5 (Figures 6.2, 6.3, 6.4). A very short first metacarpal was observed, giving the appearance of a very proximally placed thumb. The third to fifth metacarpals showed less marked shortening. The feet were likewise affected. The ulnar styloid process was truncated. Additionally, the two affected sisters were treated for clubfoot as children, and all homozygous affected siblings are shorter than their unaffected sisters. There are no other health concerns. The proband's son was examined and was noted to be of average

Figure 6.2. Photographs and hand radiographs of the severely affected proband of family 18. (A) Picture of the hands of the adult proband, individual 18-01, showing short fingers and a proximally-placed thumb. (B) Radiographs of the left and right hands of the proband. The middle phalanges in digits 2 to 5 are very short. The first metacarpal of both hands is also very short.

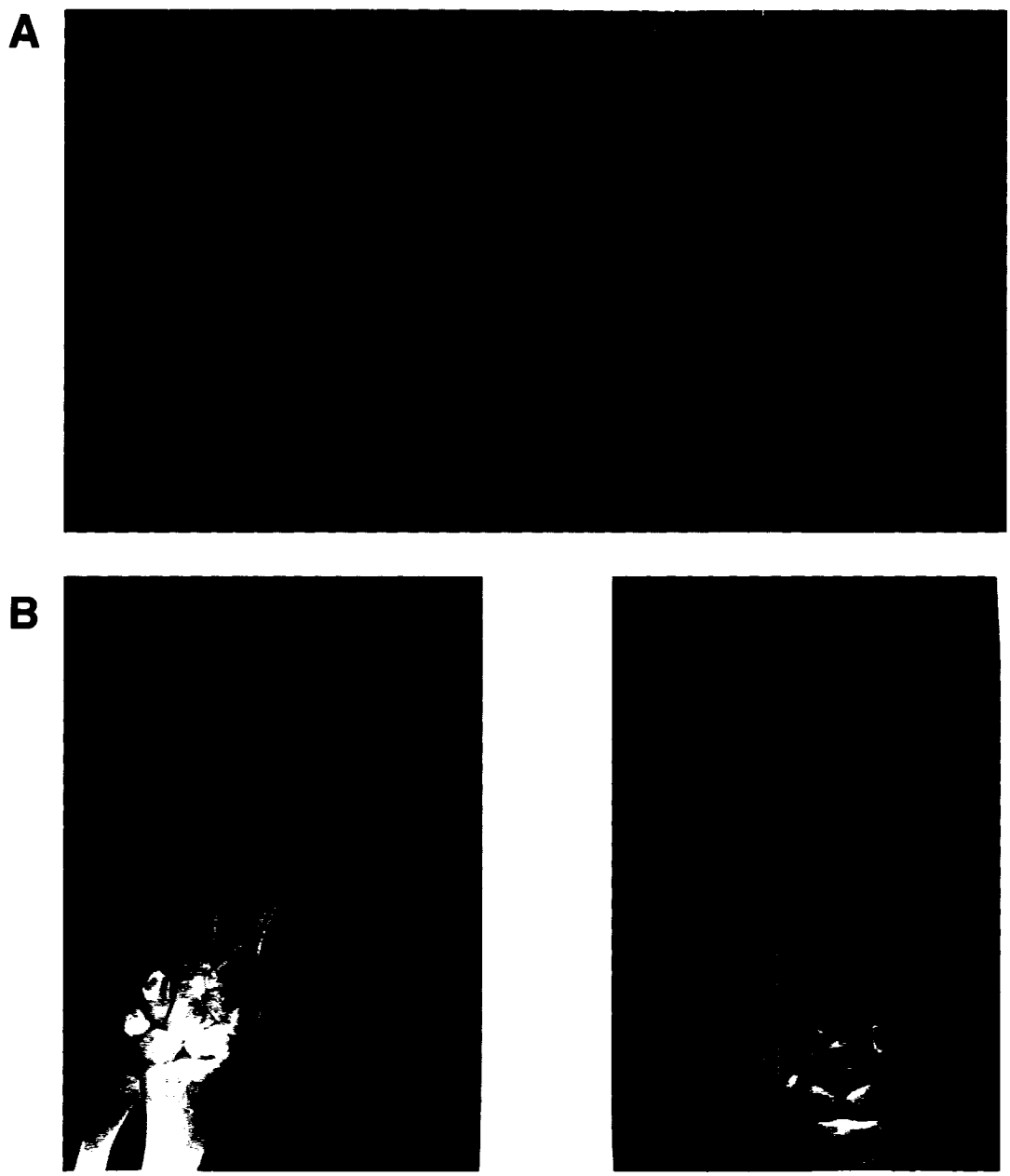
A
B

Figure 6.3. Photographs and hand radiograph of individual 18-02. (A) Picture of the hands of individual 18-02 at 8 years of age, showing fingers that appear to be of normal length. (B) Radiograph of the right hand of individual 18-02. The physician reported that the bones appeared to be of normal length. This individual was later classified as being mildly affected.


A
B

Figure 6.4. Metacarpophalangeal profiles (MCPP) of individuals 18-01 and 18-02. The bone lengths are depicted on the graph in the sequence of distal phalanges (order digits 5-1), middle phalanges (order digits 5-2), proximal phalange (order digits 5-1), and metacarpals (order digits 5-1). The MCPP of individual 18-01 (A) shows an extremely short first metacarpal and middle phalanges and first metacarpal. Individual 18-02 (B) shows the same general pattern as 18-01 with a short first metacarpal and short middle phalanges, but is a much less severe case. A normal individual would be expected to have phalanges within +/- 2 standard deviations from the age-and-sex-matched average (denoted as "0").

A

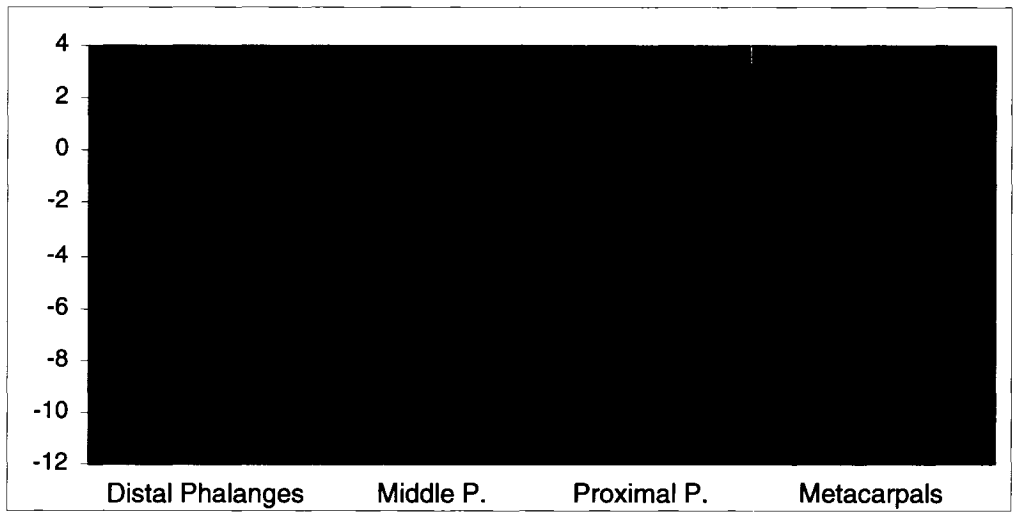
4
2
0
-2
-4
-6
-8
-10
-12
Distal Phalanges
Middle P.
Proximal P.
Metacarpals

B

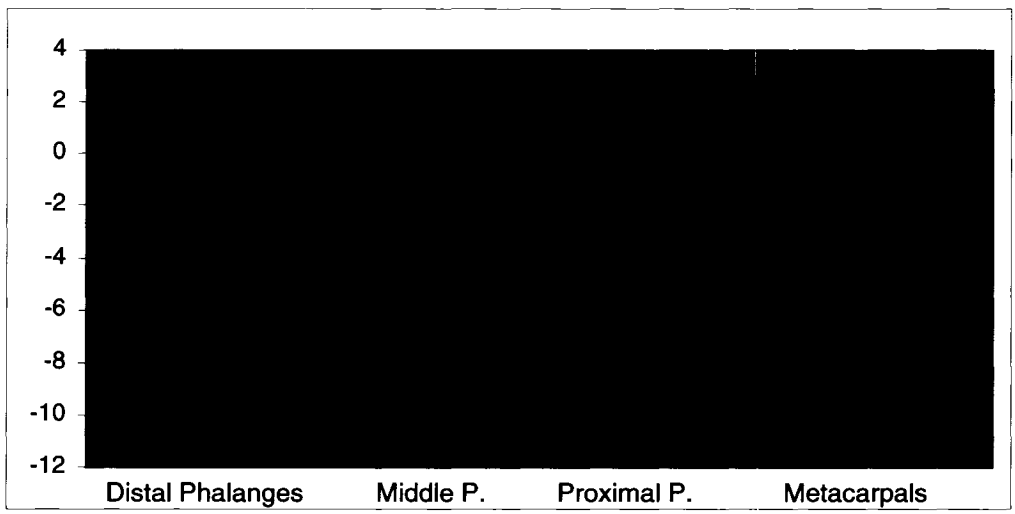
4
2
0
-2
-4
-6
-8
-10
-12
Distal Phalanges
Middle P.
Proximal P.
Metacarpals

height. His hands and feet appeared unremarkable. Radiographs of his hands did not reveal any striking changes, however his MCPP revealed that his middle phalanges of the second to fifth digits were short, especially for the second digit (Figures 6.3, 6.4). His first metacarpal was also short.

6.3.2 Evaluation of *GDF5* by DNA Sequencing in 3 Familial and 7 Sporadic Cases of BDA1

Three families (4, 18, 21) and 6 sporadic cases (6-03, 8-01, 9-01, 11-01, 15-01, 17-01, 19-01) were evaluated for *GDF5* mutations by DNA sequencing of the two exons, flanking splice sites, and associated untranslated regions in the proband of each family (Figures 5.1, 3.1). Three exonic single nucleotide polymorphisms (SNPs) were detected in the sequence; one of these was observed in an unaffected control, and the other 2 were listed as SNPs in the Ensembl Genome Browser Transcript Report (Table 6.2, Appendix I). One SNP was silent, coding for synonymous amino acids. The other two SNPs led to p.A117S and p.S275A substitutions. Additionally, 3 other SNPs were observed in the 3' un-translated region (UTR) of GDF5. All of these SNPs were observed in an unaffected control.

A heterozygous c.1138C>T nucleotide change was present in the DNA of individual 4-Pp (Figure 6.5). Sequence analysis confirmed that this c.1138C>T change was present exclusively in the affected family members. None of the unaffected family members carried the nucleotide change. In order to determine if this change was simply a rare polymorphism, the DNA of 100 control individuals was amplified and probed by ASOH with both wild-type and mutant oligonucleotides. The c.1138C>T nucleotide

Table 6.2. List of nucleotide and amino acid changes seen in the *GDF5* gene of individuals 1-19, 6-03, 8-01, 9-01, 11-01, 17-01, 19-01, 21-01, 4-Bb and 18-01.

GDF5 exon	Nucleotide change	Position of nucleotide change	SNP status	Codon change	Amino acid or splice site change	Genotypes observed
5'UTR	T>C	-48 of ATG	rs143384	---	---	T/T, C/C, T/C
Exon 1	G>T	c.349	Seen in unaffected parent 17-02	GCT>TGC	Ala117Ser	G/G, G/T
Exon 2	T>G	c.826	rs224331	TCC>GCC	Ser275Ala	T/G, G/G, T/T
Exon 2	G>A	c.1017	rs224330	AAG>AAA	Synonymous	G/A, G/G, A/A
Exon 2	C>T	c.1138	---	CGG>TGG	Arg380Trp	C/T, C/C
Exon 2	C>T	c.1195	---	CGC>TGC	Arg399Cys	C/C, T/T
3'UTR	A>C	+335 of exon 2	Seen in unaffected control	---	---	C/C, A/A
3' UTR	T>C	+425 of exon 2	Seen in unaffected control	---	---	T/T, C/C, T/C
3' UTR	T>C	+520 of exon 2	Seen in unaffected parent 17-02	---	---	T/C, T/T

Figure 6.5. Chromatograms showing the *GDF5* mutation found in affected members of family 4. (*A*) Wild type sequence and (*B*) the mutant heterozygous c.1138C>T nucleotide change (arrow) predicted to lead to the amino acid substitution R380T.

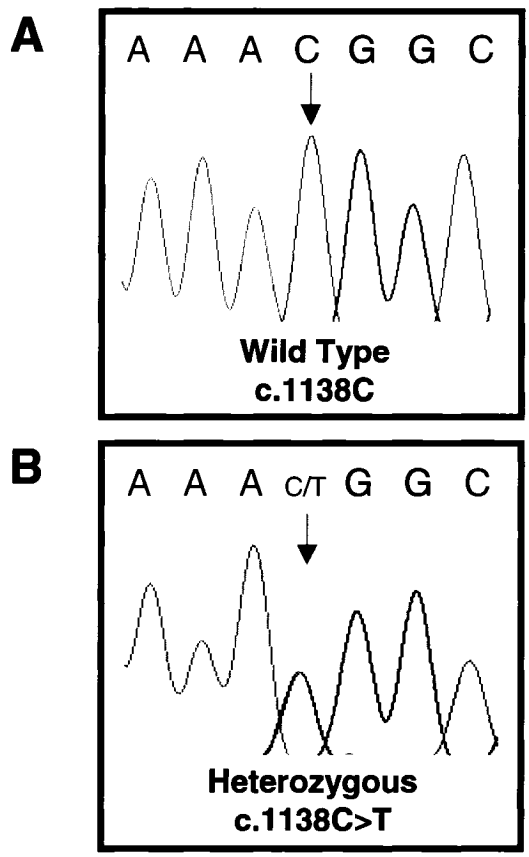
A
A A A C G G C
Wild Type
c.1138C
B
A A A C/T G G C
Heterozygous
c.1138C>T

change was not seen in any of the 200 control chromosomes evaluated.

A homozygous c.1195C>T nucleotide change was present in the DNA of individual 18-01 (Figure 6.6). Sequence analysis confirmed that all 3 affected siblings were homozygous for this c.1195C>T nucleotide change; none of the unaffected siblings carried the change. Only the DNA of the son of 18-01 was available to be examined for the mutant, and he was found to be heterozygous for the nucleotide change. In order to determine if this change was simply a rare polymorphism, the DNA of 100 control individuals was amplified and probed by ASOH with both wild-type and mutant oligonucleotides. The c.1195C>T nucleotide change was not seen in any of the 200 control chromosomes evaluated.

In summary, we have identified a heterozygous nucleotide change in affected individuals of family 4, and a homozygous nucleotide change in affected individuals of family 18. In the remaining individuals (6-03, 8-01, 9-01, 11-01, 17-01, 19-01, 21-01), we have excluded mutations in the exons, UTRs, and flanking sequences of *GDF5* as the cause of BDA1.

6.4 Discussion

6.4.1 Scope of Discussion

Here we present molecular, radiological and clinical data on a consanguineous French-Canadian family with partially dominant BDA1. Homozygous individuals display a severe phenotype, while a heterozygous individual has a mild phenotype, apparent only upon the generation of a metacarpophalangeal profile. These results

Figure 6.6. Chromatograms showing the *GDF5* mutation found in affected members of family 18. (*A*) Wild type sequence and mutant (*B*) heterozygous and (*C*) homozygous c.1195 C>T nucleotide changes (arrows) predicted to lead to the amino acid substitution R399C.

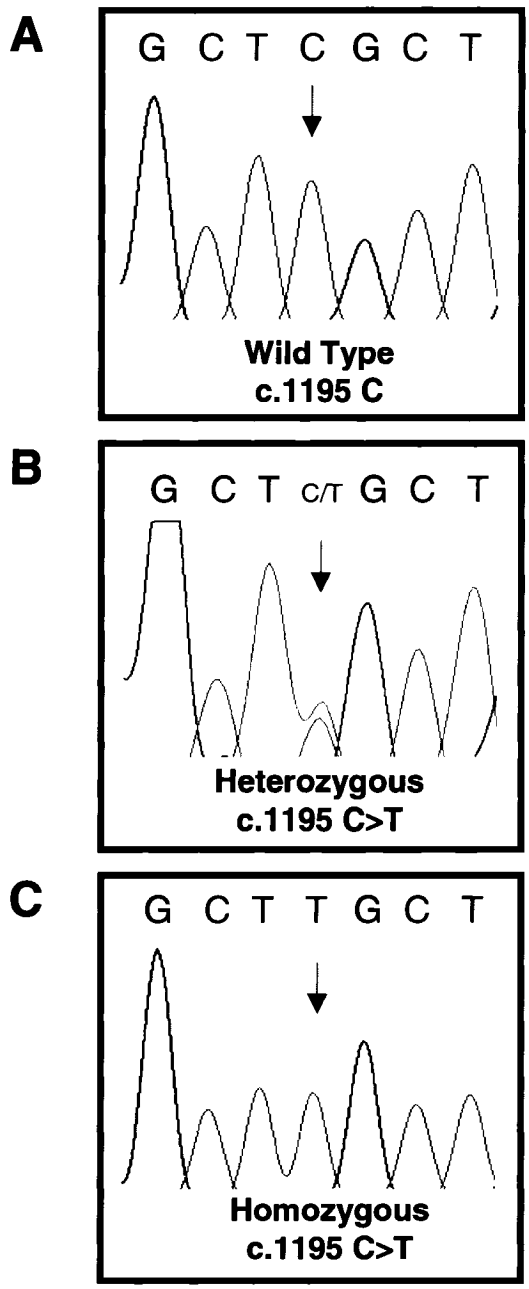
A
G C T C G C T
Wild Type
c.1195 C
B
G C T C/T G C T
Heterozygous
c.1195 C>T
C
G C T T G C T
Homozygous
c.1195 C>T

implicate mutations in *GDF5* in the development of BDA1 for the first time.

Although we have also presented data on an American family with fully penetrant, autosomal dominant BDA1, recently obtained evidence indicates that this family is actually affected with Brachydactyly type C (BDC). Close inspection of radiographs of the proband and her affected grandmother suggest that the middle phalanges are not equally affected, with the middle phalange of the fourth digit appearing normal (Figure 6.7). As previously described, this is the hallmark feature of BDC. Unfortunately, there was no mention of this feature in the physician's original report, and radiological data was only provided following the generation of the present molecular data. Therefore, for the purpose of this discussion, family 4 will be treated as a family affected with BDC.

We do not believe that the mis-diagnosis of family 4 has any effect on the outcome of molecular findings for family 18. Although the candidate gene region initially used to identify *GDF5* was based on a region of overlap for both families, if the study had been conducted with family 18 alone, chromosome 20 would still have been examined first because of the promising LOD scores obtained in that region. Furthermore, the candidate region for family 18 alone would only grow to 2.14 cM and would include a gene-poor region encompassing the centromere. *GDF5* would remain the best positional candidate for BDA1 pathogenesis in this family and would have remained the first gene examined for disease-causing mutations. That overlapping linkage data was used to identify mutations in one gene in members of 2 separate families with different diagnoses is considered a fortunate coincidence.

Figure 6.7. Hand radiographs of two members of family 4. (A) Radiographs of the left and right hands of individual 4-Ll. The middle phalanges in digits 2, 3, and 5 and the first metacarpals are very short in both hands. The proximal phalanges in digits 3 are also short. The spared middle phalanges of digit 4 in both hands warranted re-classification of this family to brachydactyly type C. (B) Radiograph of the right hand of individual 4-Pp at 2 years of age. Although the radiograph is of poorer quality, the same pattern of short middle phalanges in digits 2, 3 and 5 with a spared middle phalange in digit 4 can be seen.

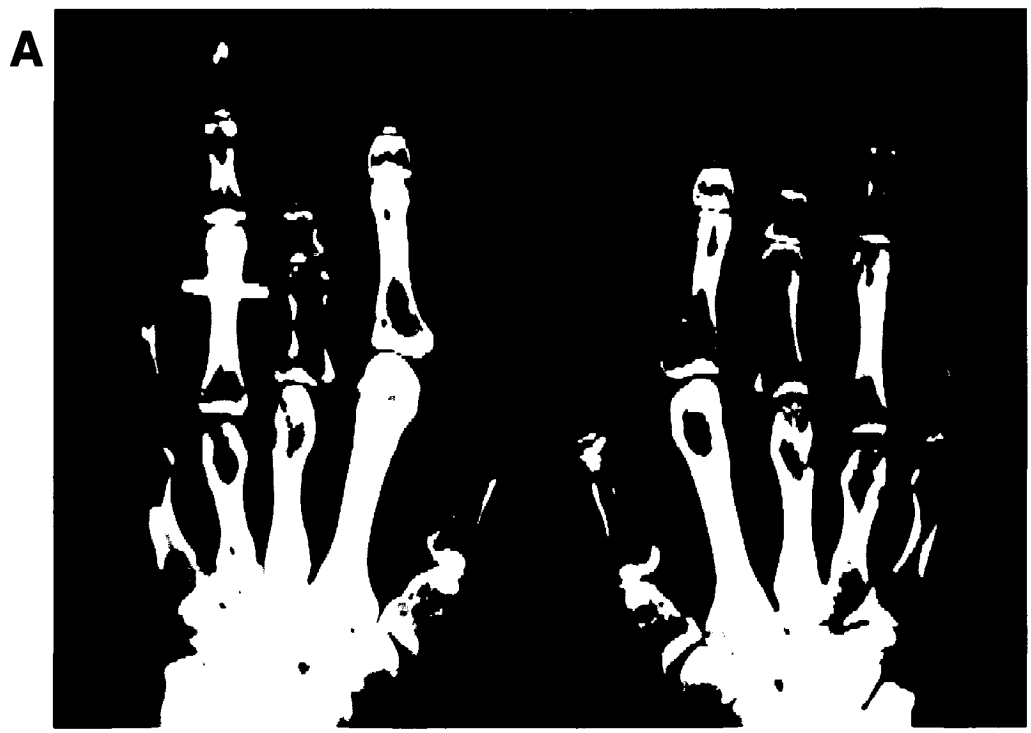
A


B

6.4.2 Molecular Findings

To investigate whether mutations in *GDF5* are the cause of BDA1 in family 18 and BDC in family 4, we determined the sequence of the two exons encoding *GDF5* in the probands of each family. In family 18, we have identified a homozygous c.1195C>T mutation in all affected siblings. The son of the proband was heterozygous for the change. The mutation caused an arginine to cysteine amino acid substitution at position 399. This nucleotide change was not seen in 200 unrelated non-brachydactyly control chromosomes.

Conservation of the Arg399 residue across species and other GDF family members (Figure 6.8) is evidence that the p.R399C mutation is disease-causing. We hypothesize that the introduction of a cysteine at this position may disrupt the highly-conserved 7-cysteine motif critical for proper dimerization and maturation of GDF5. Six of the 7 cysteines normally present in the active region of GDF5 form intra-chain disulfide bonds within the monomer, with links between cysteines 19 and 85, 48 and 117, and 52 and 119 (Figure 1.7) [140]. The last cysteine, at position 84, forms an inter-monomer disulfide bond to create a dimer (Figure 1.7) [140]. In family 18, the R399C substitution takes place in position 18 of the active region of the GDF5 monomer. It is feasible that while cysteines 19 and 85 are brought in close contact for an intra-chain disulfide bond, the mutant cysteine at position 18 would come in close contact with the cysteine at postion 84, potentially forming another intra-chain disulfide bond. Alternatively, the mutant cysteine could form an intra-chain disulfide bond with any of the other cysteines, altering the overall tertiary structure of the monomer. Either of these situations could prevent the formation of a GDF5 dimer.

Figure 6.8. Alignment of the partial amino acid sequence of human GDF5 with those of other species, as well as with human GDF6 and GDF7. The human GDF5 (amino acids 377 to 501) was aligned with GDF5 proteins from a number of species, namely the chimpanzee, mouse, horse, chicken, and frog GDF5, as well as human GDF6 and GDF7. Residues associated with disease are indicated by an arrow. The homozygous mutation R399C is associated with BDA1 in this study (denoted by an asterisk). The heterozygous mutation R380T is associated with BDC in this study (denoted by a double asterisk). Heterozygous mutations R438L are associated with SYNS1 and SYM1, R438C is associated with CVT, R438C and C498S are associated with BDC, and L441P is associated with BDA2. Homozygous mutation C400Y is associated with CGT, L441P is associated with DuPan syndrome, and 1475ins22 is associated with CHTT.

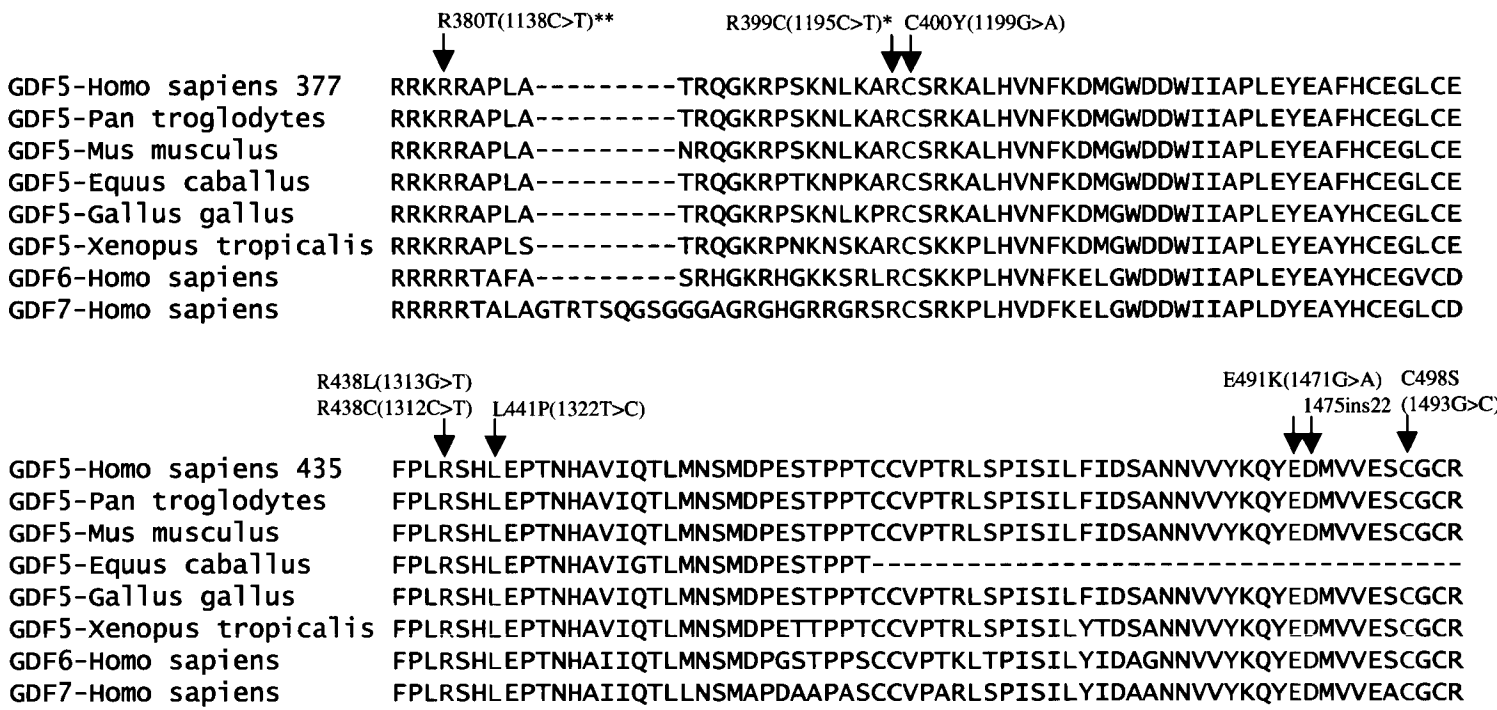
R380T(1138C>T)**
R399C(1195C>T)*
C400Y(1199G>A)
GDF5-Homo sapiens 377 RRKRRAPLA---------TRQGKRPSKNLKARCSRKALHVNFKDMGWDDWIIAPLEYEAFHCEGLCE
GDF5-Pan troglodytes RRKRRAPLA---------TRQGKRPSKNLKARCSRKALHVNFKDMGWDDWIIAPLEYEAFHCEGLCE
GDF5-Mus musculus RRKRRAPLA---------NRQGKRPSKNLKARCSRKALHVNFKDMGWDDWIIAPLEYEAFHCEGLCE
GDF5-Equus caballus RRKRRAPLA---------TRQGKRPTKNPKARCSRKALHVNFKDMGWDDWIIAPLEYEAFHCEGLCE
GDF5-Gallus gallus RRKRRAPLA---------TRQGKRPSKNLKPRCSRKALHVNFKDMGWDDWIIAPLEYEAYHCEGLCE
GDF5-Xenopus tropicalis RRKRRAPLS---------TRQGKRPNKNSKARCSKKPLHVNFKDMGWDDWIIAPLEYEAYHCEGLCE
GDF6-Homo sapiens RRRRRTAFA---------SRHGKRHGKKSRLRCSKKPLHVNFKELGWDDWIIAPLEYEAYHCEGVCD
GDF7-Homo sapiens RRRRRTALAGTRTSQGSGGGAGRGHGRRGRSRCSRKPLHVDFKELGWDDWIIAPLDYEAYHCEGLCD
R438L(1313G>T)
R438C(1312C>T)
L441P(1322T>C)
E491K(1471G>A)
1475ins22
C498S
(1493G>C)
GDF5-Homo sapiens 435 FPLRSHLEPTNHAVIQTLMNSMDPESTPPTCCVPTRLSPISILFIDSANNVVYKQYEDMVVESCGCR
GDF5-Pan troglodytes FPLRSHLEPTNHAVIQTLMNSMDPESTPPTCCVPTRLSPISILFIDSANNVVYKQYEDMVVESCGCR
GDF5-Mus musculus FPLRSHLEPTNHAVIQTLMNSMDPESTPPTCCVPTRLSPISILFIDSANNVVYKQYEDMVVESCGCR
GDF5-Equus caballus FPLRSHLEPTNHAVIGTLMNSMDPESTPPT----------
GDF5-Gallus gallus FPLRSHLEPTNHAVIQTLMNSMDPESTPPTCCVPTRLSPISILFIDSANNVVYKQYEDMVVESCGCR
GDF5-Xenopus tropicalis FPLRSHLEPTNHAVIQTLMNSMDPETTPPTCCVPTRLSPISILYTDSANNVVYKQYEDMVVESCGCR
GDF6-Homo sapiens FPLRSHLEPTNHAIIQTLMNSMDPGSTPPSCCVPTKLTPISILYIDAGNNVVYKQYEDMVVESCGCR
GDF7-Homo sapiens FPLRSHLEPTNHAIIQTLLNSMAPDAAPASCCVPARLSPISILYIDAANNVVYKQYEDMVVEACGCR

Additional evidence supporting our hypothesis is provided by reports that a p.R438C mutation, also found in the active domain of GDF5, is known to hinder monomer dimerization and secretion of the mature GDF5 protein *in vitro* [90, 97]. Although the precise effect of this additional cysteine is not known, the mutant protein is thought to lead to functional haploinsufficiency in heterozygotes, causing BDC, clinodactyly, or CVT phenotypes [89, 90]. In contrast, *in vitro* data on a p.R438L substitution at the same amino acid was shown to efficiently form and secrete mature GDF5 dimers [97]. This mutation is thought to increase GDF5 activity, and produces a phenotype of multiple synostoses syndrome [97]. These results suggest that although the same amino acid is mutated in both instances, the introduction of an additional cysteine leads to problems with formation, processing, and secretion of a mature active dimer which are not observed when R438 is replaced with a leucine. It also leads to a distinct phenotype.

Mutations that remove one of the 7 conserved cysteines have also been reported. Prior to the identification of GDF5, studies in TGF-β showed that mutating any of the conserved cysteine residues to a serine resulted in undetectable levels of the mature, secreted protein [141]. Recent studies with GDF5 have revealed similar results. In a consanguineous family with a p.C400Y GDF5 substitution, homozygotes have CGT, while heterozygote carriers have brachydactyly phenotypes [66]. Also, a heterozygous p.C498S substitution was found to cause BDC in one family [90]. In both instances, *in vitro* data showed that the mutant monomers were present in cell extracts, but that neither mutant is secreted as a mature, active dimer [66, 90]. Furthermore, Thomas et al. (1997) showed that the p.C400Y mutant can have a dominant-negative effect, inhibiting the

secretion of wild-type GDF5, BMP-2, BMP-3 and activin [66]. The GDF5 p.C400Y mutant is hypothesized to suppress the secretion of other BMP members by forming non-functional heterodimers, which are then targeted for degredation instead of secretion [66].

In family 4, we have identified a heterozygous c.1138C>T mutation in all affected members. The mutation caused an arginine to tryptophan amino acid substitution at position 380. This nucleotide change was not seen in 200 unrelated non-brachydactyly control chromosomes.

Conservation of the Arg380 residue across species and other GDF family members (Figure 6.8) is evidence that the p.R380W mutation is disease-causing. Furthermore, the R380 residue is the last arginine in the highly-conserved RXXR cleavage site of all orthologs of GDF5, RRKR [75]. Mutating the cleavage sites of Xenopus BMP7, BMP4 and activin resulted in the generation of monomers that could successfully dimerize but not be cleaved, making them incapable of maturing to active dimers. These mutant peptides acted in a dominant negative fashion, interfering with the signaling of other wild-type BMPs [142]. We hypothesize that p.R380W mutant monomers are able to dimerize but not cleave, preventing maturation and leading to haploinsufficiency of mature GDF5 during critical stages of development. The ability of these mutants to dimerize with wild-type monomers may further reduce the amount of active GDF5 available.

Although beyond the scope of this thesis, *in vitro* studies to determine the impact of the p.R380W and p.R399C mutations on GDF5 functionality have been initiated in the lab of a collaborator.

6.4.3 Genotypic Heterogeneity

Family 18 - Brachydactyly Type A1

To date, all BDA1 families with *IHH* mutations or linkage to the chromosome 5p13.3-p13.2 critical region display an autosomal dominant mode of transmission [16-23, 137]. In contrast, our *GDF5* family displays a partially-dominant mode of transmission. Individuals who are homozygous for the *GDF5* mutation display a BDA1 phenotype, while heterozygous individuals have a very mild phenotype apparent only upon the generation of a metacarpal phalangeal profile. Identifying this third BDA1 locus raised the question of whether a consistent phenotype exists between individuals with mutations in *IHH* and *GDF5*, and with those showing linkage to the 5p13.3-p13.2 critical region.

Typically, individuals with *IHH* mutations display a phenotype of short middle phalanges in digits 2-5 and a short proximal phalange in digit 1 [16, 18, 19, 21, 22]. However, one case has been described where the proximal phalange of digit 1 is spared [20]. Terminal symphalangism, in which a rudimentary middle phalange is fused to the distal phalange, has been described in many *IHH* cases [16, 17, 20-22, 143]. Individuals linked to the 5p13.3-13.2 critical region reportedly display a similar phenotype, though in a milder form [23, 137]. Metacarpophalangeal profiles revealed shortening of all phalanges and metacarpals in affected individuals, especially the middle phalanges. The middle phalange in digit 2, distal phalange in digit 1, and fifth metacarpal were noted to be the most affected bones. Terminal symphalangism was not observed in this family [23, 137].

In family 18, affected individuals homozygous for *GDF5* mutations display a

phenotype of very short middle phalanges in digit 2-5 with no terminal symphalangism. They also lack the shortening of the first proximal phalange seen in most families with *IHH* mutations. The unique clinical feature that distinguishes this family from all others described is a very short first metacarpal, giving the appearance of a very proximally placed thumb. This is a feature commonly observed in BDC, suggesting that GDF5 plays an important role in development of the first metacarpal. Additional features described in the homozygous individuals are short stature, a truncated ulnar styloid process, and club feet. Short stature and ulnar malformations have been described in some families with *IHH* mutations [3, 16, 18]. Club foot seems to be associated strictly with *GDF5* mutations. The MCPP of the one heterozygous individual examined clinically displayed the same general pattern as homozygous individuals, but with only very minor shortening of the middle phalanges and first metacarpal.

In summary, shortening or absence of the middle phalanges 2-5 is the only consistent feature seen in all BDA1 families. Mutations in *IHH*, *GDF5*, and the 5p13.3-p13.2 critical region can cause the same general BDA1 phenotype, with additional associated features depending on the causative gene in each family. Insight gained from murine models, such as the heterozygous *Short digits* (*Dsh/+*) mouse, indicates that there may be other genes able to produce the human BDA1 phenotype [135].

Family 4 – Brachydactyly Type C

In family 4, a heterozygous mutation in *GDF5* has been found to cause fully penetrant, autosomal dominant BDC. Previously, both heterozygous and homozygous mutations in *GDF5* have been shown to cause autosomal dominant and partially

dominant BDC [28, 29, 89-93, 139]. Variable expression and non-penetrance have also been observed in many affected families [89, 90, 93], but this was not observed in the kindred examined here.

BDC was initially thought to be a genetically heterogeneous disorder, as initial studies into the genetic basis of BDC led to the identification of linkage to chromosome 12q24 in one family [144]. However, following the identification of BDC-causing mutations in *GDF5* [28], the 12q24 family was found to carry a 23-bp insertion in *GDF5* that was co-inherited with the disorder [90]. Following this discovery, BDC returned to being described as locus homogeneous, as the identification of linkage at 12q24 in one family was a false positive, type I error [90].

However, it is important to note that a p.R486Q mutation in the bone morphogenetic protein receptor 1B (*BMPR1B*) gene has recently been reported in one individual with a phenotype resembling a combination of BDC and SYM1 [30]. The hallmark features of typical BDC involve shortening of the first metacarpal and the middle phalanges of digits 2, 3 and 5; hyperphalangy of digits 2 and 3 has also been observed. In this case, the proband had severely shortened digits 2 and 3, with relatively normal digits 1, 4, and 5. Radiographs revealed that middle phalanges were very small in digit 2, and absent in digit 3. Furthermore, the proximal phalanges in digit 3 developed with an abnormal curve, and the proximal and middle phalanges in digit 2 of the right hand were fused [30].

GDF5 acts through the receptor BMPR1B to assemble a receptor complex and activate the Smad signalling pathway, effectively regulating transcription of target genes (Figure 1.8) [70, 145]. Evidence from human and murine mutations prove that mutations

in *GDF5* and *BMPR1B* can cause similar phenotypes, as mutations in both genes are known to cause Brachydactyly Type A2 (BDA2), and the *BMPR1B*$^{-/-}$ mouse closely resembles the *GDF5*-null *brachypodism* (*bp*) mouse [24, 25, 94, 145]. Although the features described in the BDC-SYM1 individual are somewhat distinct from other reported cases of BDC, the direct interaction of GDF5 and BMPR1B during skeletal development suggests that mutations in either gene could cause a broad spectrum of BDC-like phenotypes.

6.4.4 Phenotypic Heterogeneity

In this study, we have identified mutations in *GDF5* that cause BDA1 in one family and BDC in another. Extensive phenotypic heterogeneity, in which mutations in the same gene yield a range of phenotypes [123], has been observed in families with *GDF5* mutations. The only general feature shared by families with *GDF5* mutations reported to date are malformations of the appendicular skeleton, with the more distal elements most severely affected. Previous studies have revealed that heterozygous mutations in *GDF5* can cause BDC, BDA2, angel-shaped phalangoepiphyseal dysplasia (ASPED), DuPan Syndrome, multiple synostoses syndromes (SYNS1 and SYNS2), proximal symphalangism (SYM1), and congenital vertical talus (CVT) [24, 28, 88-94, 97]. Additionally, homozygous mutations in *GDF5* can cause severe BDC, DuPan syndrome, Hunter-Thompson Type chondrodysplasia (CHTT), and Grebe Type Chondrodysplasia (CGT) [29, 83-87, 139]. The brachydactylies, chondrodysplasias, ASPED and CVT are all likely the result of haploinsufficiency, null, or dominant-negative mutations leading to impaired bone formation [28, 87, 139]. In contrast, the

synostoses and symphalangism phenotypes are thought to arise from gain of function mutations, which somehow increase signaling and prevent the formation of certain joints [94, 97].

Family 18, a consanguineous French Canadian family, represents the first case of true BDA1 reported to be caused by mutations in *GDF5*. Severely affected individuals had very short middle phalanges in digits 2-5, the hallmark feature of BDA1. It differs from other *GDF5* families described with BDC, in which the fourth middle phalange is spared, and *GDF5* families described with BDA2, in which only middle phalanges of digits 2, and sometimes 5, are affected [24, 28, 88-94]. In two instances, families have been described in which most individuals were affected with autosomal dominant BDC, but variable expression of the phenotype led to a very mild BDA1- or BDA2-like phenotype in a few individuals [91, 146].

Family 4 was initially described by Mastrobattista et al. (1995) and Kirkpatrick et al. (2003) [19, 99]. The family was initially diagnosed with BDA1, but radiographic evidence suggests the family is actually affected with BDC. Radiographs of the proband and her affected grandmother showed shortened middle phalanges of digits 2, 3, and 5 as well as shortened first and third to fifth metacarpals (Figure 6.7). In the grandmother, the proximal phalange of digit 3 was also quite short, especially on the left hand. A very short first metacarpal was also observed in affected individuals in family 18, with less marked shortening in the third to fifth metacarpals. This short first metacarpal gave the appearance of a very proximally placed thumb. This feature is very frequently observed in individuals with *GDF5* mutations, and has been observed in BDC, ASPED, DuPan syndrome, and CGT heterozygous carriers [29, 83, 92, 95, 139, 146, 147]. Interestingly,

the proband in family 4 also had a single bilateral simian crease, in place of the usual 3 creases. This feature has been observed in one other BDC family [148].

Foot anomalies were observed in both families 4 and 18. Two of the 3 affected individuals in family 18 were treated for clubfoot as children, and the proband in family 4 had her feet casted as a child for correction of bony malformations of the feet. Furthermore, the proband of family 4 had flat feet, but this may have been inherited independently of the brachydactyly phenotype as her unaffected mother also has flat feet. Many foot anomalies, including two forms of club foot (talipes equinovarus, where the foot is turned inwards, and congenital vertical talus, where the foot is rounded upwards like a rocker) have previously been observed in individuals with heterozygous mutations in *GDF5*. In 2 BDC families, three individuals who were non-penetrant for the BDC phenotype had bilateral congenital vertical talus (CVT), and one had BDC with bilateral calcaneovalgus feet (a malformation where the feet are pushed upwards towards the calf) [89, 93]. In 2 families with CGT, heterozygous mutation carriers were reported to have talipes equinovarus and/or hallux valgus (a malformation where the big toe is turned towards the outside of the foot) [83, 95]. Furthermore, in one family with proximal symphalangism, many affected individuals were reported to have an absent cuboid bone and very flat feet [149]. Additional features observed in the affected individuals of family 18 were a truncated ulnar styloid process and short stature, both of which have been previously noted in individuals with *GDF5* mutations [93, 139].

A comparison of the homozygote and heterozygote phenotypes provides information regarding the nature of the abnormal course of embryonic development, resulting in the complete syndrome [150]. The 3 severely affected siblings of family 18

embody only the second report of a homozygous *GDF5* mutation causing a brachydactyly phenotype; heterozygous mutation carriers have a very mild phenotype. In 2004, Schwabe et al. described a consanguineous family in which homozygous individuals had BDC with severe ulnar clinodactyly, and heterozygous carriers had only mild shortening of the fourth and fifth metacarpals [29]. Due to the existence of a mild phenotype in heterozygous carriers in both families, in both cases the disease transmission has been described as partially dominant.

Prior to these accounts, the only reported consanguineous mating of individuals with heterozygous *GDF5* mutations led to the development of severe chondrodysplasias in homozygotes. Consanguineous mating between heterozygous individuals with BDC- or BDA-like phenotypes led to many cases of CGT [83, 86, 95, 139], while consanguineous mating between heterozygous individuals with no discernible phenotype have led to cases of CHTT, CGT and DuPan syndrome [84, 85, 87, 88]. Additionally, a report of a consanguineous mating in a family with BDA2 caused by heterozygous mutations in *GDF5* led to the birth of one female child who was speculated to be homozygous for the mutation [24, 151]. This individual died at the age of 1 year, and family descriptions indicate that "her whole osseous system was in disorder" and that "her hands and feet...were entirely absent" [151]. Although this individual was never examined by the reporting physician, this account describes a condition similar to the CGT phenotype.

Wide variation in clinical expression of bone malformations amongst many families who share mutations in the same gene may reflect the interaction of other factors with the mutant allele. Evidence exists that epigenetics, transcriptional initiation, mRNA

splicing and stability, translational controls, post-translational modifications, and protein degradation can all lead to changes in gene expression that may have a direct effect on a phenotype [152]. Furthermore, genes at other loci, as well as non-genetic factors such as environmental and physiological conditions, can also play a role [124, 152]. These genetic and non-genetic modifiers can control penetrance, dominance, expressivity and pleiotropy of characteristic phenotypes in carriers of a particular mutant genotype [124]. These modifiers are likely responsible for the appearance of varied skeletal traits associated with mutations in *GDF5*.

6.4.5 Conclusions

In summary, we have presented evidence that mutations in *GDF5* are the cause of BDA1 in one family and BDC in another. These mutations cause amino acid substitutions at highly conserved codons and are predicted to disrupt the highly-conserved 7-cysteine motif and cleavage site critical for the dimerization and maturation of GDF5. The identification of *GDF5* mutations in kindreds with BDA1 and BDC supports ongoing findings implicating GDF5 in the pathogenesis skeletal malformations. Finally, this report identifies *GDF5* as the second gene for BDA1.

Chapter 7. Conclusions

7.1 Summary of Findings

Brachydactyly Type A1 has a long literary history. In 1903, BDA1 was the first human disease described in terms of autosomal dominant Mendelian inheritance. However, little was known about the molecular or genetic etiology of BDA1 until recently. A resurgence in research related to degenerative bone diseases has peaked research interest in bone development, and as such, studies to determine the molecular and genetic basis for the brachydactylies have increased in recent years.

Indian hedgehog (*IHH*) was the first gene reported to cause BDA1 [16]. A second BDA1 locus was subsequently described on chromosome 5, although a disease gene has yet to be identified [23]. We identified *GDF5* as a novel BDA1-causing disease gene, which allowed us to confirm the hypothesis that there are additional loci which, when mutated, can lead to BDA1.

The first objective of this project was to identify novel mutations in the *IHH* gene of BDA1-affected individuals. This goal was based on numerous reports that pathogenic mutations in this gene have caused a BDA1 phenotype in numerous other affected families [16, 18-22]. In this thesis, I have identified novel *IHH* mutations in two families. In a third family, I identified a previously described mutation. It is unlikely that this third family and the previously-described family with the same mutation share a common founder, as they have different ethnic backgrounds and geographical roots. This implies that this particular codon may be a mutational hotspot.

As an extension of the *IHH* project, a genetic link has been established between a New Zealand family and the previously published descendants of the Farabee and Drinkwater families. It is likely that descendants of one common founder, who carried the original *de novo* c.G298A *IHH* mutation, migrated to different parts of England, the United States, New Zealand and Australia. Throughout the years, the trait has been maintained amongst the families in an autosomal dominant fashion.

With one exception, all of the *IHH* mutations resulting in BDA1 are hypothesized to lie in a region which could interrupt receptor-ligand interactions [16]. Further investigations, including *in vitro* and *in vivo* studies, are beyond the scope of this thesis but are currently underway in the laboratory of Dr. Dennis Bulman (Ottawa Health Research Institute).

The second objective of the project was to identify one or more novel genes which, when mutated, cause BDA1. In this manuscript, we have identified linkage to a region on chromosome 20 in one family with BDA1. Subsequent narrowing of the region of interest led to the screening of the candidate gene *GDF5*, with the successful identification of a homozygous change in all affected individuals. Interestingly, we have described the first case of BDA1 which does not follow a strict autosomal dominant transmission pattern. Rather, the consanguineous nature of the parents of the affected sibship led to the hypothesis that the disorder may have been transmitted as an autosomal recessive disease. However, a mild phenotype observed in a heterozygous individual warranted classification of the disease in this family as a semi-dominant form of BDA1, in which both heterozygous and homozygous individuals display varying severities of a phenotype. Another family, in which the affected individuals also carried a mutation in

GDF5, was later determined to have been misdiagnosed. The family is actually affected with brachydactyly type C.

The *GDF5* mutation in the BDA1 family removes a highly-conserved cysteine, which may disrupt the tertiary structure of the mature GDF5 molecule. The mutation in the BDC family is located in the highly-conserved cleavage domain, thereby preventing cleavage of the mature region from the prodomain. Both mutants are hypothesized to prevent the formation of mature GDF5 dimers, thus interrupting standard GDF5 signaling and leading to the development of a BD phenotype. Further investigations into the molecular pathogenesis of these mutants are currently underway in the laboratory of Dr. T. Michael Underhill (University of British Columbia).

7.2 Conclusions on Genetic and Phenotypic Heterogeneity

A great deal of inter- and intra-familial heterogeneity was encountered in our studies of familial BDA1. The identification of a second disease-causing gene, *GDF5*, is evidence that BDA1 is in fact a genetically heterogeneous disease. Although a consistent shortening or absence of the middle phalanges in digits 2-5 was observed in all BDA1 families, a slightly different phenotype was observed in the *GDF5* family than in the *IHH* families. This gene-dependent variation is to be expected, as these two proteins may bear some individual functions that do not overlap, thus leading to slightly different phenotypes.

Phenotypic heterogeneity has also been observed within and between families with mutations in the same gene. However, this can be accounted for, as mutations at different codons in the same gene may adversely affect the protein's function in different

ways; this may lead to different variations of a phenotype, or entirely distinct phenotypes. This is especially true with *GDF5*, in which mutations have been reported to cause both mild to severe limb shortening diseases, as well as digit symphalangism phenotypes. The genetic background of an individual is also an important factor in determining the effect of a mutation on one's development, as modifier genes may have an effect on phenotypic outcome. This is especially evident when examining a variation in phenotype between family members who share an identical mutation.

7.3 BDA1-Causing Loci

The investigation to identify novel genes that cause BDA1 has been an ongoing project in the Bulman laboratory. A table listing all of the familial and sporadic cases of BDA1 that have been examined in this manuscript, as well as those previously studied by numerous predecessors in the lab, is shown in Appendix V. Tables A4 and A5 summarize the pertinent details of each family studied, including where a disease-causing mutation is located, if available. Of the twenty-one BDA1 cases examined in this lab, nearly 48% had a mutation in the Indian hedgehog gene, while only 5% had a mutation in *GDF5*. Only one family, representing 5%, has been demonstrated to be linked to a region on chromosome 5; an additional BDA1-causing disease gene is hypothesized to lie in this region. Finally, in 42% of our familial and sporadic BDA1 cases, a disease-causing mutation was not found. These families are of particular interest, as their lack of mutations in *IHH* and *GDF5* increases the likelihood that they may also have mutations in the chromosome 5 critical region. However, it does remain possible that there are additional genes whose protein products participate in the same bone

development pathway and which, when mutated, can cause BDA1. Additional work is required to identify the disease-causing mutations in these individuals.

Appendix I
Electronic Database and Sequence Accession Information

University of California Santa Cruz (UCSC) Genome Browser:
http://genome.ucsc.edu/

Genomic Accession:
- IHH – NCBI Build 36.1, NM_000557
- GDF5 – NCBI Build 35, NM_002181

Ensembl Genome Browser Transcript report:
http://www.ensembl.org/index.html

Transcript Reports:
- GDF5 – ENST00000374369
- IHH – ENSG00000163501

Swiss Prot UniProt Protein knowledgebase,
http://www.expasy.org/sprot/

UniProtKB/TrEMBL entry:
- IHH Homo sapiens – Q14623
  - IHH Mus musculus – P97812
  - IHH Gallus gallus – Q98938
  - Banded HH Xenopus laevis – Q91612
  - Echidna Hh Danio rerio – Q98862
  - SHH Homo sapiens – Q15465
  - DHH Homo sapiens – O43323
- GDF5 Homo sapiens – P43026
  - GDF5 Mus musculus – P43027
  - GDF5 Equus caballus – Q3LSM3
  - GDF5 Gallus gallus – Q9W6G0
  - GDF5 Xenopus tropicalis – Q68KG0
  - GDF6 Homo sapiens – Q6KF10
  - GDF7 Homo sapiens – Q7Z4P5

National Center for Biotechnology Information (NCBI):
http://www.ncbi.nlm.nih.gov/

NCBI Entrez Protein Sequence Viewer:
http://www.ncbi.nlm.nih.gov/entrez/query.fcgi?db=Protein

Protein Accession:
- GDF5 Pan troglodytes – XP_001164592

NCBI Single Nucleotide Polymorphism Database:
http://www.ncbi.nlm.nih.gov/entrez/query.fcgi?db=snp

NCBI Map Viewer:
http://www.ncbi.nlm.nih.gov/mapview/

NCBI UniSTS:
http://www.ncbi.nlm.nih.gov/entrez/query.fcgi?db=unists

NCBI Online Mendelian Inheritance in Man (OMIM):
http://www.ncbi.nlm.nih.gov/entrez/query.fcgi?db=OMIM

BDA1: 11250, 607004
BDC: 113100
IHH: 600726
GDF5: 601146

Primer3 online primer design software:
http://frodo.wi.mit.edu/cgi-bin/primer3/primer3_www.cgi

Appendix II
Thermal Cycling PCR Programs for Amplification, Sequencing and Genotyping

Program Temperature (TM) X°C:

1. 94°C for 2 min
2. 94°C for 30 sec
   X°C for 30 sec
   72°C for 30 sec
3. Go to step 2, 29 times
4. 72°C for 10 min
5. 15°C forever

Program TM X°C, 40 cycles:

1. 94°C for 2 min
2. 94°C for 30 sec
   X°C for 30 sec
   72°C for 30 sec
3. Go to step 2, 39 times
4. 72°C for 10 min
5. 15°C forever

Program Touchdown (TD) 50°C:

1. 94°C for 5 min
2. 94°C for 30 sec
   66°C for 30 sec; -1°C per cycle
   72°C for 30 sec
3. Go to step 2, 14 times
4. 94°C for 30 sec
   50°C for 30 sec
   72°C for 30 sec
5. Go to step 4, 20 times
6. 72°C for 10 min
7. 15°C forever

Program Touchdown (TD) 55°C:

1. 94°C for 5 min
2. 94°C for 30 sec
   66°C for 30 sec; -1°C per cycle
   72°C for 30 sec
3. Go to step 2, 14 times
4. 94°C for 30 sec
   55°C for 30 sec
   72°C for 30 sec
5. Go to step 4, 20 times
6. 72°C for 10 min
7. 15°C forever

Appendix III
PCR Primers Used to Obtain Genotypes for the Farabee Haplotype

M13 Tail added to the forward primer, used in conjunction with IRD-700 or IRD-800 labeled M13 primers for genotyping:

CACGACGTTGTAAAACGAC

Table A1. Sequence of primers and conditions used to amplify and genotype seven microsatellite markers and five SNPs flanking the *IHH* c.G298A Farabee mutation. Parameters of the amplification programs are described in Appendix II.

Marker	Primer Name	Primer Sequence (5' to 3')	Primer Annealing Temp	PCR Product Size
D2S2250	D2S2250-FM13	CACGACGTTGTAAAACGACCTGAAAC TCACCGAACACC	55 (40 cycles)	169-183 bp
	D2S2250-R	CCCAAATAGGCAGGGAAAT		
D2S433	D2S433-FM13	CACGACGTTGTAAAACGACCCTGGAG TGTCATTGTTTCC	59	179-195 bp
	D2S433-R	TGAACTCATTGTTTTTTACATGG		
SNP D	IHHx3.3F	TGGGGCGTCTCCTGCTA	58	491 bp
	IHHx3.3R	GCATCGGGTCCAGCCAGA		
SNP C	IHHx3.2F	TGCTCTTTACGGCTGACAATC	64	534 bp
	IHHx3.2R	CAGAGGAGATGGCAGGAG		
SNP E	IHHx3.1F	AAGGGAGGGTCGTTGTG	65	494 bp
	IHHx3.1R	TTGTGAGCGGGGCGTAG		
c.G298A	IHHx1F	TGCCCATCAGCCCACCAG	TM 62 (40 cycles)	470 bp
	IHHx1R	GAGCGTGCCAGCCAGTCG		
SNP B	IHHsnp12-F	CGCACAGGGAGGAAAGG	TM 60	237 bp
	IHHsnp12-R	GCAGGAGTGTCGGCATC		
SNP A	IHHsnp12-F	CGCACAGGGAGGAAAGG	TM 60	237 bp
	IHHsnp12-R	GCAGGAGTGTCGGCATC		
D2S163	D2S163-FM13	CACGACGTTGTAAAACGACGTATCCCAGG GCAGGAC	53 (40 cycles)	213-231 bp
	D2S163-R	TAGTTTTTGGATGTTTAGCCTC		
D2S1242	D2S1242-FM13	CACGACGTTGTAAAACGACTGACATAGCG AGACCCTGTC	60	117-172 bp
	D2S1242-R	CCATTCTCATCCAGCAGGA		
D2S424	D2S424-FM13	CACGACGTTGTAAAACGACTGGTGGAGAT GTTTAAAGGC	TD 50	158-194 bp
	D2S424-R	GGGCAGGAAAAGGATTGTAT		
D2S1323	D2S1323-FM13	CACGACGTTGTAAAACGACACATTCAGCA CCAGAATGGT	TD 50	324-332 bp
	D2S1323-R	ATTTGCAGCAGAGACTCTGG		
D2S126	D2S126-FM13	CACGACGTTGTAAAACGACTGCCTAGCAC AGAGCCTACT	TD 50	141-161 bp
	D2S126-R	TCCATGGCATAGAACAAAAGT		

Appendix IV
Additional Primers Used to Genotype on Chromosomes 2, 5, 7, and 20

Table A2. Sequence of primers and conditions used to amplify and genotype nine microsatellite markers on chromosomes 2, 5 and 7. Parameters of the amplification programs are described in Appendix II.

Marker	Primer Sequence (Top, Forward with M13 tag; Bottom, Reverse)	PCR Product Size
D2S164	CACGACGTTGTAAAACGAC GTCCTAACAGGCCACAGACC	265-303 bp
	GCTGGCAGTATCACATGACA	
D2S433	CACGACGTTGTAAAACGACCCTGGAGTGTCATTGTTTCC	179-195 bp
	TGAACTCATTGTTTTTTACATGG	
D2S1242	CACGACGTTGTAAAACGACTGACATAGCGAGACCCTGTC	117-172 bp
	CCATTCTCATCCAGCAGGA	
D5S2854	CACGACGTTGTAAAACGACCTTTTGGGAAACAGAAGCAA	157-175 bp
	CTACAGATGGTACAGTGTAGGACG	
D5S583	CACGACGTTGTAAAACGACGGCTGAGGCAGAAGAATCT	250 bp +
	TCATGGGAGGTCTTCACATG	
D5S663	CACGACGTTGTAAAACGACTTACTGAGATGCAGTCACCTT	205-238 bp
	CCTGAAGACATTAATCATGGA	
D7S3070	CACGACGTTGTAAAACGACCCCCCATGAGTTATTCCTCT	184-208 bp
	GGAAGCCAAATGTTGAATTG	
D7S1823	CACGACGTTGTAAAACGACTCCAAGTAAAGGACAGACTTCC	207-235 bp
	AGCCTCTGTGCAGATCCTC	
D7S2465	CACGACGTTGTAAAACGACACCTGGGCAACAGAGTGAG	158-181 bp
	CTTCAAAGAGTTTATGCTTATGTGG	

Table A3. Sequence of primers and conditions used to amplify and genotype nine microsatellite markers on chromosome 20. Parameters of the amplification programs are described in Appendix II.

Marker	Primer Sequence (Top, Forward with M13 tag; Bottom, Reverse)	PCR Product Size
D20S471	CACGACGTTGTAAAACGACGGGATGCAGAAATTGCAGTA	257-326 bp
	TTTTCTCTTTGCCACTGACC	
D20S912	CACGACGTTGTAAAACGACCGGCTCTAGCATTCATTTG	243-283 bp
	GGCTACTTAGACTAANTCATGGACC	
D20S486	CACGACGTTGTAAAACGACGAAGGGCTTTAATGTTCAGTG	231-251 bp
	AGAAGCCTTGGAGAACGATT	
D20S601	CACGACGTTGTAAAACGACGGTACCAGAGCAACACCTTG	125-145 bp
	ATAAAGGAAAATCCCCCTACC	
D20S106	CACGACGTTGTAAAACGACTGAAAACCCTCCACCTGAAC	316-332 bp
	ACTGAGGTCATGCAAGAGGC	
D20S914	CACGACGTTGTAAAACGACGCATACCCATGCTTGCT	166-204 bp
	CTGCACCCAGCCTCTT	
D20S870	CACGACGTTGTAAAACGACAGTTCCCGCTCCCTACAG	147-181 bp
	ATTGCCAGGGCTGTGA	
D20S865	CACGACGTTGTAAAACGACCCCTGGCTCAGAGGTCAA	247-257 bp
	CTGGTGGTGGCAGCAGTAA	
D20S834	CACGACGTTGTAAAACGACTTGAAACCAGGTAAGCC	126-156 bp
	CCTCTGGCAAGGAGAC	

Appendix V
History of this study

The study of BDA1 has been an ongoing project in the laboratory of Dr. Dennis Bulman. In my project, four new BDA1 families have been studied, as well as numerous additional families that have been studied in the past by many predecessors. Tables A4 and A5 summarize the pertinent details of the families that have partaken in the study since its inception. The number of total participants and affected individuals in each family, their geographical origin, the mutated disease-causing gene (if known), and the texts in which each of the kindreds have been published are described.

Table A4. Details of families 1-10 that participated in the BDA1 study. The number of total participants and affected individuals in each family, their geographical origin, the mutated disease-causing gene (if known), and the texts in which each kindred has been published are listed. A "*" denotes that the family has the Farabee c.G298A mutation.

Pedigree	Mutation	Origin	Participants	BDA1 Affected	Reference Text
1	Chr. 5	Ontario, Canada	60	35	Armour et al 2000 McCready 2004 Grimsey 2006
2	IHH*	Liverpool, England	12	5	McCready et al 2002 McCready 2004
3	IHH*	Manchester, England	6	3	McCready et al 2002 McCready 2004
4	Reclassified as BDC: GDF5	Houston, USA	11	5	Mastrobatistta et al 1995 Kirkpatrick et al 2003 McCready 2004 Byrnes 2007
5	IHH	Houston, USA	6	4	Mastrobatistta et al 1995 Kirkpatrick et al 2003 McCready 2004
6	--	Wellington, NZ	3	1	McCready 2004 Byrnes 2007
7	IHH*	Oxford, England	1	1	McCready et al 2002 McCready 2004
8	--	Ottawa, Canada	1	1	McCready 2004 Byrnes 2007
9	--	Ottawa, Canada	1	1	McCready 2004 Byrnes 2007
10	IHH*	Oregon, USA	1	1	Brown 1998 McCready 2004 McCready et al 2005

Table A5. Details of Pedigrees 11-12 and 14-23 that participated in the BDA1 study. The number of total participants and affected individuals in each family, their geographical origin, the mutated disease-causing gene (if known), and the texts in which each kindred has been published are listed. A "*" denotes that the family has the Farabee c.G298A mutation.

Pedigree	Mutation	Origin	Participants	BDA1 Affected	Reference Text
11	--	Edinburgh, Scotland	1	1	McCready 2004 Byrnes 2007
12	--	Los Angeles, USA	1	1	McCready 2004
14	IHH*	Pennsylvania, USA	9	6	McCready 2004 McCready et al 2005 Grimsey 2006
15	--	Los Angeles, USA	1	1	Grimsey 2006
16	IHH*	Wellington, NZ	7	7	McCready et al 2005 Grimsey 2006 Byrnes 2007
17	--	London, England	3	1	Grimsey 2006 Byrnes 2007
18	GDF5	Quebec, Canada	8	3	Grimsey 2006 Byrnes 2007
19	--	Toronto, Canada	1	1	Grimsey 2006 Byrnes 2007
20	IHH	Los Angeles, USA	4	2	Byrnes 2007
21	--	Los Angeles, USA	3	2	Byrnes 2007
22	IHH	Hong Kong, China	3	3	Byrnes 2007
23	IHH	Tel Aviv, Israel	3	2	Byrnes 2007

Appendix VI
Reproduction Authorizations

Permission to reproduce Figure 1.1:

Reproduced with permission from Journal of Genetics (J. Genet. 1912, **2**, 21-40), Copyright Indian Academy of Sciences.

Permission to reproduce Figure 1.8:

Reprinted from Biochemical and Biophysical Research Communications, Vol. 329, Schreuder H., Liesum A., Pohl J., Kruse M., Koyama M., Crystal structure of recombinant human growth and differentiation factor 5: Evidence for interation of the type I and type II receptor-binding sites, pp. 1076-1086, Copyright (2005), with permission from Elsevier.

Contribution of Collaborators

Dr. Sara Nikkel (Children's Hospital of Eastern Ontario in Ottawa, Ontario): Patient examination and diagnosis, metacarpophalangeal profiles of family 18.

Dr. Alexa Kidd (Central and Southern Regional Genetics Services, Wellington Hospital, Wellington, New Zealand); Dr. Hope Northrup (Shriners Hospital for Children in Houston, Texas); Dr. Louanne Hudgins (Stanford University Medical Center in Stanford, California); Prof. Yuval Yaron (Tel Aviv Sourasky Medical Center in Tel Aviv, Israel); Dr. Yu Lung (The University of Hong Kong's Queen Mary Hospital in Hong Kong): Patient examination and diagnosis.

Ruobing Zou and Kelly Westaff (Laboratory Technicians, the Ottawa Health Research Institute, Ottawa, Ontario): Genotyping of numerous microsatellite markers in families 4 and 18.

Lemuel Racacho and Heather MacDonald (Laboratory Technicians, the Ottawa Health Research Institute, Ottawa, Ontario): Sequencing of *GDF5* in families 4, 6, 8, 9, 15, 17, 18, 19 and 21.

Jessica Skof (Summer Student, the Ottawa Health Research Institute, Ottawa, Ontario): Optimization and sequencing of many amplicons at the chromosome 5 locus.

References

1. Bell, J., *On Brachydactyly and Symphalangism*, in *Treasury of Human Inheritance*, L.S. Penrose, Editor. 1951, Cambridge University Press: London. p. 1-31.
2. Fitch, N., *Classification and identification of inherited brachydactylies.* J.Med.Genet., 1979. **16**: p. 36-44.
3. Temtamy, S.A. and V.A. McKusick, *Brachydactyly as an Isolated Malformation*, in *The Genetics of Hand Malformations*, D. Bergsma, J.R. Mudge, and K.W. Paul, Editors. 1978, Alan R. Liss: New York. p. 187-197.
4. Johnson, D., et al., *Missense mutations in the homeodomain of HOXD13 are associated with brachydactyly types D and E.* Am J Hum Genet, 2003. **72**(4): p. 984-97.
5. McKusick, V.A. and S.A. Temtamy, *Brachydactyly as an Isolated Malformation*, in *The Genetics of Hand Malformations*. 1978, Alan R. Liss: New York. p. 187-197.
6. Osebold, W.R., et al., *An autosomal dominant syndrome of short stature with mesomelic shortness of limbs, abnormal carpal and tarsal bones, hypoplastic middle phalanges, and bipartite calcanei.* Am J Med Genet, 1985. **22**(4): p. 791-809.
7. Farabee, W.C., *Hedeitary and sexual influences in meristic variation: A study of digital malformations in man.*, in *Anthropology*. 1903, Harvard University: Boston.
8. Slavotinek, A. and D. Donnai, *A boy with severe manifestations of type A1 brachydactyly.* Clin Dysmorphol, 1998. **7**(1): p. 21-27.
9. Tsukahara, M., Y. Azuno, and T. Kajii, *Type A1 brachydactyly, dwarfism, ptosis, mixed partial hearing loss, microcephaly, and mental retardation.* Am J Med Genet, 1989. **33**(1): p. 7-9.
10. Grange, D.K., et al., *Familial syndrome of progressive arterial occlusive disease consistent with fibromuscular dysplasia, hypertension, congenital cardiac defects, bone fragility, brachysyndactyly, and learning disabilities.* Am J Med Genet, 1998. **75**(5): p. 469-480.
11. Piussan, C., et al., *[Regular dominance of thumb ankylosis with mental retardation transmitted over 3 generations].* J Genet Hum, 1983. **31**(2): p. 107-14.
12. Raff, M.L., et al., *Brachydactyly type A1 with abnormal menisci and scoliosis in three generations.* Clin Dysmorphol, 1998. **7**(1): p. 29-34.
13. Sillence, D.O., *Brachydactyly, distal symphalangism, scoliosis, tall stature, and club feet: a new syndrome.* J Med Genet, 1978. **15**(3): p. 208-211.
14. Fukushima, Y., et al., *De novo apparently balanced reciprocal translocation between 5q11.2 and 17q23 associated with Klippel-Feil anomaly and type A1 brachydactyly.* Am J Med Genet, 1995. **57**(3): p. 447-449.
15. Ohashi, H.W., K; Nishimoto, H; Sato, M; Aihara, T; Nishida, T.; Fukushima, Y., *Klippel-Feil syndrome and de novo balanced autosomal translocation [46,XX,t(5,17)(q11.2;q23)].* Am. J. Hum. Genet. Suppl., 1992. **51**: p. A294.

16. Gao, B., et al., *Mutations in IHH, encoding Indian hedgehog, cause brachydactyly type A-1.* Nat.Genet., 2001. **28**(4): p. 386-388.
17. Yang, X., et al., *A locus for brachydactyly type A-1 maps to chromosome 2q35-q36.* Am.J.Hum.Genet., 2000. **66**(3): p. 892-903.
18. Giordano, N., et al., *Mild brachydactyly type A1 maps to chromosome 2q35-q36 and is caused by a novel IHH mutation in a three generation family.* J Med Genet, 2003. **40**(2): p. 132-5.
19. Kirkpatrick, T.J., et al., *Identification of a mutation in the Indian Hedgehog (IHH) gene causing brachydactyly type A1 and evidence for a third locus.* J Med Genet, 2003. **40**(1): p. 42-4.
20. Liu, M., et al., *A novel heterozygous mutation in the Indian hedgehog gene (IHH) is associated with brachydactyly type A1 in a Chinese family.* J Hum Genet, 2006.
21. McCready, M.E., et al., *A century later Farabee has his mutation.* Hum Genet, 2005. **117**(2-3): p. 285-7.
22. McCready, M.E., et al., *A novel mutation in the IHH gene causes brachydactyly type A1: a 95-year-old mystery resolved.* Hum Genet, 2002. **111**(4-5): p. 368-75.
23. Armour, C.M., et al., *A novel locus for brachydactyly type A1 on chromosome 5p13.3-p13.2.* J Med Genet, 2002. **39**(3): p. 186-8.
24. Kjaer, K.W., et al., *A mutation in the receptor binding site of GDF5 causes Mohr-Wriedt brachydactyly type A2.* J Med Genet, 2006. **43**(3): p. 225-231.
25. Lehmann, K., et al., *Mutations in bone morphogenetic protein receptor 1B cause brachydactyly type A2.* Proc Natl Acad Sci U S A, 2003. **100**(21): p. 12277-82.
26. Oldridge, M., et al., *Dominant mutations in ROR2, encoding an orphan receptor tyrosine kinase, cause brachydactyly type B.* Nat.Genet., 2000. **24**(3): p. 275-278.
27. Oldridge, M., et al., *Brachydactyly type B: linkage to chromosome 9q22 and evidence for genetic heterogeneity.* Am J Hum Genet, 1999. **64**(2): p. 578-585.
28. Polinkovsky, A., et al., *Mutations in CDMP1 cause autosomal dominant brachydactyly type C.* Nat Genet, 1997. **17**(1): p. 18-19.
29. Schwabe, G.C., et al., *Brachydactyly type C caused by a homozygous missense mutation in the prodomain of CDMP1.* Am J Med Genet, 2004. **124A**(4): p. 356-63.
30. Lehmann, K., et al., *A novel R486Q mutation in BMPR1B resulting in either a brachydactyly type C/symphalangism-like phenotype or brachydactyly type A2.* Eur J Hum Genet, 2006.
31. Schuster, H., et al., *Severe autosomal dominant hypertension and brachydactyly in a unique Turkish kindred maps to human chromosome 12.* Nat Genet, 1996. **13**(1): p. 98-100.
32. Drinkwater, H., *An Account of a Brachydactylous Family.* Proc.Roy.Soc.Edin., 1908. **28**: p. 35-57.
33. Drinkwater, H., *Account of a family showing minor brachydactyly.* J.Genet., 1912. **2**: p. 21-40.
34. Drinkwater, H., *A second brachydactylous family.* J.Genet., 1915. **4**: p. 323-339.
35. Haws, D.V. and V.A. McKusick, *Farabee's brachydactylous kindred revisited.* Bull.Johns Hopkins Hosp., 1963. **113**: p. 20-30.
36. Lai, L.P. and J. Mitchell, *Indian hedgehog: its roles and regulation in endochondral bone development.* J Cell Biochem, 2005. **96**(6): p. 1163-73.

37. Minina, E., et al., *Interaction of FGF, Ihh/Pthlh, and BMP signaling integrates chondrocyte proliferation and hypertrophic differentiation.* Dev Cell, 2002. **3**(3): p. 439-49.
38. Vortkamp, A., et al., *Regulation of rate of cartilage differentiation by Indian hedgehog and PTH-related protein.* Science, 1996. **273**(5275): p. 613-622.
39. Kronenberg, H.M., *Developmental regulation of the growth plate.* Nature, 2003. **423**(6937): p. 332-6.
40. Provot, S. and E. Schipani, *Molecular mechanisms of endochondral bone development.* Biochem Biophys Res Commun, 2005. **328**(3): p. 658-65.
41. St-Jacques, B., M. Hammerschmidt, and A.P. McMahon, *Indian hedgehog signaling regulates proliferation and differentiation of chondrocytes and is essential for bone formation.* Genes Dev., 1999. **13**(16): p. 2072-2086.
42. Levin, M., et al., *A molecular pathway determining left-right asymmetry in chick embryogenesis.* Cell, 1995. **82**(5): p. 803-14.
43. Tsukui, T., et al., *Multiple left-right asymmetry defects in Shh(-/-) mutant mice unveil a convergence of the shh and retinoic acid pathways in the control of Lefty-1.* Proc Natl Acad Sci U S A, 1999. **96**(20): p. 11376-81.
44. Echelard, Y., et al., *Sonic hedgehog, a member of a family of putative signaling molecules, is implicated in the regulation of CNS polarity.* Cell, 1993. **75**(7): p. 1417-30.
45. Riddle, R.D., et al., *Sonic hedgehog mediates the polarizing activity of the ZPA.* Cell, 1993. **75**(7): p. 1401-16.
46. Bitgood, M.J., L. Shen, and A.P. McMahon, *Sertoli cell signaling by Desert hedgehog regulates the male germline.* Curr Biol, 1996. **6**(3): p. 298-304.
47. Hebrok, M., et al., *Regulation of pancreas development by hedgehog signaling.* Development, 2000. **127**(22): p. 4905-13.
48. Lee, K., et al., *Indian hedgehog is a major mediator of progesterone signaling in the mouse uterus.* Nat Genet, 2006. **38**(10): p. 1204-9.
49. Ramalho-Santos, M., D.A. Melton, and A.P. McMahon, *Hedgehog signals regulate multiple aspects of gastrointestinal development.* Development, 2000. **127**(12): p. 2763-72.
50. Bijlsma, M.F., C.A. Spek, and M.P. Peppelenbosch, *Hedgehog: an unusual signal transducer.* Bioessays, 2004. **26**(4): p. 387-94.
51. Porter, J.A., et al., *The product of hedgehog autoproteolytic cleavage active in local and long-range signalling.* Nature, 1995. **374**(6520): p. 363-6.
52. Porter, J.A., K.E. Young, and P.A. Beachy, *Cholesterol modification of hedgehog signaling proteins in animal development.* Science, 1996. **274**(5285): p. 255-9.
53. Wendler, F., X. Franch-Marro, and J.P. Vincent, *How does cholesterol affect the way Hedgehog works?* Development, 2006. **133**(16): p. 3055-61.
54. Lum, L. and P.A. Beachy, *The Hedgehog response network: sensors, switches, and routers.* Science, 2004. **304**(5678): p. 1755-9.
55. Bijlsma, M.F., et al., *Repression of smoothened by patched-dependent (pro-)vitamin D3 secretion.* PLoS Biol, 2006. **4**(8): p. e232.
56. Chuang, P.T. and A.P. McMahon, *Vertebrate Hedgehog signalling modulated by induction of a Hedgehog-binding protein.* Nature, 1999. **397**(6720): p. 617-21.

57. Chung, U.I., et al., *Indian hedgehog couples chondrogenesis to osteogenesis in endochondral bone development.* J.Clin.Invest.. 2001. **107**(3): p. 295-304.
58. Karp, S.J., et al., *Indian hedgehog coordinates endochondral bone growth and morphogenesis via parathyroid hormone related-protein-dependent and -independent pathways.* Development, 2000. **127**(3): p. 543-548.
59. Hellemans, J., et al., *Homozygous mutations in IHH cause acrocapitofemoral dysplasia, an autosomal recessive disorder with cone-shaped epiphyses in hands and hips.* Am J Hum Genet, 2003. **72**(4): p. 1040-6.
60. Mortier, G.R., et al., *Acrocapitofemoral dysplasia: an autosomal recessive skeletal dysplasia with cone shaped epiphyses in the hands and hips.* J Med Genet, 2003. **40**(3): p. 201-7.
61. McCready, M.E.B., D.E., *The Genetics of Indian Hedgehog*, in *Hedgehog-Gli Signaling in Human Disease*, A. Ruiz i Altaba, Editor. 2006, Landes bioscience/Eurekah.com: New York. p. 146-152.
62. Massague, J., *The transforming growth factor-beta family.* Annu Rev Cell Biol, 1990. **6**: p. 597-641.
63. Storm, E.E., et al., *Limb alterations in brachypodism mice due to mutations in a new member of the TGF beta-superfamily.* Nature, 1994. **368**(6472): p. 639-643.
64. Ducy, P. and G. Karsenty, *The family of bone morphogenetic proteins.* Kidney Int, 2000. **57**(6): p. 2207-14.
65. Settle, S.H., Jr., et al., *Multiple joint and skeletal patterning defects caused by single and double mutations in the mouse Gdf6 and Gdf5 genes.* Dev Biol, 2003. **254**(1): p. 116-30.
66. Thomas, J.T., et al., *Disruption of human limb morphogenesis by a dominant negative mutation in CDMP1.* Nat Genet, 1997. **17**(1): p. 58-64.
67. Chang, S.C., et al., *Cartilage-derived morphogenetic proteins. New members of the transforming growth factor-beta superfamily predominantly expressed in long bones during human embryonic development.* J Biol Chem, 1994. **269**(45): p. 28227-34.
68. Storm, E.E. and D.M. Kingsley, *GDF5 coordinates bone and joint formation during digit development.* Dev.Biol., 1999. **209**(1): p. 11-27.
69. Schreuder, H., et al., *Crystal structure of recombinant human growth and differentiation factor 5: evidence for interaction of the type I and type II receptor-binding sites.* Biochem Biophys Res Commun, 2005. **329**(3): p. 1076-86.
70. Massague, J. and D. Wotton, *Transcriptional control by the TGF-beta/Smad signaling system.* Embo J, 2000. **19**(8): p. 1745-54.
71. Chen, D., M. Zhao, and G.R. Mundy, *Bone morphogenetic proteins.* Growth Factors, 2004. **22**(4): p. 233-41.
72. Nishitoh, H., et al., *Identification of type I and type II serine/threonine kinase receptors for growth/differentiation factor-5.* J Biol Chem, 1996. **271**(35): p. 21345-52.
73. Derynck, R. and Y.E. Zhang, *Smad-dependent and Smad-independent pathways in TGF-beta family signalling.* Nature, 2003. **425**(6958): p. 577-84.
74. Mikic, B., *Multiple effects of GDF-5 deficiency on skeletal tissues: implications for therapeutic bioengineering.* Ann Biomed Eng, 2004. **32**(3): p. 466-76.

75. Thomas, J.T., et al., *CDMP1/GDF5 has specific processing requirements that restrict its action to joint surfaces.* J Biol Chem, 2006. **281**(36): p. 26725-33.
76. Sammar, M., et al., *Modulation of GDF5/BRI-b signalling through interaction with the tyrosine kinase receptor Ror2.* Genes Cells, 2004. **9**(12): p. 1227-38.
77. Francis-West, P.H., et al., *Mechanisms of GDF-5 action during skeletal development.* Development, 1999. **126**(6): p. 1305-15.
78. Storm, E.E., et al., *Limb alterations in brachypodism mice due to mutations in a new member of the TGF beta-superfamily.* Nature, 1994. **368**(6472): p. 639-43.
79. Storm, E.E. and D.M. Kingsley, *Joint patterning defects caused by single and double mutations in members of the bone morphogenetic protein (BMP) family.* Development, 1996. **122**(12): p. 3969-79.
80. Brunet, L.J., et al., *Noggin, cartilage morphogenesis, and joint formation in the mammalian skeleton.* Science, 1998. **280**(5368): p. 1455-7.
81. Pathi, S., et al., *Interaction of Ihh and BMP/Noggin signaling during cartilage differentiation.* Dev Biol, 1999. **209**(2): p. 239-53.
82. Chhabra, A., et al., *GDF-5 deficiency in mice delays Achilles tendon healing.* J Orthop Res, 2003. **21**(5): p. 826-35.
83. Al-Yahyaee, S.A., et al., *Clinical and molecular analysis of Grebe acromesomelic dysplasia in an Omani family.* Am J Med Genet A, 2003. **121**(1): p. 9-14.
84. Faiyaz-Ul-Haque, M., et al., *Frameshift mutation in the cartilage-derived morphogenetic protein 1 (CDMP1) gene and severe acromesomelic chondrodysplasia resembling Grebe-type chondrodysplasia.* Am J Med Genet, 2002. **111**(1): p. 31-7.
85. Faiyaz-Ul-Haque, M., et al., *Mutation in the cartilage-derived morphogenetic protein-1 (CDMP1) gene in a kindred affected with fibular hypoplasia and complex brachydactyly (DuPan syndrome).* Clin Genet, 2002. **61**(6): p. 454-8.
86. Stelzer, C., et al., *Grebe dysplasia and the spectrum of CDMP1 mutations.* Pediatr Pathol Mol Med, 2003. **22**(1): p. 77-85.
87. Thomas, J.T., et al., *A human chondrodysplasia due to a mutation in a TGF-beta superfamily member.* Nat.Genet., 1996. **12**(3): p. 315-317.
88. Szczaluba, K., et al., *Du Pan syndrome phenotype caused by heterozygous pathogenic mutations in CDMP1 gene.* Am J Med Genet A, 2005. **138**(4): p. 379-83.
89. Dobbs, M.B., et al., *Variable hand and foot abnormalities in family with congenital vertical talus and CDMP-1 gene mutation.* J Orthop Res, 2005. **23**(6): p. 1490-4.
90. Everman, D.B., et al., *The mutational spectrum of brachydactyly type C.* Am J Med Genet, 2002. **112**(3): p. 291-6.
91. Galjaard, R.J., et al., *Differences in complexity of isolated brachydactyly type C cannot be attributed to locus heterogeneity alone.* Am J Med Genet, 2001. **98**(3): p. 256-62.
92. Holder-Espinasse, M., et al., *Angel shaped phalangeal dysplasia, hip dysplasia, and positional teeth abnormalities are part of the brachydactyly C spectrum associated with CDMP-1 mutations.* J Med Genet, 2004. **41**(6): p. e78.

93. Savarirayan, R., et al., *Broad phenotypic spectrum caused by an identical heterozygous CDMP-1 mutation in three unrelated families.* Am J Med Genet, 2003. **117A**(2): p. 136-42.
94. Seemann, P., et al., *Activating and deactivating mutations in the receptor interaction site of GDF5 cause symphalangism or brachydactyly type A2.* J Clin Invest, 2005. **115**(9): p. 2373-81.
95. Costa, T., et al., *Grebe syndrome: clinical and radiographic findings in affected individuals and heterozygous carriers.* Am J Med Genet, 1998. **75**(5): p. 523-529.
96. Akarsu, A.N.R., T; Demirtas, M.; Farhud, D.D.; Sarfarazi, M., *Multiple synostosis type 2 (SYNS2) maps to 20q11.2 and is caused by a missense mutation in the growth/differentiation factor 5 (GDF5).* Am. J. Hum. Genet. Suppl., 1999. **65**: p. A281.
97. Dawson, K., et al., *GDF5 Is a Second Locus for Multiple-Synostosis Syndrome.* Am J Hum Genet, 2006. **78**(4): p. 708-712.
98. Hoeffel, J.C., et al., *Brachydactyly secondary to pheochromocytoma [letter].* Am J Dis Child, 1993. **147**(3): p. 260-261.
99. Mastrobattista, J.M., et al., *Evaluation of candidate genes for familial brachydactyly.* J Med Genet, 1995. **32**(11): p. 851-4.
100. Nissen, K.I., *A Study in Inherited Brachydactyly.* Annals of Eugenics, 1933. **5**: p. 281-301.
101. Dixon, M.E., et al., *Identical mutations in NOG can cause either tarsal/carpal coalition syndrome or proximal symphalangism.* Genet Med, 2001. **3**(5): p. 349-53.
102. Gong, Y., et al., *Heterozygous mutations in the gene encoding noggin affect human joint morphogenesis.* Nat Genet, 1999. **21**(3): p. 302-4.
103. Mangino, M., et al., *Identification of a novel NOG gene mutation (P35S) in an Italian family with symphalangism.* Hum Mutat, 2002. **19**(3): p. 308.
104. Takahashi, T., et al., *Mutations of the NOG gene in individuals with proximal symphalangism and multiple synostosis syndrome.* Clin Genet, 2001. **60**(6): p. 447-51.
105. Brown, D.J., et al., *Autosomal dominant stapes ankylosis with broad thumbs and toes, hyperopia, and skeletal anomalies is caused by heterozygous nonsense and frameshift mutations in NOG, the gene encoding noggin.* Am J Hum Genet, 2002. **71**(3): p. 618-24.
106. Botstein, D. and N. Risch, *Discovering genotypes underlying human phenotypes: past successes for mendelian disease, future approaches for complex disease.* Nat Genet, 2003. **33 Suppl**: p. 228-37.
107. Kleinjan, D.A. and V. van Heyningen, *Long-range control of gene expression: emerging mechanisms and disruption in disease.* Am J Hum Genet, 2005. **76**(1): p. 8-32.
108. Baralle, M. and F.E. Baralle, *Genetics and molecular biology: single nucleotide polymorphism associations and their functional significance.* Curr Opin Lipidol, 2006. **17**(3): p. 360-2.
109. Grimsey, A., *Brachydactyly Type A1*, in *Department of Microbiology and Immunology*. 2006, University of Ottawa: Ottawa.

110. Silva, E.O., *An unusual family with brachydactyly.* Am J Med Genet A, 2003. **117**(2): p. 191-3.
111. Park, H.W., et al., *Correction of lumbosacral hyperlordosis in achondroplasia.* Clin Orthop Relat Res, 2003(414): p. 242-9.
112. Kahanovitz, N., D.L. Rimoin, and D.O. Sillence, *The clinical spectrum of lumbar spine disease in achondroplasia.* Spine, 1982. **7**(2): p. 137-40.
113. Karadimas, C., et al., *Prenatal diagnosis of hypochondroplasia: report of two cases.* Am J Med Genet A, 2006. **140**(9): p. 998-1003.
114. Rousseau, F., et al., *Clinical and genetic heterogeneity of hypochondroplasia.* J Med Genet, 1996. **33**(9): p. 749-52.
115. Dlugaszewska, B., et al., *Breakpoints around the HOXD cluster result in various limb malformations.* J Med Genet, 2006. **43**(2): p. 111-8.
116. Kimberley, K.W., C.A. Morris, and H.H. Hobart, *BAC-FISH refutes report of an 8p22-8p23.1 inversion or duplication in 8 patients with Kabuki syndrome.* BMC Med Genet, 2006. **7**: p. 46.
117. Kline, A.D., et al., *A de novo complex karyotype with two independent balanced translocations and a double inversion of chromosome 6 presenting with multiple congenital anomalies.* Am J Med Genet A, 2004. **129**(2): p. 124-9.
118. Gorlin, R.J., H.O. Sedano, and Odont, *Cryptodontic brachymetacarpalia.* Birth Defects Orig Artic Ser, 1971. **7**(7): p. 200-3.
119. Hunter, A.G., et al., *A 'new' syndrome of mental retardation with characteristic facies and brachyphalangy.* J.Med.Genet., 1977. **14**(6): p. 430-437.
120. Nance, W.E., et al., *Congenital X-linked cataract, dental anomalies and brachymetacarpalia.* Birth Defects Orig Artic Ser, 1974. **10**(4): p. 285-91.
121. Robinow, M., F.N. Silverman, and H.D. Smith, *A newly recognized dwarfing syndrome.* Am J Dis Child, 1969. **117**(6): p. 645-51.
122. Soliman, A.T., et al., *Recessive Robinow syndrome: with emphasis on endocrine functions.* Metabolism, 1998. **47**(11): p. 1337-43.
123. Wolf, U., *Identical mutations and phenotypic variation.* Hum Genet, 1997. **100**(3-4): p. 305-21.
124. Nadeau, J.H., *Modifier genes in mice and humans.* Nat Rev Genet, 2001. **2**(3): p. 165-74.
125. Slavotinek, A. and L.G. Biesecker, *Genetic modifiers in human development and malformation syndromes, including chaperone proteins.* Hum Mol Genet, 2003. **12 Spec No 1**: p. R45-50.
126. Bilginturan, N., et al., *Hereditary brachydactyly associated with hypertension.* J Med Genet, 1973. **10**(3): p. 253-259.
127. Nagai, T., et al., *Del(12)(p11.21p12.2) associated with an asphyxiating thoracic dystrophy or chondroectodermal dysplasia-like syndrome.* Am J Med Genet, 1995. **55**(1): p. 16-8.
128. den Hollander, N.S., et al., *Prenatal diagnosis of type A1 brachydactyly.* Ultrasound Obstet Gynecol, 2001. **17**(6): p. 529-30.
129. Bronshtein, M., S. Stahl, and E.Z. Zimmer, *Transvaginal sonographic diagnosis of fetal finger abnormalities in early gestation.* J Ultrasound Med, 1995. **14**(8): p. 591-5.

130. Reiss, R.E., et al., *Ease and accuracy of evaluation of fetal hands during obstetrical ultrasonography: a prospective study.* J Ultrasound Med, 1995. **14**(11): p. 813-20; quiz 821-2.
131. Collins, F.S., *Positional cloning moves from perditional to traditional.* Nat Genet, 1995. **9**(4): p. 347-50.
132. Broeckel, U. and N.J. Schork, *Identifying genes and genetic variation underlying human diseases and complex phenotypes via recombination mapping.* J Physiol, 2004. **554**(Pt 1): p. 40-5.
133. Ott, J., *Analysis of Human Genetic Linkage.* 3 ed. 1999, Baltimore: John Hopkins University Press.
134. Lander, E. and L. Kruglyak, *Genetic dissection of complex traits: guidelines for interpreting and reporting linkage results.* Nat Genet, 1995. **11**(3): p. 241-7.
135. Niedermaier, M., et al., *An inversion involving the mouse Shh locus results in brachydactyly through dysregulation of Shh expression.* J Clin Invest, 2005. **115**(4): p. 900-9.
136. McCready, M.E., *Brachydactyly Type A1: Short Fingers, Lengthy History*, in *Department of Microbiology and Immunology.* 2004, University of Ottawa: Ottawa.
137. Armour, C.M., D.E. Bulman, and A.G. Hunter, *Clinical and radiological assessment of a family with mild brachydactyly type A1: the usefulness of metacarpophalangeal profiles.* J.Med.Genet., 2000. **37**(4): p. 292-296.
138. Lin, K., et al., *Assignment of a new TGF-beta superfamily member, human cartilage-derived morphogenetic protein-1, to chromosome 20q11.2.* Genomics, 1996. **34**(1): p. 150-151.
139. Thomas, J.T., et al., *Disruption of human limb morphogenesis by a dominant negative mutation in CDMP1.* Nat.Genet., 1997. **17**(1): p. 58-64.
140. Luyten, F.P., *Cartilage-derived morphogenetic protein-1.* Int J Biochem Cell Biol, 1997. **29**(11): p. 1241-4.
141. Brunner, A.M., et al., *Site-directed mutagenesis of glycosylation sites in the transforming growth factor-beta 1 (TGF beta 1) and TGF beta 2 (414) precursors and of cysteine residues within mature TGF beta 1: effects on secretion and bioactivity.* Mol Endocrinol, 1992. **6**(10): p. 1691-700.
142. Hawley, S.H., et al., *Disruption of BMP signals in embryonic Xenopus ectoderm leads to direct neural induction.* Genes Dev, 1995. **9**(23): p. 2923-35.
143. Giordano, N., et al., *Weill-Marchesani syndrome: report of an unusual case.* Calcif Tissue Int, 1997. **60**(4): p. 358-360.
144. Polymeropoulos, M.H., et al., *Brachydactyly type C gene maps to human chromsome 12q24.* Genomics, 1996. **38**(1): p. 45-50.
145. Yi, S.E., et al., *The type I BMP receptor BMPRIB is required for chondrogenesis in the mouse limb.* Development, 2000. **127**(3): p. 621-630.
146. Burgess, R.C., *Brachydactyly type C.* J Hand Surg [Am], 2001. **26**(1): p. 31-9.
147. Camera, G., G. Stella, and A. Camera, *New X linked spondyloepimetaphyseal dysplasia: report on eight affected males in the same family.* J Med Genet, 1994. **31**(5): p. 371-376.
148. Robin, N.H., et al., *Clinical and locus heterogeneity in brachydactyly type C.* Am J Med Genet, 1997. **68**(3): p. 369-377.

149. Wang, X., et al., *A novel mutation in GDF5 causes autosomal dominant symphalangism in two Chinese families.* Am J Med Genet A, 2006. **140**(17): p. 1846-53.
150. Beighton, P., *Heterozygous manifestations in the heritable disorders of the skeleton.* Pediatr Radiol, 1997. **27**(5): p. 397-401.
151. Mohr, O.L.W., C., *A new type of hereditary brachyphalangy in man.* 1919, Washington: Carnegie Institute.
152. Yan, H. and W. Zhou, *Allelic variations in gene expression.* Curr Opin Oncol, 2004. **16**(1): p. 39-43.